AD-A074 104 WESTINGHOUSE RESEARCH AND DEVELOPMENT CENTER PITTSBU--ETC F/G 11/6
ENVIRONMENTAL HYDROGEN CRACKING OF HY STEEL WELD METALS.(U)
AUG 79 E W JOHNSON, B J SHAW N00014-77-C-0372
UNCLASSIFIED 79-9D9-HONRY-R1 NL

1 OF 2
AD A074104

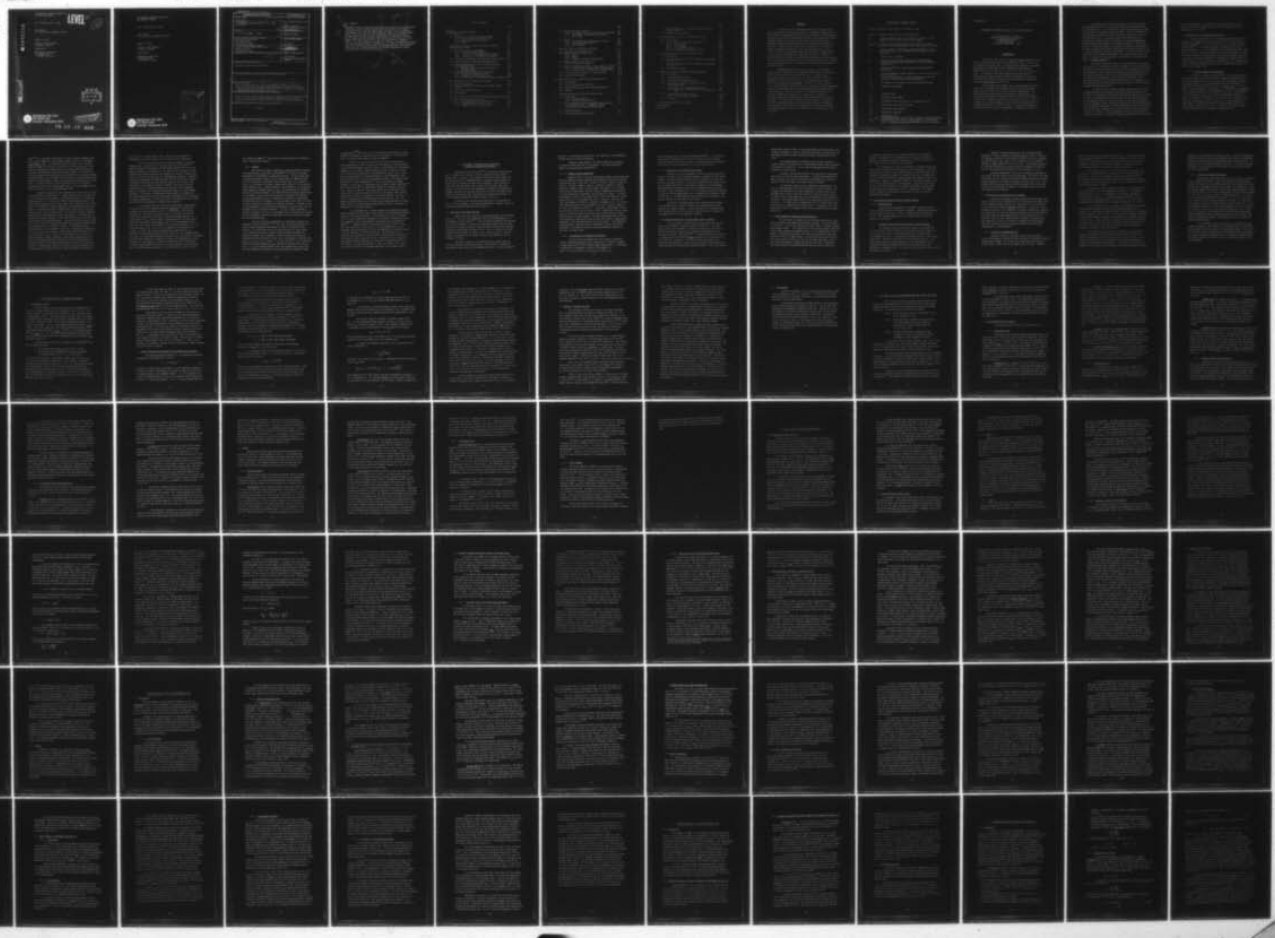

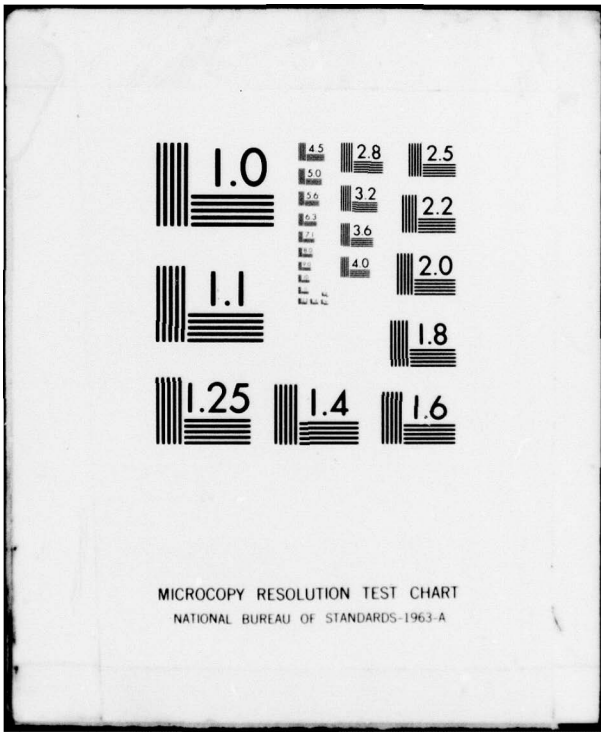
1.0
1.1
1.25
1.4
1.6
1.8
2.0
2.2
2.5
2.8
3.2
3.6
4.0
4.5
5.0
5.6
6.3
MICROCOPY RESOLUTION TEST CHART
NATIONAL BUREAU OF STANDARDS-1963-A

ENVIRONMENTAL HYDROGEN CRACKING OF HY STEEL WELD METALS

LEVEL II

E. W. Johnson and B. J.Shaw

Final Report
U.S. Navy Contract N00014-77-C-0372

August 15, 1979

Office of Naval Research
Arlington, Virginia

Submitted by

Westinghouse R&D Center
1310 Beulah Road
Pittsburgh, PA 15235

ENVIRONMENTAL HYDROGEN CRACKING OF HY STEEL WELD METALS

E. W. Johnson and B. J.Shaw

Final Report
U.S. Navy Contract N00014-77-C-0372

August 15, 1979

Office of Naval Research
Arlington, Virginia

Submitted by

Westinghouse R&D Center
1310 Beulah Road
Pittsburgh, PA 15235

Westinghouse R&D Center
1310 Beulah Road
Pittsburgh, Pennsylvania 15235

UNCLASSIFIED
SECURITY CLASSIFICATION OF THIS PAGE (When Data Entered)

REPORT DOCUMENTATION PAGE

READ INSTRUCTIONS BEFORE COMPLETING FORM

1. REPORT NUMBER: Final Report	2. GOVT ACCESSION NO.
3. RECIPIENT'S CATALOG NUMBER	
4. TITLE (and Subtitle): ENVIRONMENTAL HYDROGEN CRACKING OF HY STEEL WELD METALS.	5. TYPE OF REPORT & PERIOD COVERED: Final 5/1/77 - 6/30/79
	6. PERFORMING ORG. REPORT NUMBER: 79-9D9-HONRY-R1
7. AUTHOR(s): E. W. Johnson and B. J. Shaw	8. CONTRACT OR GRANT NUMBER(s): N00014-77-C-0372
9. PERFORMING ORGANIZATION NAME AND ADDRESS: Westinghouse R&D Center, 1310 Beulah Road, Pittsburgh PA 15235	10. PROGRAM ELEMENT, PROJECT, TASK AREA & WORK UNIT NUMBERS: NR 036-122
11. CONTROLLING OFFICE NAME AND ADDRESS: Office of Naval Research (Code 471), 800 North Quincy, Arlington, VA 22217	12. REPORT DATE: August 15, 1979
	13. NUMBER OF PAGES: 170
14. MONITORING AGENCY NAME & ADDRESS (if different from Controlling Office): 174 p.	15. SECURITY CLASS. (of this report): Unclassified
	15a. DECLASSIFICATION/DOWNGRADING SCHEDULE

16. DISTRIBUTION STATEMENT (of this Report)

Approved for unlimited distribution

17. DISTRIBUTION STATEMENT (of the abstract entered in Block 20, if different from Report)

Final rept 1 May 77 - 30 Jun 79,

18. SUPPLEMENTARY NOTES

Work coordinated with that of Contract N00600-77-C-0991, a part of an overall Naval Sea Systems Command (NAVSEA) program on "Subcritical Cracking of High Strength Steel Weldments" (Code SEA 05R). Excerpts to be presented at AIME Milwaukee Meeting Sept. 16-19, 1979.

19. KEY WORDS (Continue on reverse side if necessary and identify by block number)

stress corrosion, accelerated testing, test methods, cracks, crack propagation, steel, low alloy steels, welds, weld metal, degradation, environments, hydrogen embrittlement, hydrogen sulfide, incubation, fracture (mechanics).

20. ABSTRACT (Continue on reverse side if necessary and identify by block number)

(See Over)

DD FORM 1 JAN 73 1473 EDITION OF 1 NOV 65 IS OBSOLETE

UNCLASSIFIED 376 625
SECURITY CLASSIFICATION OF THIS PAGE (When Data Entered)

20. ABSTRACT

Techniques used in a program to develop HY steel weld metals with improved resistance to environmental hydrogen cracking include (1) levitation melting and chill casting of Charpy-size specimens, and (2) accelerated environmental testing by the H_2S rising-load method. The measured values of K_{or}, the stress intensity of crack-growth onset, had satisfactory reproducibility as well as sensitive response to composition. However, K_{or} is larger than the threshold stress intensity K_{arr} (or K_{Iscc}) by an amount that varies directly with t_{io}, the incubation-time constant. Since t_{io} is short relative to design life, only K_{arr} has design significance. Two new accelerated methods of determining K_{arr} are (1) a modified rising-load test in which the displacement is held constant after crack-growth onset, and (2) a similar procedure substituting environmental fatigue precracking for the rising-load phase.

TABLE OF CONTENTS

SYNOPSIS

The extensive alloy screening needed in the development of HY steel weld metals with improved resistance to hydrogen cracking requires that suitable techniques be used for both the preparation of representative specimens and accelerated environmental testing. The procedure for these purposes studied in the present work included levitation melting of candidate weld-metal compositions and chill casting to make Charpy-size specimens, which were then tested (as precracked) by the rising-load method in hydrogen sulfide (H_2S). The resulting values of K_{or}, the stress intensity of crack-growth onset, had satisfactory reproducibility as well as sensitive response to composition variations. The K_{or} of actual weld-metal specimens were usually higher than those of the castings (due to finer grain structure) but also more scattered due to microstructure variations within the weld. Base-metal K_{or} results were higher than the weld-metal results.

The relationship of K_{or} to K_{arr} (or K_{Iscc}), the threshold stress intensity below which no crack growth ever occurs, was examined in both the present work and a related effort (1-1). Usually K_{or} is appreciably larger by an amount that is a direct function of both the loading rate used in the test and t_{io}, the incubation-time constant. These relationships have been modeled. Usually t_{io} is short relative to the required design life and only K_{arr} (or K_{Iscc}) has design significance. Attention was therefore given to the development of accelerated methods of measuring K_{arr}. One such technique is a modified rising-load test for determining both K_{or} and K_{arr} in a single test. Another is a procedure substituting environmental fatigue precracking for the rising-load phase. The final step of either test method consists of holding constant displacement until the crack arrests, where K_{arr} is measured. Both methods are more suitable for sidegrooved CT or WOL specimens than for Charpy specimens in view of the difficulty of determining K_{arr} with the latter.

DEFINITIONS OF ALGEBRAIC SYMBOLS

Note: These and all other symbols are defined in text,

K_I or K	Tensile stress intensity of opening mode I.
K_{Ic}	Fracture toughness (Ref. 1-4): Value of K for onset of crack growth in air or other nonreactive environment.
K_{Iscc} or K_{arr}	Threshold stress intensity below which there is no crack growth in specified environment (esp. after long waiting time).
K_o	Stress intensity exceeding K_{Iscc} that causes onset of crack growth (at time t_i) in a constant-load or constant-displacement test.
P	Load applied to specimen.
v_C	Crack-opening displacement registered by suitable gauge situated at distance from load line (of CT or WOL specimen) indicated by C.
v_t	Measured deflection of Charpy specimen (includes machine deflection).
v	Actual deflection of Charpy specimen or load-line displacement of CT or WOL specimen
a	Total effective length of crack as measured from load line (in WOL) or tensile-loaded surface (in Charpy).
a_1	Net length of crack measured from root of machined notch.
a/W	Normalized crack length.
t_i	Incubation time.
t_{io}	Incubation time constant.
t_g	Crack growth time, especially in a constant-load test.
t_f	Failure time of constant-load test.
t_{go}	Crack-growth time constant.
t_{fo}	Failure-time constant.
$\dot{a}$	Crack-growth rate.
Note:	dotted symbols stand for time rate of change of symbolized quantity.
K_{or}	Stress intensity for onset of crack growth in a constant-rate step- or rising-load or rising-displacement test in environment.

ENVIRONMENTAL HYDROGEN CRACKING OF HY STEEL WELD METALS

E. W. Johnson and B. J. Shaw
Materials Evaluation and Application
Westinghouse R&D Center
1310 Beulah Road
Pittsburgh, Pennsylvania 15235

1. INTRODUCTION

This is the final report of a two-year program sponsored by the Office of Naval Research under Contract N00014-77-C-0372. The work was coordinated closely with that of a related program sponsored by the Naval Ship Research and Development Center (Annapolis) under Contract N00600-77-C-0991, the final report of which (Ref. 1-1) was recently prepared. The purpose of the latter program was the evaluation of environmental-hydrogen-assisted cracking susceptibilities of HY steel plate materials, while the present work had the purpose of similarly evaluating welded joints in such plates.

The HY (High-Yield strength) steels were developed under Navy sponsorship as weldable, high-toughness steels with yield strengths ranging from 80 to 180 ksi for marine structural applications. In a high-strength steel welded structure containing ordinary flaws, the limiting design parameter in long-term exposure to marine environments is often the structure's resistance to environment-assisted subcritical cracking (scc). The environment of Navy ship hulls is seawater with cathodic polarization to inhibit corrosion. The cathodic polarization also enhances the structure's susceptibility to hydrogen-assisted scc.

The welded joints of steel structures are usually more prone to environment-enhanced scc than are the wrought steel base materials. The crack growth can occur at relatively low stress intensities in either the weld metal or the heat-affected zone (HAZ). The HAZ is derived from the base metal and cannot be readily altered in composition to improve its resistance to scc. On the other hand, alloy modification is a feasible way of improving the scc resistance of steel weld metals and thereby improving the integrity of the entire structure. The overall purpose of the present program, accordingly, has been the development of HY steel weld-metal compositions characterized by improved resistance to scc while cathodically polarized in seawater. Since the subcritical crack growth is due to hydrogen embrittlement, the actual purpose of the program is to develop HY steel weld-metal compositions with improved resistance to hydrogen-enhanced scc.

The planned technical approach to achieving this goal includes the preparation of simulated weld-metal specimens of numerous compositions by induction-levitation melting and chill casting, followed by the screening evaluation of the hydrogen scc resistance of these specimens by the H_2S rising-load method. The initial program phase reported here has as its purposes the development, qualification and calibration of the laboratory methods for both specimen preparation and scc testing. For these purposes the only weld metals thus far studied are those with yield strengths approximating 130 ksi.

The success of the planned technical approach (to improve the hydrogen-assisted scc resistance of HY-130 weld metal) depends on the success of the technique of induction-levitation melting and chill casting as a way of simulating the HY-130 weld metal (for at least the purposes of the program) as well as on the success of the H_2S rising-load test as a way of obtaining useful comparative information on the scc propensities of the respective specimens. The latter should be suitable for evaluating not only the chill castings but also the weld metals these castings are intended to simulate. Critical assessments of both techniques are presented in this report. Although the specimen preparation technique occurs

first chronologically, the success of the testing method is the more vital to the overall program objectives and was therefore given the greater share of attention.

1.1 Suitability of H_2S Rising-load Test Method

The H_2S rising-load test for assessing environmental cracking resistance was suggested by McIntyre and Priest[1-2] and evaluated by Clark and Landes[1-3]. The test is similar to that prescribed by ASTM Standard E399[1-4] for fracture toughness testing but differs in two important respects: (a) the environment is H_2S (hydrogen sulfide) rather than air, and (b) the rate of increase of the stress intensity is lower by a factor of about 1000 than that of the fracture toughness (K_{Ic}) test. In both tests the stress intensity is increased (at a constant rate $\dot{K}$) until either (a) there is evidence of crack growth or (b) there is gross plastic yielding of the specimen, such that the plane-strain premise of the test is no longer valid.

1.1.1. Test Data Symbols and Definitions

In a test conforming to ASTM E399[1-4], the stress intensity at crack-growth onset is termed the fracture toughness and symbolized K_{Ic}. In the H_2S rising-load test it is customary for some workers to refer to the stress intensity at the corresponding point of (environmental or subcritical) crack-growth onset as K_{Iscc} or "apparent K_{Iscc}". In other kinds of testing, however, the symbol K_{Iscc} is reserved for the threshold stress intensity below which no crack growth will occur. This duality of the definition of K_{Iscc} is the source of potentially dangerous confusion. To prevent such ambiguity in the present report, we shall avoid using the symbol K_{Iscc} in favor of others, viz. K_{arr} to designate the crack-arrest or infinite-time threshold stress intensity below which no crack growth can ever occur, and K_{or} to designate the stress intensity of crack-growth onset in a rising-load or step-load test.

The ambiguity of the definition of K_{Iscc} appears to have originated in early studies of low-alloy steels suggesting that (a) the threshold stress intensity K_{arr} of a particular material might be the same in all hydrogenous environments, and (b) this same stress intensity is seemingly measured as K_{or} in the H_2S rising-load test. When later work failed to confirm the equivalence of K_{arr} and K_{or}, it became customary to refer to K_{or} as "apparent K_{Iscc}". Such terminology only compounds the confusion, however.

The results of our recent study of H_2S and H_2 crack growth in HY steel plates (Ref. 1-1) and other work have indicated that (a) the threshold stress intensity K_{arr} of a given material is a sensitive function of the hydrogenous environment composition and other conditions, viz. whether the environment is of H_2, H_2S or seawater as well as the gas pressure or applied cathodic potential, and (b) the value of K_{or} measured in a rising-load test usually exceeds K_{arr} by a factor of at least two. The difference between K_{or} and K_{arr} is a direct function of $\dot{K}$, the rate of increase of the stress intensity in the rising-load or step-load test, as discussed in Part 10 of this report.

The ambiguity of the meaning of K_{Iscc} originates in part from fundamental differences of the time dependence of fracture toughness testing on the one hand and environmental crack-growth testing on the other. To a first approximation K_{Ic} is not time dependent if a specimen can be held at a stress intensity only slightly below K_{Ic} for an indefinite length of time without failure. In environmental scc testing, on the other hand, the phenomenon of <u>incubation time</u> is universal, such that there is an inverse correlation between the time consumed by the test (or $1/\dot{K}$) and the stress intensity of crack-growth onset. The only exception is at very long test times (or at very low $\dot{K}$ values) where the crack-growth-onset stress intensity (e.g. K_{or}) closely approximates K_{arr}. Under such conditions, of course, the ambiguity in the definition of K_{Iscc} no longer exists. However, many tests must usually be performed before it can be established that a given crack-onset stress intensity is equivalent to K_{arr}. Otherwise, such equivalence should never be assumed for individual

rising-load tests. Instead, the working premise must be that K_{or} is larger than K_{arr} by a significant (and usually unknown) amount.

Incubation times are usually long in comparison with desired durations of laboratory tests but short in comparison with design lifetimes of actual structures. Accordingly, the only environment-related property of practical interest is K_{arr}, the stress intensity below which no crack growth will ever occur. Shorter-term laboratory test results such as K_{or} have no utility in design except as relative indicators of the environmental cracking susceptibility. In the present report, accordingly, we shall avoid referring to quantities like K_{or} as "apparent K_{Iscc}" and reserve the symbol K_{Iscc} for only the long-term threshold stress intensity K_{arr}.

The subscript "arr" (for arrest) may seem less appropriate than "th" (for threshold) to indicate the threshold stress intensity. However, Novak and Rolfe[1-5] have demonstrated that K_{arr}, the crack-arrest value of K in a bolt-load (nearly constant-displacement, declining K) test is equivalent to K_{th}, the infinite-time threshold stress intensity measured in multiple constant-load tests performed at different values of K_o, the stress intensity of a single-load test. This important contribution confirms the intuitive conclusion that $K_{arr} = K_{th} = K_{Iscc}$, or that the final, crack-arrest value of the stress intensity measured in a constant-displacement test is indeed identical to the threshold stress intensity defined as the crack-onset value of K at infinite incubation time. Accordingly, no distinction is made between the "arrest" and "threshold" definitions of K_{arr} (or K_{Iscc}) in the present report. The data of Novak and Rolfe on which this conclusion is based are additionally reviewed in Section 10.2.

1.1.2. Crack Tunneling Consequences

Although K_{Ic} is a design-useful quantity if it is truly time-independent, it is still the stress intensity of crack-growth onset only. The accompanying stress intensity of crack arrest in a fracture toughness test is more difficult to measure but is usually 50 to 75% of K_{Ic}.

Neale [1-6] has described crack "pop-in" during a fracture-toughness test as the rapid propagation and subsequent stable arrest of a more deeply tunnel-shaped crack. His analysis indicates that the stress intensity along the tunnel crack front is very much lower than that usually calculated by combining any average value of the crack length with the conventional two-dimensional calibration function (K/P). The formation of the tunnel-shaped crack during pop-in was initiated from a nearly straight-fronted precrack at K_{Ic} and ended in crack arrest at a tunnel-shaped crack front with the much lower, stable stress intensity characteristic of crack arrest. As Neale points out, this is possible only if the effective calibration (K/P) for the tunnel-shaped crack is very much lower than the usual such function for a straight-fronted crack.

Numerous instances of crack tunneling were seen in the H_2S tests of HY steel plate and weld metal. A common pattern was for the H_2S crack to grow internally in the interior, plane-strain region of the specimen while the ends of the crack front, being in plane-stressed material that could deform plastically rather than crack, often exhibited no local crack growth. This behavior confirms suggestions that hydrogen-assisted crack growth is initiated internally in plane-strain zones while the specimen surface layers, being in plane stress, are relatively immune to hydrogen-enhanced failure and therefore resist crack growth. The consequence is successively deeper penetration of the tunnel-shaped crack into the plane-strain zone of the specimen interior. The actual stress intensity at the tip of the crack in the plane-strain material decreases drastically while this tunneling occurs, according to Neale. In environmental tests characterized by crack tunneling, therefore, a reasonable interpretation is that the crack front assumes a stable tunnel shape where the actual stress intensity is K_{arr}. Since no crack growth may be visible on the specimen surface, indirect methods of crack-length evaluation such as elastic compliance measurement constitute the only available means of determining whether crack growth has occurred, short of destroying the specimen. Unfortunately, there is at present no widely accepted way of reformulating the calibration factor (K/P) to provide an evaluation of

K at the tip of a tunnel-shaped crack. The basic tools needed for evaluating K_{arr} from the results of such tests are thus unavailable.

A way of eliminating the crack tunneling tendency is specimen sidegrooving. In H_2S tests of 1T WOL specimens of HY-130 plate[1-1], ungrooved specimens consistently yielded tunnel-shaped crack fronts that defied quantitative interpretation. The addition of 0.05"-deep V-shaped sidegrooves eliminated the tunneling tendency and provided straight crack fronts at arrest, from which K_{arr} was unambiguously evaluated. Tunneling persisted in identically grooved specimens of HY-80 steel plate, however. A worthwhile experiment with such material might be to use even deeper sidegrooves in an attempt to obtain a straight crack front at arrest. Unfortunately, the calibration becomes less certain as the sidegroove depth is increased, and a preferred alternative might be to test thicker specimens. At present, the calibration uncertainties of interpreting the tunnel-shaped arrest crack fronts probably outweigh those of correcting for deeper sidegrooves, but in any case much of the uncertainty from either source should be eliminated by testing larger specimens.

It is evident that the realities of dealing with tunnel-shaped crack fronts at arrest introduce effective validity restrictions more stringent than those specified in Ref. 1-4 (ASTM E399). The fracture-toughness test procedure prescribed therein is concerned only with the plane-strain conditions prevailing at crack-growth onset, whereas the determination of K_{arr} usually requires interpretation of the test results under the conditions of crack arrest. Most of the environmental tests performed in the present work as well as the HY plate materials (1-1) were valid according to Ref. 1-4 as far as it applies to environmental scc testing. In cases like the H_2S rising-load test where only K_{or} is measured, the plane-strain validity limits of Ref. 1-4 are straightforward. Since K_{arr} is a more design-significant quantity than K_{or}, however, the validity specifications should now be extended to include the measurement of stress intensity at crack arrest. The proper interpetation and/or elimination of tunnel-shaped arrest crack fronts is a proper subject in this area that has not received adequate attention. Such attention as could be given in

our program for NSRDC[1-1] as well as in the present work is reviewed in Part 5 of the present report.

1.1.3. Summary

The relatively simple conditions of crack-growth-onset testing for determining K_{Ic} prescribed in ASTM E399[1-4] provide only minimum guidelines for environmental crack-growth testing. In those cases where a rising-load method is used, $\dot{K}$ must be many orders of magnitude lower than that specified in ASTM E399, and even then there is no assurance that it is low enough to deliver a design-useful value of the crack-onset stress intensity K_{or}. Preferred methods of environmental scc testing are those capable of yielding values of K_{arr}, the crack-arrest or threshold value of the stress intensity, since this should have greater significance in the design of actual structures exposed to particular environments. The valid measurement of K_{arr} is plagued with problems not anticipated in ASTM E399 such as the formation of tunnel-shaped crack fronts for which no widely-accepted K calibration is currently available. Although the use of deep sidegrooves can eliminate the tunneling, calibration data for such specimens are not currently available. The use of larger specimens is probably necessary, but this in turn implies that the plane-strain validity limits on specimen dimensions in ASTM E399 are not sufficiently stringent for tests measuring K_{arr}.

The use of H_2S as an environment of exceptional severity was proposed by earlier workers[1-2,1-3] as a way of simulating seawater and other, milder hydrogenous environments in tests of relatively short duration. Such short-term tests are always desirable if their results can be positively related to those of slower-acting environments of practical interest such as seawater, and for certain alloy steels it appeared that such correlations might exist. For example, it has been suggested (1-3) that the K_{or} results of rising-load tests in H_2S essentially agree with the much longer-term K_{arr} results of bolt-load tests in seawater. It is now realized, however, that such correlations do <u>not</u> exist for most materials and therefore cannot be arbitrarily assumed to exist

for any material.[1-1] This lack of a firm correlation has necessarily raised questions concerning the applicability of the results of tests performed in H_2S to material performance in other environments.

While it is true that the results of H_2S crack-growth tests cannot necessarily be used to predict the performance of a given material in any other environment, the use of H_2S as a test medium is scientifically valuable if for no other reason than the fact that its kinetics of both crack initiation and growth are so extraordinarily rapid. H_2S is therefore an ideal medium for accelerated studies of the fundamental crack-growth processes that occur in all hydrogenous media. For example, Novak has shown by careful measurements[1-7] that crack growth in seawater becomes so slow as K_{arr} is approached that the actual arrest condition of zero crack-growth rate is unachievable within any reasonable period of time. In H_2S, on the other hand, crack growth is so rapid that arrest occurs after a relatively short period (of a few weeks at most) and can therefore be studied in experiments of practical duration. The same is true of incubation time, discontinuous crack growth, and so on. The highly favorable kinetics of all aspects of H_2S testing permit all fundamental facets of the environmental degradation process to be studied in experiments of convenient duration.

In the present work it became evident that insufficient fundamental attention had been given to many aspects of environmental hydrogen-assisted crack growth processes. Such attention was seen as necessary for not only the experiments planned for the present program but also for the supposedly routine environmental crack-growth tests performed for NSRDC[1-1]. Examples include the significance of K_{or} relative to K_{arr} when these quantities differ widely, or the interpretation of ever-deepening tunnel-crack growth in fully instrumented H_2S rising-load tests of 1T WOL specimens of HY-130 steel plate. The resolution of such questions was essential to satisfying the present program's objective of qualifying the H_2S rising-load test as a (simulated) way of evaluating the seawater cracking resistance of both actual and simulated HY-130 weld metals. The detailed analysis of this test formed a major part of the present work and is accordingly emphasized in the present report.

2. EXPERIMENTAL PREPARATION AND CONVENTIONAL TESTING OF SIMULATED WELD METALS

Induction-levitation melting[2-1] is a method of melting small (up to 75-gram) metal charges in inert atmospheres without physical contact with a container. The induction coil and its power supply lift the charge and hold it suspended before, during and after melting, the latter often accompanied by substantial superheat. Final pouring (by controlled power reduction) into a copper mold provides rapid chill casting. The operation has the advantages of obviating contamination by crucible materials and of being rapid, with only about one minute being needed for heating, melting, superheating and casting each charge. Up to six 65-gram castings were routinely made in each run.

A sketch of the levitation-melting furnace is reproduced in Fig. 2-1, and a drawing for the Charpy-casting molds is shown in Fig. 2-2. These molds replaced those depicted in Fig. 2-1.

2.1 Early Work on HY Steel Castings

Early levitation melting and casting experiments were performed by Dr. F. C. Hull for a Navy (BuShips) contract with Westinghouse for development of HY-150 steel[2-2]. The levitation experiments were intended to aid the development of alloys for large high-strength steel castings. Charpy-size castings of numerous compositions were prepared and evaluated by hardness measurements and impact tests. Prior to testing, all Charpy blanks were heat treated to refine the cast structure and to bring the Rockwell C hardness into the range of 35-38, corresponding to a yield strength of 150 ksi.

The impact results at room temperature were often below the 50 ft-lbs required of HY-150 weld metal. The low impact strength was associated in many cases with intergranular failure. This was correlated

with (a) the coarse grain size and (b) the presence of thin manganese-sulfide films on the grain boundaries.

Substantial improvement of the impact properties was gained from minor (0.05%) additions of rare earths. The latter apparently destroy the grain-boundary sulfide films.

2.1.1. Optimum Casting Composition

Numerous tests of the levitation-melted Charpy castings indicated that the composition best satisfying the mechanical property requirements of HY-150 was that of Heat 7593: 0.19% C, 0.55% Mn, 0.072% Si, 4.60% Ni, 0.91% Cr, 0.59% Mo, 0.008% V, 0.87% W, 0.003% Zr, 0.062% Ce, 0.09% La, 0.002% Cu, 0.0008% P (max), 0.007% S (max), and balance Fe. Following the levitation experiments, this and similar compositions were prepared by melting high-purity ingredients and casting 25-lb ingots. To control intergranular fracture in the impact test, 0.05% Zr was added as a deoxidizer and the Ce + La was added just prior to pouring. The Heat 7593 ingot was tempered at 1050°F to a Rockwell C hardness of 38. The tensile test results included a yield strength of 155 ksi, ultimate strength of 171 ksi, 20% elongation and 64% R. A. The Charpy V-notch impact results were 56 ft-lbs at 0°F and 38 ft-lbs at -60°F. Essentially the same impact results had been obtained in the prototype levitation-melted castings heat-treated to the same hardness. The work demonstrated that low-alloy steel castings of high quality could be made from suitable (high-purity) ingredients, and, very importantly, that the extensive alloy composition screening effort required in such a development could be efficiently performed by levitation melting and casting experimental Charpy-size specimens for impact tests.

2.1.2. Correlation of R_C Hardness and Strength

The earlier Navy-sponsored work also included coordinated Rockwell hardness measurements and tensile tests of numerous specimens of experimental HY-150 (and related) wrought base metals. A correlation of these data is presented in Table 2-1 and Figure 2-3.
Table 2-1 also includes the correlation of hardness with

tensile strength given in the ASTM Metals Handbook[2-3]. The respective relationships agree exactly at 121 and 201 ksi but differ elsewhere. Since the present data are the results of averaging numerous measurements on HY steels, they are preferred for use in the present work.

2.1.3. Comparison of Castings and Weld Metals

The earlier work on development of HY-150 casting compositions served as the basis of the specimen preparation technique for the present program. The main difference between the two programs is that the composition screening criterion of the earlier program was the Charpy V-notch impact strength while that of the present program is the environmental hydrogen-enhanced cracking susceptibility as gauged by the H_2S rising-load test. Other differences are: (a) The present castings are intended to represent HY steel weld metal; (b) The target yield strength is below 150 ksi; and (c) No heat treatment was necessarily to be applied to the present castings in preparation for the tests.

The earlier work demonstrated that levitation-melted Charpy-size castings could be used to represent the compositions and impact properties of larger castings. A major objective of the present effort is to determine whether such castings can also be used to represent HY steel weld metals in the as-deposited condition.

2.2 Preliminary Composition Scan and Impact Tests: Series 0.

An early group of 9 Charpy-size castings (Series 0) was prepared with the nominal compositions listed in Table 2-2. The alloy selection basis was threefold. Castings 0-1 through 0-4 were made to the HY-150 weld-metal compositions suggested by Westinghouse at the conclusion of Contract NObs-78823[2-2]. Castings 0-5 and 0-6 were based on compositions of the HY-150 castings developed in the same program, as just discussed. Castings 0-7, 0-8 and 0-9 were duplicates of the identified compositions of actual filler-wire heats complying with Navy specifications for currently used HY-130 weld metals. All of the nominal

compositions listed in Table 2-2 are metal-powder mixing proportions with suitable allowances for carbon losses during melting; from experience, the discrepancies between these and actually analyzed compositions are not large.

The average Rockwell C hardness of each as-cast specimen is listed in Table 2-2 along with the corresponding ultimate tensile strength as obtained from Table 2-1. In all cases the hardness-derived tensile strengths are above 150 ksi.

The macro- and microstructures of the castings were comparable with those of actual HY steel weld metals. A typical macrostructure is shown in Figure 2-4, which indicates that the columnar grain pattern is similar to that often seen in low-alloy steel weld metals.

The castings of Group 0 had a thickness of approximately 0.41 inch, as contrasted with the 0.394" thickness of a Charpy specimen. The castings were fashioned into impact specimens by filing notches in the specimen sides and were then impact tested to yield the listed results. The latter cover a wide range that may be correlated with the composition variation. The highest impact results (90 ft-lbs) were those of Nos. 0-1, 0-3 and 0-7. Of these only the composition of No. 0-7 (McKay SMA) represents that of a contemporary HY-130 weld metal. Accordingly, only this formula was used as the standard Charpy casting composition in the subsequent work.

2.3 Final Technique of Charpy Casting Preparation

The two forms of charges used for levitation melting were solid (cast or wrought) and compacted metal-powder charges. The solid charges (for Series P, L and R) were machined as either cubes or equiaxed cylinders with rounded corners. The compacts (for Series A) were pressed from high-purity flake, granular and powdered metals. In the preparation of each compact, high-purity electrolytic iron was first pressed in a 3/4"-diameter die to form a 1"-high compact. An axial hole was drilled into one end of the compact to serve as a well for the alloy additions. Each of the latter was separately weighed and placed in the well. Additional iron flake material was then pressed into the hole and over the top of

the compact for retention of the contained powders in the subsequent melting. The weights of all components were carefully controlled to reproduce the McKay SMA weld-metal composition of 0.10% C, 0.9% Mn, 0.3% Si, 3.4% Ni, 0.45% Cr, 0.75% Mo, and balance Fe.

All castings were x-rayed for detection of internal flaws, and those found to be defective were rejected. The radiographs of some early castings made from mixed metal powders exhibited a few high-density spots eventually identified as images of unmelted Mo particles. Changing (at A-17) from coarse particles to finely powdered Mo eliminated these x-ray indications. However, a remaining question of composition uniformity led to the trial double melting of a few castings. The special copper mold for the first melt provided a 3/4"-diameter cylindrical casting, which was later levitation remelted and cast in a Charpy mold. The double-melted castings are identified by the suffix "R" after the casting identification numbers.

2.4 Conventional Mechanical Tests of Charpy Castings

2.4.1. Hardness Tests

Each casting was subjected to a Rockwell C hardness scan in 6 to 10 locations and the readings were averaged. Satisfactory uniformity was indicated by these data, a typical standard deviation (SD) being 1.0 R_c. The average hardnesses of all castings tested are listed in Tables 2-2, 2-3 and 2-4.

2.4.2. Mechanical Characterization of Series A Charpy Castings

The castings made from mixed metal powders to the McKay SMA HY-130 weld-metal formula (Series A) were divided into three groups for (a) tensile tests, (b) conventional Charpy V-notch impact tests at room temperature, and (c) environmental cracking tests by the H_2S rising load method. Results of the tests of (c) are reported in Part 3. The tensile specimens had a gauge diameter of 0.252" and length of 1.00". Conventional Charpy specimens (with 0.010" root-radius notch) were machined for the impact tests. The results of the tensile and impact tests are listed in Table 2-5.

Rockwell C hardness traverses of four as-machined Charpy specimens of Series A yielded the (average) results listed in Table 2-4. The hardness variability of the average readings for the four specimens was significantly larger (with SD $\sim$2 R_c) than that of the individual readings of each specimen (SD $\sim$1.0 R_c or less). The average hardness of 33 correlates satisfactorily with the tensile strength of 156 ksi but not with the average yield strength of 116 ksi (Tables 2-1, 2-5).

Hardness measurements of all other castings were performed on the as-cast surfaces rather than after machining. The results were somewhat higher but less variable, the overall average hardness of acceptable castings numbered A-11 through A-20 being 34.6 with SD of 0.8 R_c. Comparison with the machined-casting hardness indicates that the castings' surfaces were harder than the interior. The higher surface chill rate would explain this difference.

2.5 Uniformity and Reproducibility of Castings

The plan of screening candidate weld-metal compositions on the basis of possibly small differences of any given property is viable only if the differences being measured are large relative to the variability of the property in nominally identical specimens. In the case of the castings of Series A, the variability of any given property can originate from variations of either the charge preparation or the melting practice. The former might include weighing errors in the preparation of the compacts, while the latter might include variations of superheat time and temperature as well as of possible contamination during melting. These two potential sources of specimen variability were evaluated independently, as next described.

2.5.1. Influence of Melting Practice

Specimen variability associated solely with the melting practice was studied by making replicate castings from nominally identical wrought-steel charges. The charge sources were four steel plates, of which one was of 1018 steel and the others were of HY-130. Chemical

analyses of the latter are presented in Table 2-6. Plate FKS was studied in the program for NSRDC[1-1]. The plates identified as "L" and "R" were the left and right-hand base-metal plates for Weld D, which was supplied by NSRDC for evaluation in the present program. The largest number of such castings was that of Series R, as derived from Plate R.

The castings derived from the 1018 steel had the largest number of defects, including external and internal cracks, shrinkage pipes and gas porosity, and all were discarded. The castings derived from the HY-130 steel plate charges had fewer defects but did exhibit an incidence of transverse surface cracks higher than that in the castings derived from the mixed-metal-powder compacts.

The results of the R_c hardness traverses of the castings derived from HY-130 plates L and R are summarized in Table 2-3. The standard deviation (SD) of the 6 to 10 readings of an individual casting was usually between 1 and 2 R_c. The average hardness readings of the four L castings had an overall average of 35.3 with SD of 1.4. For the ten castings derived from plate R, the respective results were 35.7 and 0.7.

It is concluded that (a) at least six hardness readings should be taken on each casting to establish the average hardness, (b) the variability of individual hardness readings is characterized by a standard deviation between 1 and 2 R_c, and (c) the specimen-to-specimen variability of the average hardness readings is characterized by a standard deviation of about 1.0 R_c. Since the latter is no greater than that of the individual readings of a given casting, the casting-to-casting variability (of average R_c readings) probably cannot be reduced unless the hardness readings of each can be made more uniform.

The levitation-melting practice included an adequate period of superheat during which the melt was vigorously stirred. Significant chemical nonuniformity of the castings therefore seems unlikely. A more probable explanation of the nonuniformity of the individual hardness readings is the surface chilling effect. This could be relieved by heat treatment, which would also be beneficial in eliminating through-thickness

variations of both hardness and residual stress. Such heat treatment was omitted in order that the as-cast specimens would simulate as-deposited weld metal with its hardness nonuniformities and residual stresses. In comparisons of the as-cast specimens, therefore, no specimen-to-specimen variability can be attributed to variations of the levitation-melting and chill-casting steps.

2.5.2. Influence of Compact Preparation

The additional variability associated with errors of preparation of the compacted metal-powder charges can be studied by comparing the hardness variations of the castings derived from such charges with those derived from the wrought charges just described. The presumption is that the wrought charges were identical whereas the mixed-metal-powder compacts may not have been. Of all of the castings made from metal powder compacts, one (No. A-14) was rejected because of subnormal hardness: the average of six individual readings was 27.1 with SD of 1.1 R_c. In this case, at least, a major error in charge preparation is evident. Of seven other such castings, the overall average hardness was 34.6 (Table 2-4). The SD of individual readings of a given casting (taken on the as-cast surface) was typically 1.0, and that of the overall average was 0.8 R_c. Except for A-14, therefore, the castings derived from the mixed-metal-powder compacts exhibited no greater hardness variability than did those made from the wrought-metal charges, and therefore no errors of charge preparation were detectable.

It is noteworthy that the variability of individual hardness readings was less, on the average, in the castings made from the powder compacts than in those made from the wrought metal charges. This confirms the conclusion that the variability of the individual hardness readings is not due to chemical nonuniformity but is probably associated instead with minor variations of thermal history of the surface regions of the chill castings.

An unexpected result was the hardness increase that accompanied levitation remelting. Five double-melted castings had an overall average hardness of 36.2 (Table 2-4). For the individual readings of a given such specimen the standard deviation was typically 1.0, and for the overall average it was 1.6 R_c. An explanation for the hardness increase is contamination.

The double-melted specimen with the highest average hardness (of 37.9) was A-27R. X-radiography showed this specimen to be grossly defective with respect to both gas porosity and internal longitudinal cracks. Although no other casting had such defects, contamination from unknown sources during levitation melting and/or remelting is suspected.

2.5.3. Reproducibility of Tensile and Impact Properties

The results of six tensile tests and four Charpy V-notch tests of castings of Series A (made by levitation melting of mixed-metal-powder compacts to the McKay SMA weld-metal formula) are listed in Table 2-5. The castings were nominally identical except that two (viz. A-23R and A-21R) were double melted. The largest variability was that of the four room-temperature Charpy V-notch impact results, which averaged 60 ft-lbs with a standard deviation (SD) of 9 ft-lbs. Of the six room-temperature tensile tests, the average elongation was 14.8% with SD of 0.8% el., and the average reduction of area was 57% with SD of 4% R.A.

The smallest variability was that of the yield and tensile strengths, for which the respective standard deviations were each 4% of the average results of 116 and 159 ksi, respectively. The corresponding SD of the hardness (from Table 2-1) would be 1.4 R_c, which is consistent with the specimen-to-specimen variability of the average hardness readings.

The standard deviation quantifies the breadth of the data range containing 2/3 of the points. If three additional, nominally identical tensile specimens of the present series were to be made and tested, two

would be expected to have ultimate tensile strengths falling within ±6 ksi of the average of 159 ksi, and one would be expected to fall outside this range.

Let us assume that a single casting of a <u>different</u> composition is made and tested for determining the effect of the composition change on the tensile strength. If the result falls between 153 and 165 ksi, the effect of the composition variation is undetectable. To demonstrate a significant such effect, one must make and test at least two duplicate specimens of the new composition and show that both have tensile strengths either below 153 ksi or above 165 ksi.

In this example, the tensile strength has been used for illustration because its variability is lower than that of the other properties measured. In terms of the latter (e.g. impact strength or K_{or}) the effects of composition variations are more difficult to prove because of the greater variability (scatter) of the measurements. The quantification of variability, therefore, is a prerequisite to laboratory screening evaluations in which the normal scatter of the data may be appreciable.

3. H_2S RISING-LOAD TESTS OF CHARPY-SIZE CASTINGS

3.1. Description of Test

The environmental crack-growth tests of this program were performed in hydrogen sulfide (H_2S) at a pressure of 65 to 75 psia. All tests of Charpy-size specimens were performed by the rising-load method in displacement control. The specimens were machined from the castings to standard Charpy dimensions except that the machined notch root radius was 0.002" (instead of 0.010") to facilitate fatigue precracking. The latter was performed in air to a net side-measured crack length, a_{ledge}, of 0.030". This crack length plus the 0.080" notch depth provided a total side-measured precrack length, a_{edge}, of 0.110" or a normalized precrack length, a_{edge}/W, of 0.28. The final maximum fatigue precracking load, P_{max}, was 600-700 lb, for which the corresponding stress intensity, K_{max}, was about 15 ksi $in^{1/2}$.

The tests were performed in accordance with ASTM E399[1-4] with the following exceptions:

1) The specimen environment was H_2S at 65 to 75 psia;
2) The loading rate corresponded to a rate of increase of stress intensity, K, of 5 to 15 ksi $in^{1/2}$/h.

All tests were performed in displacement control such that $\dot{v}$, the rate of increase of the measured deflection, v, was constant. Three-point loading was performed with a span, S, of 1.6". The loading was performed by a servohydraulic machine with continuous feedback control based upon output from an LVDT sensing the location of an unloaded extension of the loading yoke. Autographic records of both load (P) and displacement (v) were made on both an x-y recorder (as P vs v) and a strip-chart recorder (as P and v vs time).

In those tests where the onset of crack growth occurred within the linear-elastic range, the load, P_{or}, of such crack-growth onset was taken as either the point of 5%-secant offset (as instructed in Ref. 1-4) or as the point of maximum load, whichever seemed more appropriate. From this P_{or} the stress intensity for crack-growth onset, K_{or}, was calculated from the tabulated calibration factor, K/P (Table 3-1), for the weighted-average length of the air-fatigue precrack. The latter was determined after the test from a formula described in Sec. 5.5 (p. 5-17).

Crack growth in H_2S was usually allowed to continue for an arbitrary period after onset. In some tests the slow displacement increase was continued until substantial extension of the crack was indicated by a significantly higher compliance, and the test was terminated. In other cases the displacement rate was switched to zero soon after crack-growth onset. The resulting condition of nominally constant displacement did not lead to crack arrest, however, because of the finite elasticity of the displacement-measurement system, as discussed in Ref. 1-1. A consequence of the latter was to cause K to increase with crack length over most of the latter's range. This behavior is evident from the column headed "Effective K/v_t" in Table 3-1. Since v_t was constant, the consequent increase of K with crack length made it impossible for the crack to arrest.

3.2 Limit of Plane-Strain Validity in Precracked Charpy Specimen

The limiting specimen dimension, x, for plane-strain validity is specified in ASTM E399 (Ref. 1-4) as:

$$x \geq 2.5 \, (K_{Ic}/\sigma_y)^2 \qquad (3\text{-}1)$$

in which x is either the crack length, a, or the specimen thickness, B, whichever is less. Surprisingly, no mention is made of the relation of the validity limit to the ligament length, W - a. The specimens described in ASTM E399 have W/B ratios of 2 or greater, and an implciation is that W - a should approximate B. If W - a is much smaller than B or

a, it would determine the validity limit in a way that might be indicated by substituion of W - a for x in Equation 3-1 or some similar expression. This subject is relevant in testing Charpy specimens, where W = B = 1 cm and therefore B cannot be the validity-controlling dimension.

The precracked specimens in the present study had a total crack length (a) of at least 0.11". This would be the validity-controlling dimension x in a strict interpretation of Equation 3-1. If x is taken instead as W - a, which was as large as 0.28", a considerably higher limit of load and stress intensity could be accepted as valid.

A discussion of the validity of fracture toughness tests of precracked Charpy specimens is included in Reference 3-1, page 137 of which states: "If the material is sufficiently brittle, K_{Ic} can be obtained directly from the fracture load in a test of a precracked C_V specimen. For strict adherence to ASTM E399 requirements, the following measurement capacities apply for a typical a/W of 0.25 (a = 0.1 in.) and the dimensions of a Charpy specimen:

$$K_{Ic}/\sigma_y \leq 0.4 \sqrt{\text{in.}} \text{ to meet thickness requirement}$$

$$\leq 0.2 \sqrt{\text{in.}} \text{ to meet crack length requirement}$$

Even if the crack length requirement is neglected, the measurement capacity is limited to a fairly low value.

"A considerably more liberal requirement would be that fracture must occur before general yield.... For an a/W of 0.25.... the measurement capacity would become:

$$K_{Ic}/\sigma_y \leq 0.56 \sqrt{\text{in.}}$$

Note that this interpretation ignores any crack length requirement. Based on this approach plus the results of transverse contraction measurement that indicate that the central 90 percent of the Charpy specimen thickness is in plane strain up to $K_I/\sigma_y = 0.5 \sqrt{\text{in.}}$, researchers have estimated K_{Ic} from the load provided that:

$$K_{Ic}/\sigma_y \leq 0.5 \sqrt{\text{in.}}$$

At this limit, the thickness, B, of the Charpy specimen (0.394 in.) corresponds to $B = 1.6 (K_{Ic}/\sigma_y)^2$ whereas ASTM E399 requires $B \geq 2.5 (K_{Ic}/\sigma_y)^2$.

"If the fracture conditions exceed the above limit, then other methods based on elasto-plastic fracture mechanics (e.g. J-integral) must be used to derive fracture toughness quantities from precracked C_V test records."

The load for "general yielding" is defined on page 126 of Ref. 3-1 for an uncracked Charpy specimen as $0.03 \sigma_y$, for the load in lbs and σ_y, the yield strength, in psi. This "general yielding" load is equivalent to the "fully plastic" load P_{fp} given by the formula:

$$P_{fp} = 0.31 \sigma_y (W - a)^2$$

The proportionality of P_{fp} to the square of (W - a) indicates the extreme sensitivity of the limiting load to the ligament size.

At longer crack lengths where a/W > 0.60, the formula for the stress intensity is

$$K = \frac{SP}{B(W - a)^{3/2}}$$

in which S is the span (= 1.6" usually). Combining this with the expression for P_{fp} yields

$$K_{Ic}/\sigma_y \leq 1.24 \sqrt{W - a}, \text{ or } \quad W - a \geq 0.65 \left(\frac{K_{Ic}}{\sigma_y}\right)^2$$

This allowance is far more liberal than that formulated by equating W - a to x in Equation 3-1. The limiting ligament size formulated in this way is only about 1/4 of that obtained from the latter; viewed in another way,

the limiting stress intensity for a given ligament size is nearly double that computed from the ASTM formula with (W - a) replacing x. The corresponding load, P_{fp}, is also well above that of plasticity-caused deviation of the load-displacement record from linearity. In tests of precracked, uniform Charpy specimens of HY-130 steel in which there was no crack growth at loads below P_{fp}, the latter corresponded to a secant offset of about 40%.

The possibility of errors of K must also be considered. The crack-tip blunting that accompanies local yielding decreases the actual value of K below that for the infinitely acute crack tip for which the calibration function K/P was formulated. Hence the actual stress intensity is systematically below that calculated from the combination of load and crack-length values alone. On the other hand, J-integral calculations and conversion to stress intensities yield erroneously high values of K due to inclusion of major plastic strain energy in the calculated J.

The description of the limiting load as that for "general yielding" or "fully plastic" suggests that the size of the plastic zone adjacent to the crack tip approximates (W - a) at such a load. Since the same limiting load applies in J analysis, we must question the above recommendation that "If the fracture conditions exceed the above limit, then other methods based on elasto-plastic fracture mechanics (e.g. J-integral) must be used...." Since the J analysis route is also suspected of overestimating K, such that the systematic error increases with the degree of plasticity, it is suggested that K be estimated instead by the more conventional method of combining the tabulated calibration factor (K/P) with the load up to P_{fp}. It must be emphasized that this load range is highly liberalized with respect to the ASTM-prescribed limit of Eq. (3-1) and that this admits the possibility of a large error of K. The error may be tolerable, however, if the alternative is scrapping the experimental measurements.

In the treatment of precracked Charpy specimen tests in the present report, the highly liberalized "fully plastic" criterion of validity is applied only in special cases such as QS 2-3, as described

in Section 4.3.2. The routinely applied validity criterion is the more conservative limit obtained by substituting the ligament size (W - a) for x in Equation 3-1. The latter also coincides approximately with the point of plasticity-caused deviation of the load-displacement curve from linearity.

3.3 Results of Rising-load Tests

The principal conditions and results of the H_2S rising-load tests of precracked Charpy castings are presented in Table 3-2. The usual ligament length was 0.28" and the average yield strength, σ_y, of the castings of Series A was 116 ksi (Table 2-5); hence the maximum stress intensity measurable in a valid plane-strain test was 39 ksi $in^{1/2}$ according to the "conservative" criterion just described. All of the K_{or} results in Table 3-2 were below this limit and therefore satisfy the corresponding specimen dimensional requirements for plane-strain validity.

Of the five tested castings of Series A (i.e. those made from mixed-metal-powder compacts), the average K_{or} result was 28 ksi $in^{1/2}$ with a standard deviation (SD) of ±6 ksi $in^{1/2}$ (Table 3-2). The tests of of Specimens A-4 and A-6 were completed in short times due to the use of a relatively high loading rate beginning at a finite load. The other three tests employed the lower $\dot{K}$ of 5 ksi $in^{1/2}$/h beginning at zero load and therefore consumed significantly more test time (at least 5 h, and usually much longer). Despite this range of test times, there is no apparent dependence of K_{or} on $\dot{K}$, contrary to theoretical expectations of Part 10.

One of the five specimens (A-25R) had been double levitation melted and its K_{or} result (34 ksi $in^{1/2}$) is the highest of the group. The data scatter is such, however, that no significant improvement of K_{or} can be attributed to the double melting process.

Table 3-2 also lists the K_{or} results of three tests of castings derived from HY-130 steel plate (Series P and R). The average K_{or} result of 18 ksi $in^{1/2}$ is well below that of Series A, presumably because of a higher impurity content of the wrought melting stock. It may be recalled

also (Table 2-3) that the overall average hardness of this group was 1.1 R_c higher than that of Series A, from which the ultimate tensile strength would be about 164 ksi as compared with 159 ksi in Series A. The strength difference alone seems inadequate to account for the difference of the average K_{or} values, and therefore impurity effects are the preferred explanation for this difference.

The data in Table 3-1 provide a preliminary view of the ability of the present technique to distinguish alloy composition (or impurity) effects on the environmental hydrogen-assisted cracking propensities of the cast specimens. Despite the scatter, the average results of the respective specimen groups are significantly different and indicate that one group (viz. Series A) has superior environmental hydrogen cracking resistance, presumably because of its lower impurity content.

Several additional Charpy castings had been machined in preparation for H_2S testing but were abandoned after air fatigue precracking attempts failed to yield precrack growth at both specimen sides. This difficulty, which occurred in several specimens of as-deposited weld metal as well as in the castings, is probably due to variations of fatigue strength and/or residual stress across the specimen width. A common occurrence was for the precrack to originate at the ends of the machined notch and to grow toward the center as quarter ellipses. In Specimen R-6 the precrack halves did not meet (Figure 3-7) and the effective average precrack length was assigned arbitrarily. The autographic P-v plot of the H_2S test of this specimen passed through an exeptionally sharp load maximum that may have been due to the peculiar narrowness of the effective precrack front and to the relative ease of the ensuing environmental crack growth. Although P_{or} was defined unambiguously, the same cannot be said of K_{or}, the estimation of which was rendered unsatisfactory by the peculiar shape of the precrack front. Difficulties of this kind occurred more frequently in the H_2S tests of castings and weld metals than in those of wrought specimens, thereby helping to explain the greater variability of the casting and weld-metal test results.

3.4 Fractography

Fracture macrographs of all of the H_2S-tested specimens except A-6 are presented in Figs. 3-1 through 3-7. The distinctive columnar grain patterns of the castings are evident, as are the precrack fronts and some of the H_2S crack fronts.

Scanning-electron-microscope (SEM) studies of the H_2S fracture surfaces were performed on Specimens P-C and A-4. Typical stereo SEM photographs are presented in Figures 3-8 and 3-9. Specimen P-C, which was prepared by levitation remelting HY-130 plate FKS, had exclusively intergranular fracture in H_2S, as seen in Figure 3-8. Specimen A-4, which was made by levitation remelting a high-purity mixed-metal powder compact, exhibited a mixture of intergranular and cleavage fracture in H_2S, as illustrated by Fig. 3-9. All of the as-cast specimens had a coarse columnar grain structure with a high likelihood of intergranular fracture in the H_2S test.

4. H_2S TESTS OF HY-130 (AND RELATED) WELD-METAL CHARPY SPECIMENS

This section describes the conditions and results of H_2S rising-load (displacement-control) crack-growth tests of precracked Charpy specimens machined from three weld metals received from NSRDC (Annapolis). The weld metals are identified as follows:

Weld D: HY-130 weld metal made by conventional process (yield strength 144 ksi),

Weld F: HY-130 weld metal derived from same electrode as D but deposited as a larger number of finer beads to refine the microstructure (σ_y = 151 ksi), and

Weld Q: HY-180 weld metal with as-deposited yield strength of 185 ksi, post-weld heat treated (overaged) to yield strength of 125 ksi.

Each weld was a full-thickness double-V joint in 1.5" thick HY-130 plate (or equivalent). The usable length of Weld D was about 5-1/4" in a single piece, and that of Weld F was the same. Weld Q was supplied in three pieces each having a usable length of 2-1/8".

All Charpy specimens were oriented transverse to the welding direction. A stack of three such specimens was machined from 1/2"-square cross-section blanks cut from a 1/2"-thick slice of each weldment. The identifications of the specimens of each such set ended in -1, -2 and -3, with the specimen numbered -2 being located in the plate midplane or the weld center axis.

The H_2S tests of the precracked Charpy specimens were performed in two phases that differed with respect to the specimens' notch orientations. If the weldment orientation is taken as that of downhand

(flat) welding, the specimen notches for the first test phase had conventional vertical orientation, and those for the second test phase had horizontal notch orientation.

The third phase of H_2S testing consisted of load-cell tests of 1T WOL specimens of Welds D and F. The longitudinal orientation of these specimens in the respective welds provided an intended crack-growth path running longitudinally along the vertical center plane of the weld metal, as in the Charpy specimens of the first phase. The descriptions of the load-cell tests of Welds D and F are presented in Part 5 and will be accompanied by a discussion of similar tests of HY steel base metals for NSRDC (1-1).

4.1 H_2S Rising-load Tests of Weld D

A macroetched section of Weld D is shown in Fig. 4-1.

4.1.1. First-phase Tests

Three sharp-notch Charpy specimens were machined from a 1/2" transverse slice of Weld D with vertical notch orientation. These were precracked in air at a maximum load of 700 lbs to a net side-measured crack length, a_{ledge}, of 0.06 to 0.08". Combining the weld-metal yield strength of 144 ksi with the average precrack length of 0.07" yields a calculated plane-strain stress-intensity upper limit of 45 ksi $in^{1/2}$ if the "conservative" approach is followed of substituting the ligament length, W - a, for x in Eq. 3-1. The results of the H_2S rising-load tests of the first-phase precracked Charpy specimens of this weld are listed in Table 4-1.

Specimen D1-3 was loaded at $\dot{K}$ = 18 ksi $in^{1/2}$/h to a calculated stress intensity of 50 ksi $in^{1/2}$, and the test was terminated. Two minor indications of limited or arrested crack growth in the P-v record were not confirmed in fractography, and it was concluded that the susceptibility to H_2S cracking could not be quantified under the applied conditions.

Specimen D1-2 (from the center of Weld D) was precracked and tested by procedures similar to those used with D1-3. There was definite onset of crack growth at a stress intensity (K_{or}) of 37 ksi $in^{1/2}$. This was followed by several sudden load drops, which indicated rapid (stepwise) crack growth. The test was terminated an average crack length (a_1) of 0.18". As shown in Fig. 4-2, the crack front was scalloped, with one large and three small maxima in a zigzag pattern. The spacing of these features corresponded to that of the individual beads of weld metal in the central region of the weld (Fig. 4-1). The air-fatigue precrack front exhibited similar waviness but to a much smaller degree. Thus, both the precrack and H_2S crack-front locations traced microstructural features of individual weld beads. The measured K_{or} of 37 ksi $in^{1/2}$ is a rough average of the highly variable susceptibility of the different microstructural components to crack growth in H_2S.

Specimen D1-1 had a net precrack length estimated as 0.115". It was loaded from zero at $\dot{K}$ = 26 ksi $in^{1/2}$/h. At a stress intensity of 24 ksi $in^{1/2}$ there was rapid, minor crack growth amounting to about 0.007", but this immediately arrested. Loading was continued to a calculated K_{or} of 52 ksi $in^{1/2}$, where rapid, major crack growth was indicated by a load drop from 1150 to 650 lbs. The test was then terminated.

The three first-phase tests of Weld D provided an approximate profile of K_{or} through the weld thickness. Only the material at the center had a tendency to fail within the "conservative" plane-strain validity limit (i.e. $K < 45$ ksi $in^{1/2}$). The material near the weld surfaces showed distinctly higher resistance to such failure.

4.1.2. Second-phase tests

An adjoining slice of Weld D was used for making three sharp-notch Charpy specimens with horizontal notches. Two of these, including that from the weld center, were air-fatigue precracked to a net side-measured length, a_{ledge}, of 0.03 to 0.05". (The third specimen

refused to show uniform precrack growth after 4 million cycles and was not tested.) The rising-load conditions of all second-phase tests included an elastic-range loading rate, $\dot{K}$, of 5 ksi $in^{1/2}$/h beginning at zero load.

Specimen D2-2 was centered in the weld. Its weighted-average precrack length was 0.062". The initial crack-onset-caused departure of the load-displacement curve from linearity occurred at a stress intensity of 16 ksi $in^{1/2}$. The curve exhibited a sharp maximum at 18 ksi $in^{1/2}$, which is taken as K_{or}. The subsequent crack growth was steady and quite rapid, producing a steep drop of the P-v plot. In the fractograph (Fig. 4-3), the precrack front is symmetric and the final H_2S crack is straight, indicating uniformity of the material along the crack front. The K_{or} result is only one-half that in the adjacent specimen D1-2, however.

Specimen D2-1 had an anomalous, reverse-tunnel precrack with a center net length of only 0.008" (Fig. 4-4). The effective average precrack length, a_1, was taken as 0.010". The specimen was slowly loaded past the point of yielding (at K = 50 ksi $in^{1/2}$). Rapid, stepwise crack growth through most of the ligament then occurred as the load dropped rapidly from 3400 to 1050 lbs. This was followed by much slower growth of the crack with the slowly increasing displacement. The test was terminated and the specimen was opened to reveal a smooth, somewhat tunnel-shaped crack front. Unfortunately, the latter is nearly invisible in Fig. 4-4.

4.1.3. Summary of Weld D Charpy H_2S Data

The results of the second-phase (horizontal-notch) tests of Weld D were consistent with those of the first-phase (vertical-notch) tests in demonstrating that the center of the double-V weld had significantly lower resistance to environmental crack growth than the regions nearer the surfaces. This difference was magnified in the second-phase tests due to the higher sensitivity of K_{or} to the orientations of the microstructural differences within the weld. In the first-phase tests, the

0.39" wide crack front extended over several weld-metal layers and the measured K_{or} was an effective average. In the second-phase tests the crack front was parallel to the welding direction, and this entire crack front could grow rapidly through any highly environment-sensitive band of the weld metal. This may help to explain why K_{or} was only 18 ksi $in^{1/2}$ in Specimen D2-2 as compared with the (average) K_{or} of 37 ksi $in^{1/2}$ in the neighboring center-weld Specimen D1-2.

In both of the near-surface Specimens D1-1 and D2-1, major environment-enhanced crack growth occurred only after plastic yielding, and the calculated K_{or} values are relatively high. The latter are probably overestimates of the actual stress intensities because of the crack-tip blunting that accompanied the specimens' bending. Attempts to calculate K_{or} from J-energy analyses yielded even higher estimates than the invalid K_{or} values listed in Table 4-1 and were therefore abandoned. It is concluded that the actual values of K_{or} for the plastically yielded specimens D1-1 and D2-1 were above the "conservative" plane-strain validity limit of 45 to 50 but were below the calculated values of 52 to 70 ksi $in^{1/2}$. These estimated K_{or} ranges are still significantly higher than the K_{or} results of 18 and 37 ksi $in^{1/2}$ found at the weld center.

4.2 Rising-load Tests of Weld F

Weld F was prepared from the same HY-130 base plate and filler wire as Weld D. Whereas Weld D was made by the normal practice of depositing a few large beads (Fig. 4-1), Weld F was made by depositing a much larger number of much smaller beads. The weld-metal grain refinement that resulted from the many more reheat cycles is credited with the significant improvement of environmental crack-growth resistance exhibited by Weld F in seawater tests by the NRL cantilever-beam step-load method (Ref. 4-1).

The yield strength of Weld F was 151 ksi. The H_2S rising-load tests of the precracked Charpy specimens of Weld F followed the same procedures as those for Weld D. The higher yield strength of Weld F

extended the "conservative" plane-strain stress-intensity limit to about 47 ksi $in^{1/2}$.

4.2.1. First-phase tests (Vertical Notch Orientation)

Specimen F1-2 was from the weld center location. The weighted-average length (a_1) of its air-fatigue precrack was 0.085". In H_2S at 75 psia, the specimen was loaded rapidly (at $\dot{K}$ = 200 ksi $in^{1/2}$/h) to a stress intensity of 27 ksi $in^{1/2}$, after which $\dot{K}$ was set at 20 ksi $in^{1/2}$/h. Deviation of the load-displacement record from linearity occurred at about 1400 lbs (K = 47 ksi $in^{1/2}$), after which the test was continued at constant $\dot{v}$ for a long period. There was a single instance of minor, stepwise crack growth at a calculated stress intensity of 61 ksi $in^{1/2}$, but apparently this crack arrested immediately. The displacement was subsequently increased without evident crack growth until the load passed through a maximum of 2200 lbs. This was followed by a slow decay of the load (at constant $\dot{v}$) to 1930 lbs, where the test was terminated.

Post-test examination of the fractured specimen revealed that the H_2S crack had advanced beyond the precrack by 0.055" at one side of the specimen and by 0.013" at the other (Fig. 4-5). All of the H_2S crack growth had occurred after general yielding. Although the corresponding K_{or} cannot be evaluated, it was well above the plane-strain validity limit of 47 ksi $in^{1/2}$.

Specimen F1-3 had a weighted-average precrack length of 0.065". It was tested in H_2S at 65 psia under essentially the same conditions as Specimen F1-2. Within the elastic range there were three rapid load drops indicative of minor, stepwise crack growth that immediately arrested. After yielding there were at least five more such events. The load eventually passed through a maximum at 2100 lbs, and soon thereafter a major crack-growth step was signalled by a rapid load drop to 1600 lbs. The test was then terminated and the specimen was opened to reveal that extensive H_2S crack growth had occurred on one side the the specimen while none had occurred on the other side: Fig. 4-6.

This test was one of several in which major environmental crack growth occurred along only one side of the specimen. In each case the final H_2S crack front followed a diagonal, somewhat S-shaped path across the specimen section. Without exception, the extensive crack growth occurred in coarse-grained material while the other, crack-resistant side of the specimen was fine-grained. Although most of the weld metal of Weld F was fine-grained, the grain refinement process apparently did not include the outermost surface passes. The result was a layer of coarse-grained (unrefined) weld metal near each final weld-metal surface. This surface weld metal cracked much more readily in the H_2S test than did the refined material of the weld interior.

The nonuniformity of Specimen F1-3 precludes assignment of a single value of K_{or}. There was evidence of extremely minor, arrested crack growth at stress intensities as low as 27 ksi $in^{1/2}$, and the first significant (though still minor) load drop occurred at K = 38 ksi $in^{1/2}$. This range appears to represent K_{or} for only the coarse-grained, near-surface region of the weld. Continued straining enlarged the crack in only the coarse-grained region of the specimen to produce the final diagonal crack front. The precrack end at the fine-grained side of the specimen was probably blunted plastically, and there was no crack growth along that side at any time.

4.2.2. Second-phase (Horizontal-notch) Tests

The second-phase tests of Weld F followed the same procedures as those of the second-phase tests of Weld D. The Charpy specimens were machined from a slice of Weld F adjacent to that of the first-phase specimens.

Specimen F2-2 had a weighted-average precrack length (a_1) of 0.068". The constant-$\dot{v}$ test was performed in H_2S at 65 psia. Plasticity-caused deviation of the load-displacement curve from linearity occurred at 1600 lbs, where K = 49 ksi $in^{1/2}$. Loading was continued to 2430 lbs, where the test was discontinued. Post-test fractographic examination revealed that minor H_2S crack growth had occurred, the crack having

advanced symmetrically by 0.008" at the specimen sides and 0.027" at the center. From the linearity of the load-displacement record up to the point of yielding, it was concluded that the crack growth had not occurred in this range (below 49 ksi $in^{1/2}$), and that it must have occurred instead quite slowly in the plastic range between 1600 and 2430 lbs. At 5% secant offset, the calculated stress intensity was 60 ksi $in^{1/2}$, but this cannot describe K_{or} if the offset was due primarily to plastic deformation.

Specimen F2-3 was the only other horizontal-notch Charpy specimen of Weld F tested in H_2S. The conditions of precracking and testing were essentially identical to those of Specimen F2-2. The weighted-average net length, a_1, of the air-fatigue precrack was 0.074".

The test followed the same pattern as that of F2-2 except that constant-$\dot{v}$ loading was continued to 3200 lbs before the test was terminated with no evidence of crack growth visible in the load-displacement record. The specimen was then opened by impact after chilling in liquid nitrogen, and it was seen that a small branched H_2S crack had formed (Fig. 4-7). The branches had equal angles and lengths, each having advanced beyond the precrack by about 0.005" at the specimen sides and 0.011" at the center. Evidently the crack(s) had grown slowly after yielding, and the only possible K_{or} assignment is somewhere above 50 ksi $in^{1/2}$.

The overall liquid-N_2 fracture surface of F2-3 was seen to include two distinct zones: a fine-grained zone in which the precrack and short H_2S cracks had propagated, and a coarse-grained zone at the far end of the ligament (Fig. 4-7). The boundary between the zones was parallel with the machined notch root and spaced about 0.21" from it (or 0.10" from the far specimen surface). Since the coarse-grained band was at least 1/8" away from the final H_2S crack tip, it had not influenced the test.

If the specimen's situation in the weld had been rotated or shifted to place the precrack tip within the coarse-grained zone, the results of the test would probably have been quite different, with

initiation of H_2S crack growth at a relatively low stress intensity ($K_{or} \sim 20$ ksi $in^{1/2}$) and possible crack arrest at the boundary between the coarse- and fine-grained zones. The present tests thus demonstrate that K_{or} is highly sensitive to the weld-metal microstructure, confirming earlier indications of such sensitivity in the Navy's seawater crack-growth tests of these same welds (4-2). An advantage of the testing the precracked Charpy specimens is that the microstructural features of a given weld can be individually tested to provide separate evaluations of their environmental cracking responses as gauged by K_{or}.

4.3 Weld Q

Weld Q was an HY-180 steel weld that had been postweld heat treated (at 1150°F) to yield strength of 125 ksi. Its macrostructure (Fig. 4-8) shows that it was deposited by the same small-bead practice as Weld F with grain refinement prominent in the interior but not the near-surface layers. The residual stresses in the as-deposited weld metal should have been eliminated by the postweld heat treatment.

4.3.1. First-phase Tests

Three vertical-notch (first-phase) precracked Charpy specimens from a transverse slice of Weld Q were tested in H_2S by the rising-load (constant-$\dot{v}$) method. The precracking and testing of these specimens followed the same procedures as the first-phase tests of Welds D and F.

Specimen QS1-2 had a weighted-average net precrack length (a_1) of 0.154", for which the stress intensity limit ("conservative" criterion) for plane-strain validity is 32 ksi $in^{1/2}$. The constant-$\dot{v}$ test in H_2S at 65 psia was performed at an elastic-range loading rate, $\dot{K}$, of 23 ksi $in^{1/2}$/h beginning at zero load. Yielding occurred during the second hour at a load below 600 lbs, but the test was continued for 10 additional hours during which the load rose slowly and passed through a maximum of 1515 lbs. Soon thereafter, a rapid load drop from 1510 to 980 lbs signalled the only decisive crack-growth event. The calculated K_{or} is 91 ksi $in^{1/2}$ (grossly invalid!). Fractographic examination revealed that

the H_2S crack had grown in plane (probably slowly) for 0.011" at the specimen center and then formed two branches nearly 90° from the precrack plane. The test actually yielded no quantitative result except that K_{or} was well above the plane-strain limit of 32 ksi $in^{1/2}$. This is well above the K_{or} results for the center-weld specimens of Weld D (but not Weld F).

Specimen QS1-1 was one of two specimens derived from near-surface regions of the weld metal. Its weighted average net precrack length, a_1, was 0.085". The H_2S pressure for the constant-$\dot{v}$ test was 75 psia. Both the load-displacement record and the final fracture appearance were very similar to those of F1-3 (above). There was evidence of minor, arresting crack growth at stress intensities as low as 18 ksi $in^{1/2}$, while the first significant (though still minor) load drop occurred at K = 26 ksi $in^{1/2}$. The crack growth occurred along only the one (coarse-grained) side of the specimen and not the other: Fig. 4-9. The measured stress intensities therefore represent K_{or} for only the coarse-grained portions of the weld metal.

Specimen QS1-3 exhibited a pattern of one-sided crack growth in H_2S similar to that in QS1-1 and F1-3, but the specimen was much weaker. The air fatigue precrack net length (weighted-average a_1) was 0.078" and the H_2S pressure was 65 psia. Crack-growth-caused deviation of the load-displacement record from linearity was evident at a load of 670 lbs or a 5% secant-offset stress intensity of 22 ksi $in^{1/2}$, which is taken as K_{or} for the coarse-grained zone of the weld metal. Subsequent straining at constant $\dot{v}$ produced a succession of discontinuous, rapid load drops of increasing amplitude. The highest load supported by the specimen was 920 lbs, as contrasted with 1520 lbs in QS1-1 and 2090 lbs in F1-3. The discontinuous load drops indicate that the crack growth was discontinuous, probably due to the internal nucleation and growth of new cracks that became unstable and broke through the intermediate material to join the existing crack, at which point the sudden increase of the specimen's elastic compliance was registered as a rapid load drop (at constant displacement). The test was terminated at a final load of 550 lbs and

deflection of 17 mils. Opening the specimen revealed an extreme pattern of diagonal crack-front formation: Fig. 4-10. Along the coarse-grained side of the specimen the crack front was only 0.005" from the specimen's back corner, while the other end of the crack had not advanced beyond the precrack. Most of the intervening area of the section was occupied by the H_2S crack, suggesting that the refusal of the one end of the crack to grow was due to local plane-stress blunting of the crack tip.

4.3.2. Second-phase Test

Charpy Specimen QS2-3 was a horizontal-notch Charpy specimen machined from a 1/2" thick blank sampling an outer-1/3 region of the weld. The notch situation was similar to that in F2-3, namely in fine-grained weld metal and parallel to the interface between the fine-grained and coarse-grained zones, with the latter occupying the opposite part of the ligament. A precrack of normal length would remain in the fine-grained zone, as in F2-3, and not permit study of H_2S crack-growth onset in the coarse-grained portion of the weld metal. For exploration of the latter, the air-fatigue precrack in QS2-3 was extended to a side-measured length (a_{ledge}) of 0.266 inch such that the final precrack tip coincided with the boundary between the fine- and coarse-grained zones of the specimen.

The constant-$\dot{v}$ test of QS2-3 was performed in H_2S at 100 psia, using an elastic range loading rate, $\dot{K}$, of 30 ksi $in^{1/2}/h$. Crack-growth onset was signalled by deviation of the load-displacement curve from linearity at 110 lbs.

A rising-load test is liable to give totally invalid data if the plastic zone size at the tip of the crack is larger than half the length of the test ligament. An estimate of the plastic zone size is given by the expression $0.2\ (K/\sigma_y)^2$.

The maximum value of K_{or} for QS2-3 was obtained from J-analysis of the entire load-displacement curve, which includes a component in which the crack was propagating. The resulting, upper limiting estimate of K_{or}

was 45 ksi $in^{1/2}$. Thus an overestimated plastic zone size, using the above expression, is approximately 24 mils, which is half of the test ligament length. This evidence coupled with the observation that (1) the lateral expansion of the specimen was zero and that (2) the fractographic features were those of brittle fracture (mixed cleavage and intergranular fracture with no dimpled rupture) suffices to ensure that the calculated stress intensities are reasonable.

The value of K_{or} was estimated by the use of the J-analysis technique and also for comparison by the use of the correlation equation developed by Ronald et al (4-2). The former yielded a value for K_{or} approximating 31 ksi $in^{1/2}$, whereas the latter gave K_{or} approximating 26 ksi $in^{1/2}$. These are the best currently available estimates of the H_2S crack-onset stress intensity in the coarse-grained zone of the weld metal.

4.3.3. Weld Q Summary

Weld Q was produced by NSRDC as a structure with seawater cracking resistance superior to that of any HY-130 weld, as demonstrated by cantilever-beam step-load tests performed by the Naval Research Laboratory (4-1). In the present H_2S tests, however, the cracking response was highly variable. It depended primarily upon the grain size, with fine-grained (multiply reheated and refined) material exhibiting markedly higher K_{or} than coarse-grained (unrefined) material. A specimen containing both structures consistently experienced crack onset in only the coarse-grained zone. Specimens from the centers of both Welds F and Q contained no coarse-grained material and were resistant to crack growth. The H_2S tests thus confirm the Navy's seawater tests in demonstrating the superior environmental cracking resistance of the small-bead, refined weld metal of either HY-130 or HY-180 composition.

On the other hand, neither of the present weld metals was resistant to H_2S crack growth in the coarse-grained (unrefined) condition.

The difference was quite large in Weld Q, where extensive cracking at moderately low stress intensities occurred in the coarse-grained zone of a given specimen while no such cracking occurred in the fine-grained zone.

5. LOAD-CELL TESTS OF WELD METALS AND PLATES

5.1 Description of Load-cell Test

The term "load-cell test" describes a method of static-displacement testing with an instrumented, tensile-loaded bolt for applying and continuously monitoring the load applied to the precracked specimen. The specimens tested were of the 1T WOL design (Fig. 5-1). A schematic sketch of the load-cell assembly is shown in Figure 5-2, and two versions of the load-cell device (instrumented bolt) are shown in Fig. 5-3.

The assembly used for load-cell testing in H_2S differed from that depicted in Figure 5-2 in that (a) no clip gauge or other displacement-measuring device was used, and (b) the load-cell device penetrated the wall of the H_2S container and was sealed by the O-ring shown in Fig. 5-3. The penetration was accommodated mechanically by the use of a shortened clevis (Fig. 5-2) outside the container and a pair of compressively loaded support blocks inside.

In preparation for each load-cell test, the specimen, container lid, clevis, blocks, load-cell device and nut were assembled with only enough load applied to hold the pieces together during the assembly steps and the subsequent evacuation of the container. Since the O-ring-sealed load-cell device was a 1" diameter piston, in effect, the evacuation produced an 11-lb reduction of the load applied to the specimen. The vessel was then backfilled with H_2S at a pressure of 65 to 75 psia, and the specimen was loaded to the desired level (in H_2S) by turning the nut while monitoring the load-cell output reading.

The load-cell readings were monitored at least once daily during the work week. The onset of crack growth was detected as a decline of the measured load.

A common procedure was to perform the load-cell test in steps, the initial load being well below that where crack growth was expected to initiate in a one-week exposure period. If the load-cell readings indicated that no significant crack growth had occurred during the period, the load was stepped up by 15 to 30%. Step loading was continued at weekly intervals until either there was clear evidence of crack growth or the nominal load limit of plane-strain validity was reached. The load-cell setting was then left unchanged and the load was monitored for several weeks prior to test termination.

As a rough approximation, the load-cell test is a nearly constant-displacement test like the bolt-load test. However, the elastic compliance of the load-cell and clevis assembly is much higher than that of the short, compressively loaded bolt end in the bolt-load test, and therefore the load cell is more realistically viewed as a spring-loading device. A disadvantage is that the stress intensity does not necessarily decrease as the crack grows, and crack arrest may not be achievable.

An additional piston load of 39 to 47 lbs was also exerted by the H_2S pressure of 50 to 60 psig. After the crack became quite long, this piston load tended to convert the test into a constant-load (increasing K) test. Although the load-cell test is not actually a constant-displacement test, it is nevertheless useful as a longer-term alternative to the rising-load test for determining the incubation time and stress intensity, K_o, of crack-growth onset. Additional information on the growth and arrest of tunnel-shaped cracks is also available, as will be discussed.

5.2 Load-Cell Tests of Welds D and F

Specimens of the 1T WOL configuration (Fig. 5-1) were made from both Welds D and F. The intended crack plane was the vertical center plane of the weld, such that the 3.2" length of each specimen consumed most of the 5.3" length of weld metal supplied by NSRDC. The 1" thickness of each specimen was centered in the 1.5" thickness of the weld, excluding the coarse-grained surface layers.

The specimens were ordered air fatigue precracked to a net length, a_1, of 0.3". However, such a precrack formed at only one side of each specimen. Later fractographic examination (Fig. 5-4) revealed that the fatigue crack was only a small lobe at one side and had not extended through most of the specimen thickness.

5.2.1. Weld D

The 1T WOL specimen of Weld D is identified as D-5. The initially assumed precrack net length, a_1, of 0.3" was later corrected to zero (a/W = 0.30), for which the calibration factor K/P is 4.11 $in^{-3/2}$. The specimen was load-cell loaded in H_2S to 5.6 kips (K = 23 ksi $in^{1/2}$) and held for 13 days. During the first 24 hours the load declined to 5.2 kips. It then remained essentially constant for the next 12 days (Table 5-1).

The load was then increased to 6.4 kips (K = 26 ksi $in^{1/2}$). Within 10 minutes there was a failure of the load-cell device (Fig. 5-3) in the 5/8" thread near the specimen. The test was delayed for six days, during which the unloaded specimen was stored in air. Another load-cell device was installed and the H_2S exposure at 6.4 kips was resumed. Within 18 hours the load dropped to only 70 lbs, and within 4 additional hours it was zero. The specimen had broken into two pieces except for a slight, perforated hinge at the back surface. The failure (Fig. 5-4) roughly followed the center plane of the weld metal, but with coarse longitudinal corrugations tracing the interfacial contours of the individual weld beads. This confirms the earlier observation of a significant variation of the environmental cracking resistance within each bead, with the environment-enhanced crack locally following the weakest planes.

5.2.2. Weld F

Weld F was tested (as 1T WOL Specimen F-5) by the load-cell method simultaneously with Weld D. Precracking by fatigue in air was ordered to a net precrack length (a_1) of 0.3", but this occurred on only

one side of the specimen. The initial H_2S load-cell load of 5.5 kips ($K = 23$ ksi $in^{1/2}$) declined slowly during the 13-day exposure to 5.2 kips (Table 5-1), suggesting that slow crack growth was occurring during this period. The load-cell setting was then increased to 6.4 kips ($K = 26$ ksi $in^{1/2}$). Within minutes there was failure of the loading device for Specimen D-5 in the same container, as described above.

During the subsequent 6-day delay, Specimen F-5 remained loaded at 6.4 kips in air. There was no decrease of its load during this period. The H_2S environment was then restored at 75 psia. Within 18 hours the load dropped to 1.0 kip, and within four more hours it was zero. The specimen was found to have failed completely through its pin-loaded arm, there being no indication of any crack growth in the intended weld-center plane (Fig. 5-5).

The arm failure of Specimen F-5 was accompanied by numerous other brittle cracks on the specimen sides. These cracks occurred mainly in the base-plate portion of the specimen, and their main orientation was perpendicular to the welding direction. One such crack had a semi-circular form with one end intercepting the fatigue precrack at the latter's midlength. The arm failure revealed no evidence of a fatigue crack starter, eliminating the possibility that the fatigue step had produced a precrack in this part of the specimen. Although it is tempting to conclude that the base plate had been damaged by the multiple-pass welding procedure, the crack pattern suggests instead the original plate possessed abnormally low resistance to H_2S cracking. In contrast with this plate, the weld metal of Weld F apparently resisted any tendency to crack under nominally the same conditions that had led to the complete failure of the weld metal of Weld D.

5.2.3. Comment on Load-cell Test Sequence

The accidental failure of the load-cell device for Specimen D-5 resulted in a unique sequence of testing both D-5 and F-5, namely: (1) both specimens were loaded in H_2S and remained exposed for 13 days,

(2) the load was increased to 6.4 kips and immediately thereafter the specimens were exposed to air for six days, during which the loads on F-5 and D-5 were 6.4 kips and zero, respectively, (3) the specimens were returned to H_2S and D-5 was reloaded to 6.4 kips, and (4) within 18 hours both specimens failed, D-5 by crack growth through the weld-metal center plane and F-5 by perpendicular crack growth through the base plate.

A third specimen, EZH-2, was also being load-cell tested in the same container, and it also failed within the 18-hour period of H_2S exposure after final loading. EZH-2 was of 10 Ni HY-180 base plate overaged to a yield strength of 125 ksi. A description of this test is given below, as well as on pp. D-29 and D-30 of Ref. 1-1. Just prior to the load-cell accident, EZH-2 had been loaded in H_2S to 3.6 kips, for which K = 21 ksi $in^{1/2}$. It was then stored in air for six days while still loaded. Like F-5, it was re-exposed to H_2S, and failure occurred within 18 hours.

It seems unlikely that all three specimens would have failed within 18 hours after being returned to H_2S unless there were something uniquely destructive about the particular history of these tests. Polythionic acid cracking occurs in certain materials (e.g. sensitized stainless steels) during exposure to humid air following sulfidation by H_2S. However, the present tests were performed in January when the humidity was low, and no crack growth occurred during the storage in air of the two specimens that remained loaded after at least 13 days' H_2S exposure. This lack of crack growth is clearly indicated by the constant load-cell readings of both specimens during the air storage period. The early failures of all three specimens occurred during the subsequent re-exposure to H_2S. The possible influence of the intermediate air exposure step is therefore difficult to assess at this time.

5.3. Interpretation of Load-Cell Tests

The early load-cell test setup in Figure 5.2 was viewed as a low-cost alternative to a servohydraulic machine for long-term exposures of instrumented specimens. The omission of the clip gauge in the H_2S tests precluded measurement of the displacement, v, after crack-growth onset. In theory it is possible to calculate v along with the crack length and stress intensity from the load alone if the elastic compliance of the loading system is known. The present tests used two load-cell device designs and several clevis designs; unfortunately, the compliances of the various combinations of these were never determined. The test results, therefore, consisted of quantitative data for only the conditions (stress intensity, incubation time) of crack-growth onset.

Consistent results were obtained in the load-cell tests of HY steel plates described in Ref. 1-1. These are reviewed in Sec. 5.4 to indicate the usefulness of such tests in current and future evaluations of both base metals and weldments.

5.3.1. Load-Cell Test Model

The behavior of a specimen after crack-growth onset in the load-cell test depends on both the elastic compliance of the loading system and the intensity of the piston loading effect as well as on the elastic compliance and K calibration of the specimen itself. If the loading system were infinitely stiff (or had zero compliance) and if the pressure of the environment gas in the container were exactly atmospheric to nullify the piston load, the useful form of specimen calibration function would be K/v as a function of the crack length, where v is v_o of v_{LL}, the specimen displacement at the load line. K/v is computed by dividing the calibration factor K/P by the load-line elastic compliance, C_e or v/P. Since v is a constant during crack growth in this ideal (infinite-stiffness) case, the relative behavior of K during crack growth is indicated by the values of K/v_o as a function of a_1 in Table 5-2.

Unfortunately, neither the bolt-load nor the load-cell test method is a constant-displacement method, since neither loading device has infinite stiffness. The elastic compliance of the loading member in the bolt-load method is small (viz. 0.085 mils/kip), and only a minor correction is adequate to compensate for it. The elastic compliance of the load cell is much larger, with the consequence that the specimen is more realistically viewed as spring-loaded. Adding the piston effect further shifts the test out of the area of a constant-displacement test and into that of a load-control test. This is undesirable because of the increasing-K characteristic of the load-control test, as contrasted with the decreasing-K characteristic of the constant-displacement test.

The desirable, smoothly decreasing stress intensity with increasing crack length in a constant-v test is indicated by the list of K/v_o values in Table 5-2. Since a significant overload is usually necessary to initiate crack growth within a reasonable period of time, the arrest value of the crack length may be predicted from the overload K factor and the listed K/v_o values. For example, if the precrack net length is 0.3" and the overload K factor is 2.5, the arrest value of the net crack length (a_1) is 1.40" (to make K/v_o at arrest 1/2.5 of that initially). The accompanying decrease of the load is determined by combining these figures with the listed values of the specimen's load-line elastic compliance, v_o/P, or better with its reciprocal, P/v_o. This indicates that the load at crack arrest is only 1/19 that at crack-growth onset.

More specifically, let us assume that a test is performed on a 1T WOL specimen for which K_{arr}, the arrest value of the stress intensity (also symbolized K_{Iscc}), is 10 ksi $in^{1/2}$, and the initially applied stress intensity, K_o, is 25 ksi $in^{1/2}$ to provide the overload factor of 2.5. We assume that the precrack length, a_1, is 0.30", for which $v/P = 1.036$ mils/kip, $K/P = 5.307$ $in^{1/2}$, and $K/v = 5.121$ ksi $in^{1/2}$/mil. The initial load P_o is therefore 4.71 kips and the initial load-line displacement, v_o, is 4.88 mils. For a test in which v_o remains constant during crack growth, the final arrest value of the crack length is 1.40" ($a/W = 0.85$),

and the final load P_f is 247 lbs. Since the final ligament length is 0.38", the arrest condition should satisfy plane-strain validity requirements.

Let us now compare this behavior with that in a spring-loading system that itself has an elastic compliance, C_s, of 1 mil/kip. A simplified sketch of such a system is shown in Figure 5-6, in which it is assumed that the only loading element with finite compliance is the tensile-loaded bolt. The active elastic portion of the bolt has the dimensions 5/8" dia. x 9-1/8" long, with an elastic modulus of 30,000 ksi to provide the compliance, C_s, of 1.00 mil/kip. Since the yoke and pin are assumed to constitute a nondeflecting frame we see that

$$v + v_s = \text{constant} = v_{eff} (= 9.59 \text{ mils in present example})$$

in which v is the specimen displacement at the load line and v_s is the elastic deflection of the bolt. Dividing by P yields

$$C_e + C_s = v_{eff}/P \ .$$

Since C_s and v_{eff} are constant during crack growth while C_e is a monotonic function of the crack length, this formula indicates the dependence of P on the crack length:

$$P = v_{eff}/C_e + C_s) \ .$$

The calibration factor (K/P) is also a monotonic function of the crack length. Hence the relationship of the stress intensity to the crack length is indicated by

$$K = (K/P)v_{eff}/(C_e + C_s) \ .$$

Since v_{eff} is constant, the relative behavior of the stress intensity during crack growth is indicated by

$$\frac{K}{v_{eff}} = \frac{(K/P)}{C_e + C_s}$$

Thus the effect of adding the loading-system compliance C_s to that of the specimen in the denominator of the right side of this equation is to replace the specimen load-line displacement v by v_{eff} (a constant) in the calibration function K/v. It is important to note that K/v_{eff} and therefore K do not necessarily decrease as the crack grows. This is evident in Table 5-2 where the respective values of K/v_{eff} are listed for five values of the loading-system compliance C_s, viz. 0, 0.085, 1, 2, and 3 mils/kip. As C_s increases, the spring-loaded specimen test becomes less of a constant-displacement test and more of a load-control test. At the higher values of C_s, K/v_{eff} increases with a_1 over a major range of the latter before finally passing through a maximum and rapidly declining to become zero at a/W = 1. Eventual crack arrest can therefore occur, although the crack length may be too large and both the final ligament and final load too small for satisfactory estimation of K_{arr}. The spring-loaded specimen test with appreciable loading-system compliance is therefore unsatisfactory for evaluation of K_{arr} (or K_{Iscc}).

(The bolt-load specimen is a spring-loaded case where C_s is relatively small, viz. 0.085 mils/kip, as calculated for the 1/2" dia x 1/2" long bolt end that serves as the elastic loading member. The diagrammatic analysis of this case is identical to that above if we imagine the compressively loaded bolt end to be replaced by a tensile-loaded spring of equal compliance along with the nondeflecting yoke or frame. Hence the same formulae for P and K/v_{eff} apply to the bolt-load case. The main advantage of the bolt-load over the load-cell test is its extremely compact, compressive loading member that has minimal elastic compliance; hence the bolt-load test is a far better approximation of the constant-displacement test desired.)

The crack-arrest condition in the present example is indicated by a 2.5-fold reduction of K/v_{eff} in the appropriate column of Table 5.2 (for C_s = 1.0 mil/kip). By interpolation, this crack length (a_1) is 1.67 inch (a/W = 0.96). The corresponding ligament is 0.11" and the final load is only 39 lbs. These conditions are far less favorable from the standpoint of either measuring K_{arr} or satisfying plane-strain

validity requirements than are those of the ideal constant-v test considered previously.

The final step in modelling the load-cell test is to add an allowance for the piston-loading effect. The load cells used in testing 1T WOL specimens had an O-ring diameter of nominally 1" or a piston area of $(\pi/4)$ in^2. For the usual H_2S gauge pressure of 60 psi, the piston load is 47 lbs. This is 1% of the initial applied load P_o in the present example, such that the piston load has the effect of increasing P_o, K_o and v_o by 1% to 4.76 kips, 25.25 ksi in$^{1/2}$ and 4.93 mils, respectively.

As the crack grows, the load maintained by the load cell decreases rapidly while the piston load remains constant at 47 lbs and therefore becomes an increasing proportional share of the total load, P_t. At each value of a_1, then,

$$P_t = P_s + P_p$$

in which P_s is the load provided by the load cell and P_p is the piston load. The stress intensity is given by

$$K = (K/P)(P_s + P_p)$$

and the formula for K/v_{eff} becomes

$$\frac{K}{v_{eff}} = \frac{K}{P}\left[\frac{1}{C_e + C_s} + \frac{P_p}{v_{eff}}\right]$$

in which P_p/v_{eff} is a constant having the value 4.9 lbs/mil in the present example.

Values of K/v_{eff} for the present conditions are listed in Table 5-2. The condition for crack arrest is that where K/v_{eff} has decreased to 1/2.525 of its initial value (or to 1.05 in the present example). But this is unattainable with the piston load, which produces a rapid increase of K as the crack becomes very long. For the load-cell compliance of 1.0 mil/kip, the listed minimum K/v_{eff} of 1.96 indicates that crack arrest is possible only if the initial overload K factor is

less than 1.35. This is unrealistic, since a factor of about 2 was usually necessary for visible crack growth (1-1). At overload K factors exceeding 1.35, the piston effect is sufficient to produce complete parting of the specimen. This explains the complete failures of the load-cell-tested specimens that occurred in both the present study and the simultaneous work for NSRDC (1-1).

The increasing-K tendency of the load cell is further accentuated by increasing load-cell compliance, as indicated by the K/v_{eff} values for C_s values of 2 and 3 mils/kip in Table 5-2. In effect, the influence of C_s is largest at the smallest crack lengths where the specimen compliance C_e is itself relatively low. The piston load, on the other hand, has its major influence at large crack lengths where the load-cell-applied load P_s is relatively small. When both are present, the entire K/v_{eff} calibration is degraded from the favorable characteristic of the constant-v test to the extremely unfavorable one illustrated by the case of $C_s = 3$ in combination with the piston load. The latter has K/v_{eff} increasing with a_1 over almost its entire range, affording no possibility of crack arrest. Once cracking initiates, the specimen must fail catastrophically, much as in a constant-load test.

Specimen failure under conditions of rising stress intensity occurs in two steps. The first is that of relatively slow, environment-enhanced crack growth proceeding at a nearly constant rate over a large K range (Stage II crack growth). As K closely approaches K_{Ic}, there is a (possibly discontinuous) jump of the crack growth rate and the specimen fails suddenly. An example was the load-cell test of Specimen EZH-8 described on page D-29 of Ref. 1-1. The final 0.05" band of the specimen to fail was rougher than that of the remaining H_2S fracture surface, suggesting that K_{Ic} was attained at a crack length of 1.73" (a/W = 0.98) where K/P = 900. If C_s was 1.0 mil/kip, P_s would have been about 4 lbs which, added to the piston load (P_p) of 47 lbs, would yield a K_{Ic} result of 46 ksi $in^{1/2}$. (This corrects the earlier estimate of K_{Ic} in Ref. 1-1 where P_s was disregarded.)

5.4 Review of Long-term Load-cell Tests of HY Steel Plates

The program for NSRDC (1-1) included several load-cell tests of HY steel plate specimens with yield strengths from 80 to 180 ksi. Some of these tests, including that of EZH-8 described above, were short-term, single-step tests in which complete specimen failure occurred soon after initial loading. In these cases the specimens were apparently overloaded to a major degree.

The preferred load-cell test procedure employed conservative step loading at one- to two-week intervals. The initial load was preferably below that sufficient to initiate crack growth. In a later step the onset of crack growth became evident from the load decline during H_2S exposure. Such crack growth apparently did not occur during the loading activity but instead commenced after a delay of several hours or days. In certain (tunnelling) cases it also appeared to arrest after several additional days. This consistent pattern (of crack initiation and arrest) is evident in the tests next described.

5.4.1. Load-cell Test of 10 Ni Steel Specimen EZH-2.

As described in Ref. 1-1, the 10 Ni steel plate (EZH) received from NSRDC had a yield strength of 186 ksi. Several specimen blanks of this material were overaged to a yield strength of 125 ksi, and the 1T WOL (bolt-load) Specimen EZH-2 was machined from such a blank.

The specimen was air fatigue precracked to a net side-measured length, a_{ledge}, of 0.3". Later fractographic examination revealed that the precrack front had an unusual tunnel shape resembling that of a statistical normal distribution curve. The edge length measurements were 0.30" and 0.325" for an average a_{ledge} of 0.31", while the center or maximum length of the precrack was 0.53". (The "bulge" of the tunnel precrack was 0.53" - 0.31" or 0.22".) The effective average length of this precrack, a_1, was taken as 0.42" (a/W = 0.47), for which $K/P = 5.92$ and $C_e = 1.29$ mils/kip.

As described on page D-29 of Ref. 1-1 and summarized in Table 5-3, the load-cell test of EZH-2 was conducted over a period of several weeks during which the load was increased in steps (at one- to two-week intervals) to 2.5, 2.8, 3.2 and 3.6 kips. The corresponding stress intensities (as calculated for the effective crack length, a_1, of 0.42") are 14.9, 16.6, 19.0, and 21.3 ksi $in^{1/2}$. The first clear indication of crack growth occurred during the eighth day of the fourth step as the load declined from 3.58 to 2.82 kip. One day later it was 2.72 kip, which remained constant for four days. The next successive daily load-cell readings were 2.60 and 2.52 kips. The latter remained constant from the 14th to the 19th day of the step, at which time the specimen was examined and found to exhibit surface-visible crack extension of 0.12".

The fifth step of the test included reloading (in H_2S) to 3.0 kips. In seven days the load declined slowly to 2.65 kips and then remained steady for six more days, indicating crack arrest. There was no increase of the visible crack length during this period, indicating the load drop was due to tunnel crack growth. This was confirmed in final fractography, which indicated that a deeply tunnel-shaped H_2S crack had formed (bulge = 0.41").

The load was then increased to 3.6 kips. Within 10 minutes there was a catastrophic failure of the load cell for Specimen D-5 in the same H_2S container, as already described. Specimen EZH-2 remained loaded at 3.6 kips for six days in air, then was reinstalled in the H_2S chamber at 75 psia. Within 18 hours the load dropped to 1.0 kip, and within four more hours it was zero. Since the latter reading is inconsistent with the final side-measured crack length of 1.23" (a/W = 0.78), no final evaluation of K_{arr} is possible. Interpretations of the earlier arrests associated with crack tunneling are offered below.

5.4.2. Load-cell Test of HY-80 Steel Specimen FKZ-S1

As described on page D-40 of Ref. 1-1, an H_2S environment test of several months' duration was performed on a sidegrooved 1T WOL specimen of HY-80 steel plate. The daily load readings during the successive steps of this test are listed in Table 5-4. The first four steps were performed at 5, 5.6, 6.4 and 7.2 kips (K = 27, 30, 35, and 39 ksi $in^{1/2}$)* over a period of 10 weeks, and the load readings indicated no clear evidence of crack growth in any of these steps. The fifth step was initiated at 8.24 kips (K = 44 ksi $in^{1/2}$), which was held for two days. Crack-growth initiation is indicated by the load drop to 7.84 kips on the third day, and continuation of crack growth is indicated by the load decrease to 6.89 kips on the sixth day of the step. The load then remained constant, indicating crack arrest. Since no visible crack growth had occurred, it is concluded that the load decline was due to crack tunneling.

The load-cell test was then terminated, and the specimen was bolt loaded in air. Exposure of the bolt-loaded specimen to H_2S for 13 days at 10 kips produced no indication of crack growth, as confirmed by later load remeasurement at 9.9 kips. Finally, the specimen was bolt loaded to 11 kips and exposed to H_2S for the weekend, after which it was found to be extensively cracked and to be supporting a final bolt load of only 316 lbs. The combination of the arrest load and crack length corresponded to a K_{arr} result of 27 ksi $in^{1/2}$.

Returning to the fifth step of the load-cell test, we note in Table 5-2 that K/v_{eff} for a C_s of 1 mil/kip is relatively insensitive to crack length in the short crack-length range. However, P/v_{eff} decreases rapidly with increasing crack length. The load decrease in the fifth load-cell step can therefore be attributed to crack growth at the essentially constant nominal stress intensity of 44 ksi $in^{1/2}$.

---

*(Footnote). Since the specimen was sidegrooved, both its compliance and K/P calibration differ from the values listed in Table 5-2 by the factor 1.054 while K/v_o is the same.

Apparently this was tunnel crack growth exclusively. The load decline from 8.24 to 6.89 kips amounts to a 1.20-fold reduction of P/v_{eff}, which corresponds to an increase of the effective net crack length a_1 from 0.26 to 0.44". If the crack growth consisted exclusively of tunneling, the surface-measured a_{ledge} would have remained constant at 0.18" while the center or maximum value of a_1 would have increased by 0.27" to 0.57".

5.5 Crack Tunneling and Arrest in Load-Cell Tests

The formation of thumbnail or tunnel-shaped crack fronts has often been observed. Neale (1-6) has claimed that the actual stress intensity at the tip of such a crack is far lower than that computed by the usual method of combining the average crack length with the conventional calibration factor (K/P) or f(a), which applies strictly to straight crack fronts. Neale's calculations indicate that the effective calibration factor decreases drastically as the crack tunnels. Such behavior is consistent with the stable arrest of short tunnel cracks in the present tests.

Unfortunately, there is still no widely accepted formula for calculating K at the tip of a tunnel-shaped crack. This fact, in combination with the fact that C_s was unknown for the load-cell devices, precludes the estimation of K_{arr} in the load-cell tests in which the tunnel-shaped cracks grew and arrested.

Despite the current lack of calibration data, the load-cell tests exhibited consistent patterns from which significant information can be derived. There were two extreme categories of the tests: (1) those that produced early, complete specimen failure, and (2) those in which several load steps were necessary to initiate crack growth. Another way of categorizing the tests was according to whether the H_2S crack, once started, would either (3) continue to grow in a self-accelerating manner until the specimen failed completely, or (4) arrest as a tunnel-shaped crack of relatively short length.

In the tests of Category 1 the initial loads were excessive, causing early failure of the specimen in a comparatively short time. In Category 2 the loading was more conservative, such that the K overload factor necessary for the onset of crack growth was attained only in a later step.

The distinction between Categories 3 and 4 was determined by the specimen's tendency to form tunnel-shaped crack fronts. In the HY-180 1T WOL specimens, little or no tunneling occurred except in specimens overaged to the lowest yield strength. In both HY-80 and HY-130 steel, on the other hand, tunneling occurred repeatedly. The full-strength HY-180 tests belonged in Category 3 because of the absence of tunneling while those of the lower-yield-strength, high-toughness materials belonged in Category 4 because of the readiness of the specimens of these materials to form tunnel-shaped crack fronts.

Crack tunneling is an indicator of plane-strain invalidity at arrest. Tunnel-shaped cracks can form if there is a significant thickness of plane-stressed material at the specimen sides to support the applied bending load. The latter material deforms plastically rather than cracks. The plane-strain zone at the specimen interior is not so free to deform and it cracks instead, producing the tunnel-shaped crack front. Improved plane-strain validity is gained by going to either larger specimens or higher yield strength, where the plane-stress surface layer is proportionately thinner and can crack more readily to produce straighter crack fronts. The same effect is gained by machining V-shaped sidegrooves. When such changes are made in specimens for load-cell tests, however, the probability of complete specimen failure is increased; that is, the test is transferred from Category 4 to Category 3.

Although the actual compliance of the loading device was unmeasured, we shall assume for modeling purposes that it was about 1 mil/kip. At such a C_s value a short, straight crack in a 1T WOL specimen propagates at nearly constant nominal stress intensity, as indicated by the listing of K/v_{eff} in Table 5-2. Since an overload K factor approximating 2 is usually necessary to initiate crack growth

within the one- to two-week period of a given test step, this overload is largely retained as the crack grows. As the crack becomes very long, the piston load takes over and causes complete failure of the specimen. The fact that such behavior occurred repeatedly in the load-cell tests confirms that C_s was of the magnitude assumed.

Category 4 consisted of conservatively step-loaded tests of specimens that formed tunnel-shaped cracks, which arrested. Although overload K factors approximating 2 were attained in these tests also, the crack growth was confined to the internal, plane-strain regions of the specimen while there was little or no visible crack growth at the surfaces. In spite of the condition of nearly constant nominal stress intensity resulting from spring loading, the tunnel crack arrested because, according to Neale's interpretation, the actual stress intensity at the tip of the crack decreased significantly as the tunnel formed. This K probably decreased by a factor of approximately two to K_{arr}, where the tunnel crack arrested.

The specimen load decline during tunnel crack growth indicates that the response of the specimen's elastic compliance, C_e, to tunnel crack formation is straightforward. An informative quantity is P/v_{eff}, the reciprocal of $(C_e + C_s)$. During tunnel crack growth P/v_{eff} decreased by a significant factor, and therefore C_e must have increased by an even larger factor.

The specimen compliance, C_e, is a monotonically increasing function of the crack length if the crack front is straight. In dealing with C_e for tunnel cracks we assume that the same relationship exists between C_e and an effective crack length, a_{eff}, defined as the weighted-average crack length obtained by giving the center or maximum crack length, a_{max}, twice the weight of the edge length, a_{edge}. Thus a_{eff} grows 2/3 as rapidly as a_{max} during pure tunneling (while a_{edge} remains constant). The resulting, sensitive response of C_e to crack tunnel growth is indicated by the accompanying decrease of the measured load. Accordingly, the tunnel crack length can be represented by a_{eff} in treatments of the elastic compliance alone.

The same crack-length weighted averaging that yielded a_{eff} has also been used by others (e.g. Novak and Rolfe: Ref. 1-5) in treating the stress intensity calibration factor (K/P). If this were appropriate, crack tunneling would have the same effect on K as simply increasing the length of a straight-fronted crack by 2/3 as much as a_{max}. In the present model this would correspond to the actual stress intensity's remaining essentially constant at the overload factor of 2, in which event the tunnel crack would not arrest but would continue to grow, just as in a specimen where no tunneling occurs. Since tunnel crack arrest was repeatedly observed, Neale's assertion that the calibration factor K/P is drastically reduced by tunneling is in far better accord with the load-cell test results than is the alternative view of (K/P) depending simply on a_{eff}. It is concluded, therefore, that the tabulated (K/P) factor is unsuitable for tunnel-shaped cracks and further that no simple method of crack-length averaging can be used with this calibration to yield the stress intensity at the tip of a tunnel-shaped crack. (Even a_{edge}, the minimum crack length measured at the specimen sides, is not a suitable effective crack length for this purpose.) Instead, (K/P) is apparently so low that no effective crack length can be computed. This is actually true of <u>any</u> crack front with a positive bulge. This conclusion, which originated in Neale's analysis of the tunnel cracks resulting from pop-in during fracture toughness testing, is thus confirmed by the present load-cell tests. A corollary is that K_{arr} cannot be evaluated unless the arrest crack front is straight.

An effective method of obtaining straight-fronted cracks at arrest in specimens that otherwise form tunnel-shaped cracks is by adding V-shaped sidegrooves of suitable depth. In 1T WOL specimens of HY-130 plate tested by bolt loading in H_2S, conventional 0.05"-deep grooves were sufficient, but in identically prepared and tested HY-80 specimens such grooves were insufficient to prevent tunneling. Deeper sidegrooves may be suitable in the latter case. Since K/P for the deeply grooved specimens is uncertain, the use of larger specimens may be the only satisfactory way of obviating the errors due to crack tunneling.

5.6 Load-cell Test Summary

The load-cell method appeared initially to be an improved constant-displacement technique for long-term environmental testing. In use, however, the conditions of load-cell testing were such that crack arrest at long lengths was impossible, as proved by repeated instances of complete specimen failure. The latter were eventually attributed to (1) excessive elastic compliance of the (spring-like) loading system,and (2) the piston effect, which added an undesirable component of load control at large crack lengths. The load-cell test was nevertheless useful for studying the conditions of crack-growth onset. The load could be (a) applied while the specimen was exposed to the environment, (b) readjusted without otherwise disturbing the test, and (c) monitored continuously. The measured load was extremely sensitive to crack length, and therefore the onset, progress and arrest of the cracking could be readily followed.

In addition to the final failures, the studies disclosed that a consistent pattern of minor crack growth and arrest was associated with crack tunneling, where the crack grew internally without visible growth on the specimen surface. Since the tunnel growth and arrest of the crack occurred at nearly constant nominal stress intensity, the occurrence of arrest under such conditions is interpreted as confirmation of Neale's hypothesis that the actual stress intensity declines significantly during crack tunneling. The (K/P) calibration for tunnel cracks is still unknown, and it is concluded that the use of larger specimens and/or sidegrooving is essential to attain the straight arrest crack fronts necessary for accurate evaluation of K_{arr} (or K_{Iscc}). It is clear also that the load-cell technique is not suitable for this determination.

The load-cell tests of Welds D and F were troubled by (a) incomplete formation of precracks, and (b) failure of Weld F in the base-metal arm of the specimen rather than in the weld metal. In both weldments the nominal stress intensity of crack-growth onset, K_o, was between 23 and 26 ksi $in^{1/2}$. In Weld D this result applies to the onset of H_2S crack growth in the weld metal, whereas in Weld F the weld metal survived such loading intact and therefore had a higher crack-onset K_o value.

6. MEASUREMENT OF K_{arr} IN CONSTANT-DISPLACEMENT TESTS

6.1 Introduction

The disadvantages of the load-cell test leave the bolt-load test as the technique of choice for the evaluation of K_{arr} at long exposure times. The H_2S bolt-load tests of HY steel plates performed for NSRDC (1-1) were similar to those described by Novak and Rolfe (1-5) except that the environment was gaseous rather than a liquid and arrest occurred in much shorter times. A "shim" (wedge)-loading technique was also used for constant-displacement testing WOL-outline specimens machined to a two-pin (rather than bolt-load) design.

Although both the bolt and shim had finite compliance, it was sufficiently small to permit the approximation of both methods as constant-displacement techniques. As indicated in Table 5-2 for a C_s value of 0.085 mils/kip, the effective calibration factor K/v_{eff} decreases steadily with the crack length in such a test. Similarly, the stress intensity decreases during crack growth from K_o to K_{arr}. The small elastic compliance of the loading device permits crack arrest at moderate final crack lengths where K_{arr} may be measured accurately under conditions of plane-strain validity. Hence the bolt- or shim-load test has the potential of accurately delivering design-useful values of K_{arr} at minimum cost.

The program for NSRDC included bolt- and shim-load tests in H_2S of 1T WOL-outline specimens of HY steels with yield strengths from 80 to 180 ksi. Major crack growth occurred in all specimens. The final arrest values of the crack length were unexpectedly large, and the measured K_{arr} results were unexpectedly low in all materials tested. It was evident, therefore, that the H_2S environment was far more detrimental to the steels than had been expected, and that this effect was more clearly brought out by the longer-term constant-v tests than by either the load-cell or rising-load tests.

A detailed description of the H_2S bolt- and shim-load tests of HY steel plates is presented in Section D.6 of Ref. 1-1. The brief review of those tests presented below mainly emphasizes those of HY-130 steel.

6.2 Plate Rolling Orientation Effects

The effect of plate rolling direction on cracking may be visualized by comparing the plate with a wooden board. A specimen oriented with the crack plane parallel to the grain (rolling) direction (T-L orientation) should fail easily, as wood is split. A specimen oriented perpendicularly (L-T orientation) should have greater resistance to crack growth but also a tendency for the crack to turn 90° from the precrack plane to become parallel with the rolling direction. A test where the crack turns cannot be interpreted, and therefore nearly all of the HY steel plate specimens were machined in the nominal T-L orientation. The plates had been cross-rolled, however, and the rolling-direction assignments appear to have been arbitrary.

In the case of the HY-130 (FKS) plate, all but three of the 1T WOL specimens were of nominally T-L orientation, and there was a considerable amount of crack turning and branching in the H_2S tests of these specimens. In all three specimens of L-T orientation, the crack followed the intended plane. The latter was therefore the weaker orientation, in spite of the rolling-direction assignment.

6.3. Determination of K_{arr} under Optimum Conditions

The final H_2S test of a 1T WOL specimen of HY-130 plate was performed on FKS-R3, a nominally L-T (actually weaker) specimen with 0.05" deep sidegrooves. As described on page 45 of Ref. 1-1, the specimen was shim loaded to a stress intensity of 20 ksi $in^{1/2}$ and exposed to H_2S at 75 psia for 33 days. At the end of this time it exhibited no crack growth, as confirmed by remeasurement of the elastic compliance. It was then shim reloaded to a stress intensity (K_o) of

27 ksi $in^{1/2}$ and re-exposed to H_2S for 12 days, during which the crack grew to a normalized length (a/W) of 0.93 and arrested at K_{arr} = 6 ksi $in^{1/2}$. The crack grew only in the groove plane and did not branch, and the arrest crack front was straight. It was concluded, therefore, that the orientation and sidegroove depth in this one specimen constituted the optimum combination for H_2S testing the HY-130 plate.

The K_{arr} result of 6 ksi $in^{1/2}$ was lower than had been expected on the basis of earlier tests of the same plate. Those tests, however, had produced a high incidence of crack turning, branching and tunneling. The test of FKS-R3 was the only one of the HY-130 plate in which no such aberration occurred, and the unexpectedly low K_{arr} measurement was probably the least subject to error.

Even lower K_{arr} results were obtained in H_2S bolt-load tests of the 10 Ni HY-180 plate, as listed in Table 9 of Ref. 1-1. This material was tested as ungrooved 1T WOL specimens of three yield strengths, and in no case was the tunneling as severe as that in the ungrooved HY-130 specimens. H_2S bolt-load tests of the 9 Ni 4 Co version of HY-180 steel produced higher K_{arr} results varying from 10 to 15 ksi $in^{1/2}$. The ungrooved specimens of this material had acceptably straight arrest crack fronts in H_2S.

6.4. Summary

Although the values of K_{arr} measured in the H_2S constant-displacement tests were unexpectedly low, they are nevertheless regarded as accurate estimates of the threshold stress intensities for the respective material-environment combinations. The bolt-load or shim-load method is therefore viewed as the optimum technique for reliably measuring K_{arr} (or K_{Iscc}). Acceptable tests still require careful selection (usually by trial and error) of (a) the specimen orientation relative to the nominal plate rolling direction, (b) the sidegroove depth, and (c) the initially applied stress intensity K_o. A representative H_2S K_{arr} result for HY-130 plate measured under near-optimum conditions was 6 ksi $in^{1/2}$.

7. RISING-LOAD TESTS OF HY PLATE SPECIMENS IN H_2S

7.1 Introduction

The main emphasis of the program for NSRDC (1-1) was on rising-load tests of HY plate-derived 1T WOL specimens in H_2S. Rising load tests in H_2S were also performed on precracked Charpy specimens of the same plates. This work is next reviewed for comparison of the tests on plate with those on actual and simulated weld metals.

Although "WOL" initially stood for "wedge-opening load" to indicate the method of specimen loading, it is used in this report only to represent the specimen outline proportions shown in Figure 5-1. The work for NSRDC included tests of the bolt-load version of the 1T WOL specimen by both the load-cell and bolt-load methods, as just discussed. In addition, a two-pin version of this specimen was tested by the rising-load and shim-load methods.

7.1.1. Test Description

The rising-load tests were performed with a servohydraulic machine in displacement control, much as in the precracked Charpy specimen tests already described (Parts 3 and 4). The continuously monitored displacement signal was derived from a clip gauge mounted as shown in Figure 5-2. Although the clip gauge was heavily coated with wax to protect it against corrosive attack by the H_2S, slow drifting of its output signal occurred in some tests. Corrections were applied where possible, and in no case did the clip-gauge error influence the main conclusions of a test. The principal consequence of such errors was an uncertainly of the detailed (minor cracking) behavior of the specimen during a long-term rising-load test or modification thereof.

The clip gauge was later replaced by an LVDT sealed with an O-ring against H_2S exposure of the wiring. This arrangement, which had already been used in the rising-load tests of Charpy specimens, constitutes a major improvement over the use of the clip gauge in H_2S.

7.1.2. Modified Rising-Load Test

A key modification of the rising-load test was the automatic switching from increasing displacement at constant $\dot{v}$ to holding constant displacement (zero $\dot{v}$) at a secant offset of 5, 10, 15 or 20% (individually selectable). The onset of crack growth thereby triggered automatic conversion of the rising-load test into a constant-displacement test. Accordingly, both K_{or} and K_{arr} could be measured in the same test, at least in principle. In practice, however, there was interference from (a) crack tunneling, which caused early crack arrest at erroneously high calculated values of the stress intensity, (b) impracticability of committing the rising-load test apparatus for the periods of time usually necessary for arrest, and (c) slow drift of the clip-gauge output, which led to slow drift of the specimen displacement. In view of these difficulties, the use of the modified rising-load test for determining K_{arr} was supplemented by long-term bolt-load tests (Part 6).

Modified H_2S rising-load tests were performed on ungrooved 1T WOL (2-pin) specimens of HY-130 steel (heat identification FKS) in both T-L and L-T orientations. The difficulties of measuring both K_{or} and K_{arr} (K_{Iscc}) in these tests are evident from the test descriptions in Ref. 7-1, which are excerpted below. The role of crack tunneling is discussed in relation to Neale's theory that a severe reduction of K/P accompanies formation of the tunnel crack front (Ref. 1-6).

The modified H_2S rising-load tests of the 1T WOL (2-pin) specimens of HY-130 plate FKS included two specimens of "standard" or S (T-L) orientation and two of "rotated" or R (L-T) orientation. In one of the S specimens the crack turned 90°. The relative weakness of the R (L-T)-oriented specimens was obscured by the incubation and crack tunneling effects, both of which led to severe overestimation of K_{arr}

(or K_{Iscc}). The best measurement of the latter, as obtained from the bolt-load test of FKS-R3 already discussed, was 6 ksi $in^{1/2}$. All results of the rising-load tests, including those modified for estimation of K_{arr} (in ungrooved specimens), were much higher than this, even after application of Neale's revision of the calibration factor (K/P) (also symbolized f(a)) for crack tunneling. The presumed reason is lack of sufficient time for crack arrest in the modified rising-load tests.

Many of the crack lengths in the descriptions that follow are values of a_1, the net crack length measured from the root of the machined notch. Since the latter is 0.767" from the load line, the total crack length, a, is a_1 + 0.767". The crack front bulge, b, is the difference between the maximum crack length, a_{max}, as usually measured at the specimen center, and a_{edge}, the crack length measured at the specimen side.

The rising-load tests of the 1T WOL specimens were performed at three H_2S pressures: 130, 65 and 20 psia. The effects of the H_2S pressure on K_{or} and K_{arr} were in the expected direction, but the dependence of the test data on the H_2S pressure was minor in comparison with the uncertainties associated with tunneling and incubation-time effects.

7.2. HY-130 Rising-load Test Descriptions and Discussion, as Excerpted from Ref. 7-1

Specimen FKS-S6 had "standard" (T-L) orientation. It was tested in H_2S at 130 psia in the as-air-precracked condition. The maximum fatigue load was 4.0 kips. The nominal fatigue crack length a_1, as measured on the specimen sides, was 0.149 inch. Later fractographic measurement indicated this crack had a bulge of 0.062 inch. The specimen was loaded slowly over a 40-hr period. The attended rate of loading was 8 to 18 lb/min, for which $\dot{K}$ is 2 to 5 ksi $in.^{1/2}$ hr^{-1}. During a 16-hr overnight holding period at nominally constant displacement, K increased from 27 to 31 ksi $in.^{1/2}$ due to slow drift of the displacement control system. Elastic compliance measured occasionally during the 40-hr period

gave no clear evidence of crack growth. Finally there was a sudden load drop from 15.7 to 14.7 kips (K drop from 76.5 to 74.1 ksi $in.^{1/2}$). Displacement was then held constant for the next sixteen hours, during which K dropped in three steps to 69.1 ksi $in.^{1/2}$. The latter, "arrest" value is taken as K_{Iscc}.

After an unload-reload cycle for compliance measurement, slowly rising displacement was resumed. This led to two minor load drops at K values of 70 and 74 ksi $in.^{1/2}$. Constant displacement was resumed at a K of 82.3 ksi $in.^{1/2}$. An hour later there was a load drop of 0.9 kip accompanying a K drop to 80.5 ksi $in.^{1/2}$. The test was terminated after 63 hr when the final crack length, a_1, as estimated from elastic compliance, was 0.40 inch as compared with 0.30 inch measured on the specimen surface.

The specimen was heat tinted and fractured to reveal a tunnel-shaped crack with a bulge of 0.275 inch. There was also the mark of a smoother, earlier crack that had advanced 0.030 inch beyond the fatigue crack during the initial 40-hr period while K was being slowly increased to 76.5 ksi $in.^{1/2}$. This early crack had evidently formed at relatively low stress intensity, being possibly associated with an unload-reload cycle for elastic compliance measurement.

The increasing tunneling tendency explains why the calculated K_{Iscc} increased as the crack grew in steps during the final portion of the test. There is a mounting error of the calculated stress intensity as the crack growth proceeds with increasing tunneling. The actual stress intensity at the tip of the crack is probably much lower than that calculated from the available calibration, which applies strictly to a straight, non-tunneling crack front. The assigned K_{Iscc} of 69 ksi $in.^{1/2}$, therefore, is probably an overestimate.

Specimen FKS-R2 had "rotated" (L-T) orientation. The initial precrack had been extended to 0.50 inch by fatigue in air at maximum loads decreasing in steps from 4 kips to 1.8 kips (K_{max} decreasing from 18 to 11.5 ksi $in.^{1/2}$). The purpose of the additional precracking was to bring the precrack length into the range prescribed in Ref. 1-4 as well

as to discourage rotation of the crack plane. The final precrack, from later fractography, had an average edge length of 0.521 inch and bulge of 0.062 inch. The specimen was tested in H_2S at 65 psia.

The early loading history of this test was similar to that of FKS-S6. Occasional unload-reload cycles for elastic compliance measurement during the initial, slowly rising displacement (24-hr) period indicated that at least 0.05 inch of crack growth had occurred by the time K reached 55 ksi $in.^{1/2}$, and a K_{Iscc} value of 53 ksi $in.^{1/2}$ is assigned to this specimen.

Later, slowly rising displacement testing yielded progressively higher measurements of the apparent K_{Iscc}. The final and largest load drop was from 12.46 to 11.41 kips, where the calculated stress intensity dropped from 92 to 88 ksi $in.^{1/2}$.

Fractography indicated extensive tunneling of the final crack front, which exhibited a bulge of 0.242 inch. There were actually two tunnels (eyebrows) astride the plate center plane, where numerous lamellar failures had occurred at right angles to the intended crack plane or parallel to the applied stress. These lamellar failures relieved the triaxial stress in the center plane and shifted the points of maximum tunnel-crack penetration to the 1/4- and 3/4-thickness locations.

An early, relatively smooth-surfaced environment crack was also evident. Its average edge crack length was 0.558 inch and bulge was 0.090 inch. Again, it appears that there was early crack growth (of 0.037 inch at the sides, 0.065 inch at the center) at relatively low stress intensity (estimated at 50 ksi $in.^{1/2}$) but that this was arrested until the load was much higher, when the major share of cracking occurred. The crack then grew internally but not at either specimen surface. Because of the high degree of tunneling, the final calculated K values are erroneously high.

K Recalibration for Crack Tunneling Case

The error of K_{Ic} due to crack tunnel formation has been analyzed by Neale (1-6), who refers to a three-dimensional elastic finite-element analysis idealization of a parabolic, tunnel-shaped crack (7-2) that was used for reformulating the stress-intensity calibration function f(a). The results are described by Neale for the case of a normalized surface-measured crack length, a_{edge}/W, of 0.535. Since the W dimension of our specimen was 2.55 inch, the corresponding a_{edge} is 1.364 inch and the edge-measured crack increment beyond the machined notch, a_{ledge}, is 0.597 inch. The present specimen's calibration, f(a), for this crack length is 7.13 $in.^{1/2}$, which represents K/P for only a straight-fronted crack (b = 0).

The calibration function f(a) increases with increasing crack length in the absence of tunneling. For the case where b alone increases at a constant value of a_{edge}, Neale indicates that the calibration function $f(a_{max})$ decreases sharply. For example, the present HY-130 specimens exhibited bulges of at least 0.24 inch. Neale's treatment indicates that a bulge of 0.24 inch corresponds to an actual K of only 45% of that determined by the conventional procedure if (1) the crack front is parabolic and (2) the weighted-average crack length is used for estimating K from f(a). Since the final estimates of K_{Iscc} for the HY-130 specimens were from 80 to 88 ksi $in.^{1/2}$, the effect of applying Neale's tunneling correction is to reduce these to the range of 36 to 39 ksi $in.^{1/2}$.

7.3 Updated Discussion

Although the K_{Iscc} results of 36 to 39 ksi $in^{1/2}$ seemed low when they were obtained, the subsequent bolt-load tests produced much lower results. The difference is probably due to the difference of test time. The discontinuous crack growth in the modified rising-load tests consisted of rapid crack advances alternating with periods of several hours each in which no cracking activity was apparent. This behavior suggests that the existing crack does not actually grow but instead

serves as a stress concentrator to aid the nucleation and growth of a new, internal crack near the tip of the "old" crack. The latter process was assisted by hydrogen diffusion into and accumulation within the new, internal crack. The apparently discontinuous crack growth observed would thus have resulted from the periodic breakthroughs of the new crack(s) to join the "old" crack.

Even though many hours were consumed in performing the modified rising-load tests during which such discontinuous crack growth occurred, the time allowed for crack arrest was short in comparison with the one- to two-weeks' duration of an H_2S bolt-load test. The apparent K_{arr} results were also considerably higher, even after application of Neale's correction for crack tunneling.

In summary, the major difference between the results of the rising-load and bolt-load tests of the same HY-130 plate material in the same H_2S environment are attributed to the difference of test time in combination with the effects of crack tunneling. The preferred way of contending with the latter is to eliminate it by adding sidegrooves to the specimen. The evidently true K_{arr} value was then measurable in a constant-displacement test of at least one week's duration. The modified rising-load tests of ungrooved specimens did not satisfactorily approach such conditions and therefore delivered erroneously high K_{arr} results, even after major correction for the tunneling.

7.4 Precracked Charpy Specimen Tests

The work for NSRDC included six H_2S rising-load tests of precracked Charpy specimens of the HY-130 steel plate; these are described in Sections 4.5.1 and D.4.4 of Ref. 1-1 and are briefly reviewed here. Both S (T-L) and R (L-T) orientations of the plate (FKS) were tested in H_2S at 65 psia. The initial, constant-$\dot{v}$ portions of the modified rising-load tests were performed at elastic-range values of $\dot{K}$ between 6 and 25 ksi $in^{1/2}/h$.

The tests of the precracked Charpy specimens differed markedly from those of either the actual or simulated weld metals described earlier in this report in that they exhibited no definite crack growth prior to the onset of major plastic deformation. This was true of both T-L and L-T orientations, of all loading rates including the lowest, and even of specimens precracked by fatigue in the H_2S environment. In every test there was significant deviation of the load-displacement curve from linearity due to plastic deformation alone prior to crack growth. In a few tests where the specimen was subjected to occasional, partial unload-reload cycles for remeasurement of the elastic compliance, the latter confirmed that no crack growth had occurred either before or after yielding.

Continuation of loading into the plastic range resulted in some cases in the sudden onset of fairly rapid crack growth. There was often a discontinuous (stepwise) pattern of such crack growth alternating with apparent arrest, much as in the modified rising-load tests of the 1T WOL specimens. The Charpy rising-load tests were similarly modified by switching from the constant-$\dot{v}$ to a zero-$\dot{v}$ (constant-v) loading condition. However, holding nominally constant displacement in these tests did not lead to crack arrest, since all crack growth occurred under conditions of increasing stress intensity. (The latter was due to an elastic component in the deflection measurement system, as discussed in Ref. 1-1.) Since crack arrest was unattainable, K_{or} was the only measurable result of the Charpy specimen tests.

K_{or} results interpretable by linear-elastic fracture mechanics were obtained in the tests of precracked Charpy specimens of the actual and simulated HY-130 weld metals where crack growth initiated at stress intensities below those of plastic yielding. In the tests of the HY-130 plate, however, the only observed crack growth initiated at loads in the plastic range where the evaluation of K_{or} is extremely difficult. In a few of these tests the load passed through a smooth maximum and gradually declined as the displacement was slowly increased (at constant $\dot{v}$). Such specimens usually showed minor tunnel crack growth associated with

the load maximum. The nominal (invalid) values of K_{or} estimated for the HY-130 plate-derived Charpy specimens were in the range 83 to 93 ksi $in^{1/2}$.

7.5 H_2S Rising-load Test of Deeply Sidegrooved Charpy Specimen FKS-R22

As an experiment, a Charpy specimen of HY-130 steel plate was machined with deep (0.10") sidegrooves and tested in the as-machined (unprecracked) condition by the H_2S rising-load method. The H_2S pressure was 65 psia.

The first part of the test was performed at a constant displacement rate corresponding to an elastic-range loading rate of 4.6 lbs/min. Visible deviation of the load-displacement curve from linearity due to yielding occurred at 1.7 kips. Continued slow loading to 2.1 kips produced no evidence of crack growth, and the specimen was unloaded.

Although the specimen had been machined with a 0.002" root radius in all three notches, fatigue precracking was deemed necessary for crack growth in the H_2S test. The servohydraulic loading machine had a capability for cyclic loading in the H_2S environment, and the precrack was grown under such conditions. The frequency was 1 hz. Only 100 cycles at a maximum load, P_{max}, of 1500 lbs were sufficient to initiate rapid H_2S fatigue crack growth. P_{max} was then reduced to 800 lbs, and the rapid crack growth stopped. It was then increased to 1100 lbs and the rapid crack growth immediately resumed. Finally, P_{max} was returned to 800 lbs where rapid crack growth resumed after 30 cycles. The fatigue cycles were displacement controlled, and the maximum load of the final crack-growth cycle was 560 lbs.

The freshly precracked specimen was unloaded for the final rising-load step. The displacement rate was equivalent to an elastic-range loading rate of 1.4 lbs/min. The load rose linearly to 500 lbs where it passed through a sharp maximum and then declined steadily. The test was terminated after the load declined gradually to below 100 lbs. The displacement was then 7 mils, as compared with 5.1 mils at the maximum load.

Post-test examination of the fracture surface with a binocular microscope indicated the surface to be largely featureless (Fig. 7-1). The rapid fatigue crack growth in H_2S had not produced distinctively smooth zones, and precrack length could not be measured.

The deeply sidegrooved specimen had the disadvantage that neither the calibration factor K/P nor the elastic compliance is accurately calculable from available formulae. For shallow (5%) sidegrooves it is common to replace the thickness B of a flat-sided specimen by $(B_n B)^{1/2}$, where B_n is the reduced thickness in the notch plane. However, no accuracy is claimed for this formula with the present sidegroove depth of 25%. The theoretical elastic compliance is similarly uncertain.

The onset of crack growth at 500 lbs in the final rising-load step may be viewed the next load-cycle resumption of the H_2S fatigue cracking process that was previously terminated at a maximum load of 560 lbs. The rate of fatigue crack growth (in displacement control) was such that the maximum load in the next cycle would have been 540 lbs, with crack-growth resumption at a somewhat lower load. Since the fatigue cracking was so rapid, the resumption of crack growth at a comparable load in the succeeding rising-load step was not unexpected. Values of K_{or} determined under such conditions are probably a function primarily of the prior fatigue operation and therefore trivial.

In summary, the H_2S rising-load test of the deeply sidegrooved Charpy specimen did not produce crack growth until after the specimen was precracked, in this case by cyclic loading in the H_2S environment. The final maximum load of the final precracking cycle was sufficient to produce a high rate of crack growth, and the onset of crack growth in the subsequent H_2S rising-load step occurred at a comparable load. Although K_{or} could not be measured, the deeply sidegrooved Charpy specimen is viewed as promising for environmental tests of lower-yield-strength materials if it is precracked under suitably controlled conditions and if the necessary calibration data can be formulated. The deep sidegrooves have the advantage of virtually eliminating the plane-stress specimen surface layer that interferes with the acquisition of useful

results in environmental tests of materials with moderate yield strength and high toughness.

7.6 Improved Test Procedures

Although the modified rising-load tests described above did not produce the quantitative results expected, they were nevertheless extremely valuable in indicating productive directions for future environmental tests of both wrought base metal and weldments of HY steels. A serious goal of such tests is the measurement of K_{arr} (or K_{Iscc}) as well as K_{or}, since only the former now appears to be relevant in design. Both quantities may be measured in modified rising-load tests of suitably prepared specimens. Machined sidegrooves of depth suitable to prevent tunneling are desirable in such tests.

The results of testing sidegrooved, precracked Charpy specimens by the modified rising-load method include K_{or} but not K_{arr}, and therefore the testing of WOL or CT specimens is preferable. If such a specimen is sidegrooved to yield a straight crack front at arrest, it can provide values of both K_{or} and K_{arr} in the modified test without systematic errors due to crack tunneling.

In recent work the errors due to slow drift of the output of the clip gauge in H_2S have been eliminated by the use of an O-ring-sealed LVDT for displacement measurement. As a consequence, the modified rising-load technique is now far more satisfactory for use in long-term tests in H_2S.

Finally, the capability of fatigue precracking in the test environment has only recently been systematically exploited. A preferred technique of utilizing this capability was suggested by the present work. Both the overload factor and incubation time have been very significantly reduced by the use of fatigue precracking at sufficiently high levels of K_{max} in the test environment to produce initially rapid environmental fatigue crack growth. The fatiguing is performed in displacement control such that the maximum displacement, v_{max}, is constant; hence K_{max} must

decrease as the precrack grows. At the conclusion of such precracking, the loading system is shifted to a static mode in which the displacement is held constant near v_{max}. The crack then usually continues to grow and eventually arrests.* Alternatively, the displacement may be slowly decreased during the static crack-growth phase to yield arrest at more conveniently measurable values of the final load and crack length. Since the "static" rising-load phase has been replaced in this test by the environmental fatigue precracking step, the new technique is termed an "environmental precracking and static crack-arrest test" for efficiently determining K_{arr}.

The new test procedures were suggested by the laboratory experience gained in the present work as well as in that for NSRDC (1-1). Their advantages in essentially eliminating both the incubation and overloads of conventional static tests may be appreciated from the descriptions of these phenomena and their consequences in Parts 8, 9 and 10.

---

*The resulting value of K_{arr} should be unrelated to the environmental fatigue precracking conditions if the final, static crack extension to arrest is large relative to the size of the fatigue-affected zone.

8. RISING-LOAD TEST OF 9 Ni 4 Co HY-180 PLATE IN H_2

8.1 Introduction

The work for NSRDC (1-1) included several tests of 1T WOL specimens of HY steel plate in which the environment was tank H_2. In most such tests there was no apparent crack growth. In two rising-load tests of HY-180 steels, however, there was moderately rapid hydrogen-enhanced crack growth through most of the specimen ligament. The tests are identified as those of Specimens ERH-6 and EZH-23. In both cases there was a single, continuous crack growth event that was essentially complete (at arrest) within 30 minutes after onset. Such behavior is consistent with the suggested cracking mechanism in which the existing (pre)crack does not actually grow. Instead, it serves as a stress concentrator to assist the internal initiation and growth of a new crack. The early subsurface growth of the new crack probably has little detectable effect on the measured compliance and is therefore essentially invisible. Upon reaching a critical size, however, the new crack breaks through to join the "old" crack (or precrack) and the accompanying sudden increase of compliance is manifested as a rapid drop of the recorded load. This occurred in both H_2 and H_2S.

Following the initial signal of crack-growth onset, the control shifted automatically from the constant-$\dot{v}$ to the zero-$\dot{v}$ (constant-v) control mode. In specimens prone to crack tunneling, such as ungrooved HY-130 specimens in H_2S, the new tunnel-shaped crack arrested temporarily and the load remained essentially constant for several hours, following which there was another stepwise growth of the crack, and so on. In he the HY-180 specimens tested in H_2, however, all of the crack growth occurred in a single, continuous step. Detailed descriptions of these tests are presented in Section D.3 of Ref. 1-1.

The H_2 fracture surfaces were clean and therefore far better fractography subjects than the H_2S fractures, which were usually fouled by sulfides. Detailed fractography of ERH-6 revealed a great deal of significant information on the process of crack initiation. This information is presented below in the form of excerpts from an independent scientific paper (Ref. 8-1).

8.2 Test of ERH-6, as Excerpted from Ref. 8-1

8.2.1. Introduction

In a recent study of the environmental hydrogen embrittlement of HY-180 steels (1-1) it was found that K_{or}, the stress intensity of crack-growth onset in a slow rising-load test, was considerably higher than K_{arr}, the stress intensity of crack arrest in a constant-displacement test of the same material in the same environment. Since both testing methods have been used for estimating K_{Iscc}, the twofold or larger disagreement between K_{or} and K_{arr} was a matter of some concern.

The difference between K_{or} and K_{arr} is a direct function of the characteristic incubation time that must elapse between application of a given load and the onset of crack growth in an environmental test. An interpretation of the origin of this incubation phenomenon is offered in the present paper.

8.2.2. Test Procedure

All rising-load tests in hydrogen were performed at an H_2 pressure of 175 to 190 psia. The test chamber was first evacuated with a mechanical vacuum pump, purged several times with H_2, and finally backfilled with the static H_2 charge used for the test. Commercial high-purity H_2 was used in the condition drawn from the tank.

In the case of 9 Ni 4 Co HY-180 Specimen ERH-6, the air-fatigue precracking was completed at a maximum load of 4.0 kips, for which the stress intensity was 19 ksi $in^{1/2}$. The net precrack length a_1 was 0.17 inch (a/W = 0.37), for which the calibration factor K/P is 4.76 $in^{-3/2}$.

The H_2 rising-load test included two slow load-unload cycles, in each of which the load and displacement were increased slowly (at $\dot{K}$ = 5 ksi $in^{1/2}$/h), held constant for a time and returned rapidly to zero. The maximum stress intensity in these excursions was 24 ksi $in^{1/2}$.

The final rising-load part of the test consisted of an 8.95-h period during which the load was increased at a constant rate from 0.15 to 9.40 kip. During this period there was no evidence of plastic deformation or crack growth. Extensive crack growth then occurred rapidly, as signalled by a sudden decrease of the load from 9.40 to only 0.84 kip. The time for the load to drop from 9.40 to 7.25 kip was 3.0 min, during which the crack growth rate (calculated from compliance) increased from 0.03 to 0.08 inch/minute. Within 11 additional minutes the load was steady at 0.84 kip and remained so for a constant-displacement period of 11 hours, after which the specimen was unloaded and opened after air-fatigue cracking to mark the final H_2 crack front. The net crack length, a_1, was measured as 1.35 inch (a/W = 0.83) for which the calibration factor K/P is 33.3 and K_{Iscc} is 30 ksi $in^{1/2}$. (This result is based on a corrected value of the final load obtained by adding to the measured load of 0.84 kip an unmeasured increment of 0.08 kip due to the H_2 chamber pressure of 175 psig acting on the 0.75"-dia. loading ram.)

This test was of interest for a number of reasons including the fact that failure occurred in a single crack-growth event lasting less than 14 min after the specimen had been overloaded, in effect, to a stress intensity 1.5 times the final arrest K_{Iscc} value. The overload requirement is a manifestation of incubation.

In spite of the test's total finite-load time consumption of 37 hours, such a slowly rising-load test is viewed as a reasonable way of measuring K_{Iscc} in a single test of an unknown specimen. After the two false starts, the rising-load period of 8.95 hours was necessary to achieve the peak stress intensity (K_{or}) of 45 ksi $in^{1/2}$, following which the final, arrest value of the load was recorded within 15 minutes.

8.2.3. Fractographic Features

An optical photograph of the fracture surface is shown in Fig. 8-1. It is clear from this picture that the front of the fatigue precrack appears to be very irregular. The scanning electron microscope (S.E.M.) view of the fatigue front corresponding to the 5.8 cm position in Fig. 8-1 is shown in Fig. 8-2. This view shows that the tip of the fatigue crack is reasonably straight and that the apparent irregularities are due to the fracture in hydrogen not having joined directly with the fatigue crack front. Figure 8-3 is an enlargement of the center of Fig. 8-2, adjacent to the overhanging lip. It reveals that there is a ribbon of dimpled rupture between the fatigue crack, on the lower left hand corner and the primarily intergranular cracking on the upper right hand side. Fig. 8-4 is an overview of another one of the lips in which it can be seen that the lip face is very smooth and almost featureless.

The sample was tilted in such a way that the tip of the fatigue crack in Fig. 8-4 could be clearly viewed. Fig. 8-5 is an enlarged view of the fatigue crack tip corresponding to the center of Fig. 8-4 and it was noted that there was little evidence of dimpled rupture compared with that characterized in Fig. 8-3.

Fig. 8-6 gives a view of the fracture surface, in the 7.1 cm position in Fig. 8-1, taken from a point facing the fatigue fracture surface. This site corresponds to the situation where the fatigue crack front has been removed from the fracture surface, and is of course, on the other half of the specimen. Attention is drawn to the vertical "scrape" markings in the featureless zone. Replicas taken from the fracture surface and viewed in the transmission electron microscope (T.E.M.) showed the same features not only at the fatigue interface with the intergranular fracture but also at various sites within the hydrogen embrittled fracture surface. This evidence is not, however, essentially reliable since scrape markings produced in removing the replica from the fracture surface can be confused with real scrape markings as seen in Fig. 8-6. The intergranular fracture surface on

the left hand side of this fractograph extends under the fatigue fracture surface. Fig. 8-7 gives the same fracture area viewed from the upper right hand corner of Fig. 8-6. It is noted that what should be a flat fatigue plane has been substantially deformed by the fracture process. Fig. 8-8 shows another view of the fracture surface adjacent to Fig. 8-6. In the center of Fig. 8-8 evidence of pre-existing or rather smeared dimples can be seen within the featureless zone.

8.2.4. Discussion of the Cracking Mechanism

The principal fractographic details are consistent with the concept that hydrogen cracking occurs ahead of the main fatigue crack in a region of maximum stress (8-2). In this particular specimen the internal crack did not join the fatigue crack in the fatigue crack plane and hence provided additional fractographic evidence of a very interesting nature.

Figures 8-9, 8-10 and 8-11 give a schematic overview of the fracture processes. In each figure it is assumed that the internal hydrogen assisted crack, which in this instance was primarily intergranular (I.G.), starts parallel to and out of the plane of the fatigue crack. In Figure 8-9 this crack is assumed to advance to a position close to the fatigue crack tip and the remaining ligament fails by a shear overload producing dimpled rupture as shown in Fig. 8-3.

The example shown in Fig. 8-10 is that of the internal crack extending back beyond the fatigue crack tip and joining the fatigue crack by shear overload from the tip of the internal crack. The two possible fracture surfaces, from the upper and lower halves of the specimen, are shown in the fractographic overview. The final fracture ligament is smeared because the two separating halves do not pull apart as in Fig. 8-9 but instead rotate about a point close to the far end of the internally formed crack. The smeared dimples give evidence of the final fracture sequence being dimpled rupture followed by a severe one-step fretting of the two surfaces.

Figure 8-11 shows a modification of the joining of two overlapping cracks via a shear from the fatigue crack to a point not on the tip of the internal crack. The minor crack shown in the overhanging lip in the center of Fig.8-2 is an example of this crack orientation. Whereas the lower half (a) of the fractographic overview is similar to (a) of Fig. 8-10, the upper half leads to the observation seen in Fig. 8-6, in which the intergranular crack lies parallel to and extends underneath the fatigue crack. The severity of the scraping motion of the two halves is clear in Fig. 8-6, note the vertical lines in the featureless zones, and also by virtue of the substantial deformation of the fatigue surface shown in Fig. 8-7.

One of the important observations is shown in Fig. 8-5 where little or no dimpled rupture can be seen at the tip of the fatigue crack. First it demonstrates that the dimpled rupture (Fig. 8-3) was not caused directly by the presence of hydrogen, since if it were the dimpled rupture should be evident along the length of the fatigue crack tip. Secondly, if this is so, the tip of the fatigue crack did not significantly advance in the hydrogen environment test. In other words the evidence suggests that the hydrogen induced cracking did not start at the fatigue crack tip.

It is interesting to speculate on the reason for the internal crack starting out of the principal plane of fracture and subsequently circumventing the tip of the fatigue crack. Since the specimen was prepared by fatigue pre-cracking, in order to introduce a sharp crack for the hydrogen embrittlement test, a zone of heavily worked material was formed around and ahead of the tip of the fatigue crack. A heavily worked volume provides extra traps for hydrogen and is not typical of an unworked material.

Reviewing the test data, it is seen that the initial stress intensity required for cracking in hydrogen is often significantly higher than the stress intensity required to propagate the crack after it has started. Tentatively this can be interpreted as the difference between the initiation of a crack in a heavily worked zone compared with a relatively work-free zone. If so, it would be reasonable to expect

the internally formed crack to initiate and propagate around the heavily worked zone at the tip of the fatigue crack. This factor will influence the incubation time.

Even though this argument is speculative and applies only to this one material, HY-180, it does raise a very important question: is fatigue crack formation with its attendent plastic zone the correct specimen crack preparation for the measurement of K_{Iscc}?

The origin of the incubation phenomenon itself is evident from the conclusion that hydrogen-assisted crack growth begins not by propagation of the existing crack but by the nucleation and growth of an internal crack following the incubation period. The incubation time is therefore the time required for the successive steps of (a) possible hydrogen reduction of surface oxide film near the crack tip, (b) hydrogen reaction with the fresh metal surface in the crack tip vicinity, (c) hydrogen entry into the metal and diffusion to the region of maximum triaxial tensile stress, (d) hydrogen accumulation in the triaxially stressed region until a concentration sufficient for internal crack nucleation is attained, (e) nucleation of the internal crack and growth at a rate determined by the rate of supply of hydrogen in the previously described processes, and finally (f) breakthough of the internal crack to join the existing crack. To the extent that any or all of these processes do not proceed instantaneously, the delay (incubation) time between exposure of the stressed specimen to the hydrogenous environment and initiation of visible cracking is readily understood. The present fractographic study confirms that such a process actually does occur and thereby helps to clarify the basis of the incubation phenomenon.

9. RISING-LOAD TESTS OF 10 Ni HY-180 PLATE IN H_2

9.1 Introduction

The program for NSRDC (1-1) included two modified rising-load tests of 1T WOL outline specimens of as-received 10 Ni NY-180 steel plate in H_2. The tests are described in Sections 3.3.2 and D.3.2 of Ref. 1-1 and reviewed below because of (a) the close resemblance of the fractographic features to those of ERH-6 described above, (b) the distinctly different incubation kinetics of the 10 Ni and 9 Ni 4 Co alloys in H_2, and (c) the availability in one of these tests of a complete record of the load and displacement as a function of time during crack growth in H_2. The subjects of both (b) and (c) are discussed in detail in Part 10 of this report, in which a mathematical model is presented for both the incubation and crack-growth phases of the modified rising-load test.

The test of Specimen EZH-16 was performed under conditions similar to those of the test of 9 Ni 4 Co Specimen ERH-6 described above, but no crack growth occurred. The test of EZH-23 was modified to encourage crack propagation, and this eventually occurred in much the same manner as that in the test of ERH-6 just described.

9.2 Detailed Description of Test of EZH-16, as Excerpted from Ref. 1-1

Specimen EZH-16. The H_2 rising-load test of EZH-16 included several false starts that consumed 9.2 hours at finite load. The final load rise consumed 24.1 hr during which P increased from 5.3 to 17.3 kips and K increased to 81. This maximum load was held for 24 hours. There was no evidence of crack growth, and the test was terminated. Combination of these results with additional information for the same material-environment system indicates that the incubation-time constant t_{io} was at least 52 hours.

9.3. Detailed Description of Test of EZH-23, as excerpted from Ref. 1-1

Specimen EZH-23. The H_2 rising-load test of EZH-23 differed from that of EZH-16 in having two additional provisions for encouraging crack growth: (1) fatigue precracking in the test environment, and (2) the use of a lower displacement rate.

The specimen had been fatigue precracked in air at a final K_{max} value of 11 to a precrack length, a_1, of 0.30 inch. Additional fatigue precracking in the 190 psia H_2 test environment was at a frequency of 1 hz. The H_2 fatigue value of K_{max} was increased at 1-hr intervals from 11 to 13 and finally to 16 ksi $in^{1/2}$ to produce measurable fatigue crack extension in a reasonable time. The total time of fatigue in H_2 was 5.75 hours and the precrack advance was 0.023 inch.

The H_2 rising-load test immediately followed the H_2 fatigue precracking in the same apparatus. The load rise included an initial period in which P increased from 2 to 9.5 kips over a 21-hour period, following which the specimen was held at constant load for one hour. Slow loading was resumed and interrupted again at 10.0 kips for shifting chart load ranges; this necessitated rapid unloading and reloading, following which the slow loading was resumed.

At 13.2 kips (K = 71) there was a sudden drop of the load to only 0.2 kip, indicating massive crack advance. The load drop consumed about 25 minutes, during which the crack-growth rate passed through a maximum of 0.12 inch/minute. Essentially all of the load drop occurred at constant displacement (as registered by the clip gauge mounted at the end of the specimen) because of the control's automatic switching to zero displacement rate early in the load-drop event.

Constant displacement was held for 12 more hours, during which there was no indication of additional crack growth, and the test was terminated. The final crack front was marked by fatigue in air, and the specimen was opened. The extensive H_2 crack growth had left a ligament of only 0.18 inch. The arrest value of K_{Iscc} was about 30.

Although this is "valid" in terms of the final ligament size, considerable uncertainty is introduced by both the sensitive dependence of the calibration factor (K/P) on the long final crack length and the difficulty of measuring the final load. The latter was estimated by several techniques, with a correction of 0.08 kip added to allow for the H_2 chamber pressure.

An incubation time constant, t_{io}, of 14.5 hr was calculated from the results of this test on the assumption that K_{Ic} is 130. Since no crack growth had occurred in EZH-16, the present t_{io} result applies only to a specimen precracked by fatigue in the test environment. (The incubation time for a specimen not so precracked is much longer, as estimated previously.) Even so, the present t_{io} of 14.5 hr is 12 times that of the 9 Ni 4 Co HY-180 Specimen ERH-6 that was tested in the same environment and without environment fatigue precracking. These results illustrate the major difference of incubation times of the two HY-180 materials tested in H_2, even though the respective K_{Iscc} values (at arrest) were about the same.

9.4. Concluding Discussion

The fracture appearance of EZH-23 was essentially equivalent to that of ERH-6, which is described in detail in Part 8. Again there was clear evidence of the hydrogen crack's having initiated internally ahead of the precrack and of circumventing the precrack tip's fatigue-affected zone.

The incubation time associated with this process was much longer in the 10 Ni than in the 9 Ni 4 Co alloy. Since K increased continuously during the incubation period, the effect of the increasing incubation time was to increase K_{or}. The latter is also a direct function of the imposed loading rate or $\dot{K}$. The quantitative formulation of such interrelationships forms the subject of Part 10.

10. MATHEMATICAL MODEL OF MODIFIED RISING-LOAD TEST

10.1 Introduction

The nature of the incubation phenomenon is such that the results of short-time environmental cracking tests, including particularly rising-load tests, must be viewed as primarily determined by the incubation kinetics rather than by the threshold stress intensity K_{arr} or K_{Iscc}. It is therefore important that K_{or}, the stress intensity of crack-growth onset in a rising- or step-load test, be correlated with the incubation kinetics as well as with K_{arr}. A simple model for doing this was formulated in Appendix B of Ref. 1-1 and is here reviewed and extended. The main purpose of this treatment is to provide a quantitative description of the onset, growth and arrest of environment-assisted cracking in precracked-specimen tests including specifically the modified rising-load test. In view of the usual scatter of the experimental data, only a simple model is sufficient.

The premises on which the model is based are not all proven; the approach will be to construct the model and later to attempt to justify the premises. In the case of the modified rising-load test the premises include the following:

1. The rising-load portion of the test is performed entirely in the elastic range at a constant displacement rate $\dot{v}$ corresponding to a loading rate $\dot{P}$ or $\dot{K}$. Relevant relationships are $\dot{v}/\dot{P} = v/P = C_e$, the elastic compliance, and $\dot{K}/\dot{P} = (K/P)\dot{}$, the stress-intensity calibration factor.
2. There is no preliminary crack growth during the rising-load (or rising-displacement) phase of the test.
3. The onset of crack growth occurs suddenly at a stress intensity K_{or}, at which point the apparatus is switched from holding a constant,

finite $\dot{v}$ to holding zero $\dot{v}$ or constant displacement (bolt-load condition).

4. K_{or} is significantly higher than the arrest or infinite-time threshold stress intensity K_{arr} and in this sense represents an overload condition. The difference, $K_{or} - K_{arr}$, is a measure of the initial driving force for crack growth. At any time during the crack-growth process, the normalized driving force is κ, defined by

$$\kappa = \frac{K - K_{arr}}{K_{Ic} - K_{arr}}$$

5. The crack growth rate $\dot{a}$ is proportional to $\sqrt{\kappa}$:

$$\dot{a} = k\sqrt{\kappa} \qquad (\text{for } 0 < \kappa < 1)$$

in which k is a rate constant.

10.2. Constant-Load Test Model

We next briefly consider the crack growth in a simple constant-load test, as conventionally performed by constant-weight loading of a precracked specimen of either cantilever-beam or CT (or WOL) design in an environment. The main result of such a test is t_f, the failure time at the applied load, P_o. This failure time is the sum of the incubation time t_i and the crack-growth time t_g:

$$t_f = t_i + t_g$$

The assumption is next made that both t_i and t_g are proportional to $-\ln \kappa_o$, as defined by

$$\kappa_o = \frac{K_o - K_{arr}}{K_{Ic} - K_{arr}}$$

in which K_o is the stress intensity at the applied load, P_o, prior to any crack growth. The respective relationships are

$$t_i = t_{io}(-\ln \kappa_o) \qquad (10\text{-}1)$$

in which t_{io} is the incubation-time constant, and

$$t_g = t_{go}(-\ln \kappa_o) \qquad (10\text{-}2)$$

in which t_{go} is the crack-growth time constant. The failure time is then given by

$$t_f = (t_{io} + t_{go})(-\ln \kappa_o) = t_{fo}(-\ln \kappa_o) \qquad (10\text{-}3)$$

in which t_{fo}, the failure-time constant, is equal to $t_{io} + t_{go}$.

Within experimental error, Equation 10-3 is descriptive of numerous constant-load test results (1-1). These are conventionally plotted (Figs. 10-1, 10-2) as K_o against log t_f and fitted by an S-shaped curve that is asymptotic with K_{Ic} at the shortest failure times (where environmental effects are minimal) and with K_{arr} at the longest times. Success has been achieved in fitting Equation 10-3 to available failure-time data and in evaluating the failure-time constant t_{fo}, as described in Appendix B of Reference 1-1. Novak and Rolfe (1-5) have demonstrated, moreover, that the long-time threshold stress intensity (K_{th}) determined in such a series of tests is identical to the arrest stress intensity (K_{arr}) measured in individual constant-displacement tests. In the present report both kinds of test result are symbolized K_{arr}, which is equivalent to K_{Iscc} as used by Novak and Rolfe.

Since t_f has been found empirically to conform to Equation 10-3, it seems reasonable to assume that its separate components, t_i and t_g, conform to Equations 10-1 and 10-2, respectively. This assumption is consistent with the representations of these relationships in Figure 6 of Reference 10-1 as well as with the crack-growth relationship of Premise 5, as next discussed.

The crack-growth time t_g in a constant-load test is a function of both the response of å to K (e.g. Premise 5) and the size and shape of the specimen. In either the cantilever-beam or CT (or WOL) specimen the crack growth is self-accelerating in a constant-load test because of the increase of stress intensity with increasing crack length. This relationship is readily seen in the sensitive increase of the calibration factor K/P

AD-A074 104 WESTINGHOUSE RESEARCH AND DEVELOPMENT CENTER PITTSBU--ETC F/G 11/6
ENVIRONMENTAL HYDROGEN CRACKING OF HY STEEL WELD METALS.(U)
AUG 79 E W JOHNSON, B J SHAW N00014-77-C-0372
UNCLASSIFIED 79-9D9-HONRY-R1 NL

2 OF 2
AD
A074104

END
DATE
FILMED
10-79
DDC

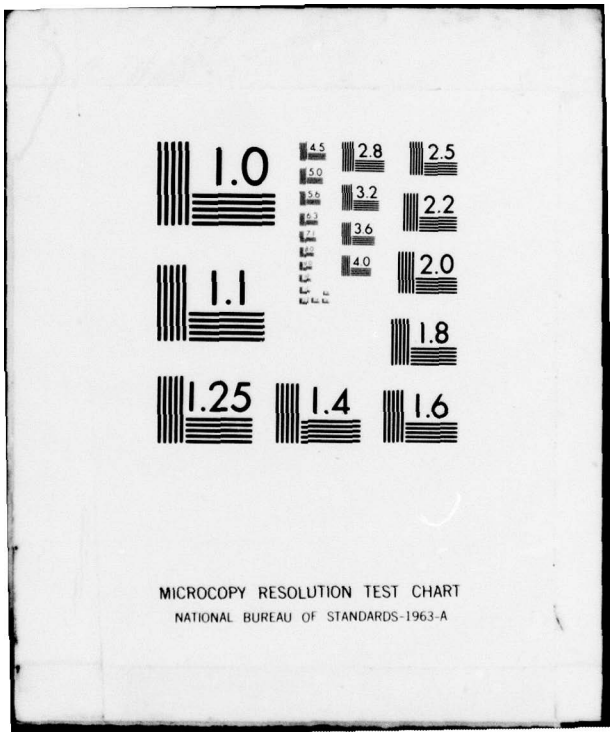
1.0
1.1
1.25
1.4
1.6
1.8
2.0
2.2
2.5
2.8
3.2
3.6
4.0
4.5
5.0
MICROCOPY RESOLUTION TEST CHART
NATIONAL BUREAU OF STANDARDS-1963-A

with increasing crack length (Table 5-2), since P is constant throughout the test.

A simple numerical method of calculation was used to describe the relationship between the crack-growth time constant t_{go} and the crack-growth rate constant k as well as other (specimen) variables for the 1T WOL specimen. During crack growth at P_o, the stress intensity increases from K_o to K_{Ic} where the test terminates in rapid failure. A test performed at a low value of K_o has a relatively long incubation time t_i as well as a relatively long crack-growth time t_g. Both times decrease as K_o increases. For the 1T WOL specimen with a normalized precrack length, a/W, of 0.42, t_{go} is related to to k by

$$k\, t_{go} = 0.8 \text{ inch.}$$

10.3. Constant-Displacement Test Model

We next examine a simple constant-displacement test, such as an idealized bolt-load test in which the displacement provided by the (ideally infinite-modulus) loading bolt remains constant during crack growth. The incubation phase of such a test is identical to that of the constant-load test just described for a specimen of identical size and shape loaded in the same environment. Bolt-load specimens are often loaded in air rather than in the test environment, however. Loading in the environment is preferable because it significantly reduces the incubation time. (It does not eliminate it, however.) Thus, a specimen loaded in air will usually have a significantly larger incubation-time constant than a similar specimen loaded in the test environment.

At the end of the incubation period in the constant-displacement test, crack growth initiates at the same rate as in the constant-load test performed at the same value of K_o. (This ignores any nonsteady crack growth prior to attainment of the crack-growth rate $\dot{a}$ expressed by Premise 5, assuming instead that $\dot{a}$ increases suddenly from zero to $k\sqrt{K_o}$ at the end of the incubation period.) As the crack grows, the stress intensity now decreases until the crack arrests at K_{arr}. The measured value of K_{arr} ($\approx K_{Iscc}$) is the main result of the test.

Since the approach of K to K_{arr} is asymptotic and the final phase of arrest is slow, it is convenient to define t_g in terms of an arbitrary degree of approach to K_{arr}. Our preference for this purpose is to use $\kappa = 0.03$. A result is that the calculated t_g is essentially independent of K_o. The tests initiated at low values of K_o have a small driving force for crack growth and t_g tends to be long. Tests at a higher K_o have a larger driving force that accelerates the crack growth, but the final length of the crack is much larger than that of the lower-K_o crack. These effects compensate to make t_g essentially independent of K_o. For the 1T WOL specimen this constant value of t_g is approximately 3 t_{go}.

The relationships of t_i and t_g in constant-displacement tests of 1T WOL specimens are

$$t_i = t_{io}\,(-\ln \kappa_o)$$

$$t_g = 3\,t_{go}$$

$$t_{arr} = t_i + t_g = t_{io}(-\ln \kappa_o) + 3\,t_{go}.$$

in which t_{arr} is the time from specimen loading to the condition of near-arrest of the crack as defined by the cutoff κ value of 0.03.

10.4. Comparison of Constant-Load and Constant-Displacement Tests

As examples of the use of the relationships just derived, we next consider two environmental crack-growth tests of 1T WOL specimens with a normalized precrack length, a/W, of 0.42 and with the following values of the respective constants:

$$K_{Ic} = 125 \text{ ksi in}^{1/2}; \quad K_{arr} = 25 \text{ ksi in}^{1/2}; \quad K_o = 45 \text{ ksi in}^{1/2};$$

$$t_{io}(\text{env}) = 250 \text{ h}; \quad t_{io}(\text{air}) = 1000 \text{ h}; \quad t_{go} = 100 \text{ h}$$

in which t_{io}(env) is the incubation-time constant for a specimen loaded

in the test environment and t_{io}(air) is for one loaded in air. One specimen is tested at a constant load after being loaded in the test environment, and the other is tested at a constant displacement after being loaded in air. In both cases the normalized, reduced initial stress intensity κ_o is 0.20 and the crack-growth rate constant k is 0.008 in/h.

The specimen tested at a constant load (of P_o = 8.5 kips) has an incubation time, t_i, of 400 h following which it experiences accelerating crack growth beginning at the rate, å, of 0.0036 in/h. The crack grows at an increasing rate to a normalized length, a/W, of 0.70 over a period, t_g, of 160 h, at the end of which the stress intensity is K_{Ic} and the specimen fails catastrophically. The failure time, t_f, is 560 h.

The specimen tested at a constant displacement is loaded in air and therefore has a much longer incubation time, t_i, of 1610 h, following which crack growth initiates at the rate 0.0036 in/h. This rate later decreases with the decreasing stress intensity. As κ declines from 0.20 to 0.03, the crack grows to a normalized length, a/W, of 0.67 during a time, t_g, of 300 h. K then is 28 ksi $in^{1/2}$. The final (infinite-time)arrest value of a/W is 0.73. This is approached asymptotically and no definite time value can be assigned to it. The time required for the entire test, therefore, is at least 2000 h. Although this is nearly 4 times the failure time of the constant-load test at the same K_o, the constant-displacement test has the important advantage that its main result is K_{arr}, while that of a single constant-load test is only the failure time (t_f).

The evaluation of K_{arr} in multiple constant-load tests requires relatively long test times even if all of the tests are started simultaneously. If one such test is performed at a K_o of 28 ksi $in^{1/2}$ or a κ_o of 0.03, the incubation time is 875 h and the crack-growth time is 350 h for a failure time of 1225 h. Tests at K_o values nearer 25 ksi $in^{1/2}$ must be run for much longer times than this to establish K_{arr} as 25 ksi $in^{1/2}$. Thus the time requirement of determining K_{arr} in this

way(in the present example at least) is of the same magnitude as that of a single constant-displacement test.

In summary, constant-load tests provide definite values of the failure time t_f, but several such tests must be performed over a range of K_o to determine K_{arr}. On the other hand, K_{arr} can be evaluated in a single constant-displacement test, but such a test is more time-consuming than a constant-load test performed at the same value of K_o because (a) the specimen is usually loaded in the air rather than in the test environment, and (b) the crack-growth process occurs under conditions of decreasing rather than increasing stress intensity. The long test-time requirements of many material-environment systems discourage the use of either testing method for determining K_{arr} of these systems.

10.5. Conventional Step- and Rising-load Tests

The use of a regularly increasing stress intensity in environmental cracking tests is a reaction to the long test-time requirements of single-step tests conducted in either load or displacement control,as just discussed. Step- or rising-load tests can be performed in either load control (i.e. at constant $\dot{P}$) or displacement control (i.e. at constant $\dot{v}$). In either case the incubation phase of the test is characterized by a constant rate of increase of the stress intensity (constant $\dot{K}$) if the loading is performed only within the linear-elastic range. The main result of the test is K_{or}, the stress intensity of crack-growth onset. This K_{or} is not K_{arr} (as represented in some reports) but is rather a function of both the incubation-time constant t_{io} and the loading rate $\dot{K}$. In many cases, in fact, K_{or} is not a suitable approximation of K_{arr} but is actually a measure of t_{io}, as will be shown.

If a simple rising-load test is performed in load control (i.e. at constant $\dot{P}$), $\dot{K}$ remains constant until the onset of crack growth at K_{or}, following which it increases because $\dot{K}/\dot{P}(= K/P)$ must increase with the crack length. Thus the crack growth and stress intensity

are mutually self-accelerating much as in a constant-load test, and the specimen fails catastrophically. If the rising-load test is performed in displacement control, $\dot{K}$ must decrease after the onset of crack growth and the crack grows at a lower rate than in the load-control test. As long as $\dot{v}$ remains finite, however, the crack cannot arrest. Hence the constant-$\dot{v}$ test is less informative than the constant-v test in that the latter yields K_{arr} while the former yields only K_{or}. To the extent that K_{arr} rather than K_{or} (or t_{io}) is the desired result, the simple rising-load test in either load or displacement control is less informative than either the bolt-load or multiple constant-load tests.

The duration of the incubation (noncrack-growth) phase of the rising-load test is $K_{or}/\dot{K}$ in those tests beginning at zero load and performed at a single value of $\dot{K}$. This time is appreciably longer than t_i, the incubation time of a single-step (constant-load or constant-displacement) test performed at a stress intensity equivalent to K_{or} if the values of t_{io} in both tests are equal. In the single-step test, K_o is held for the entire incubation period following which crack growth initiates at t_i. In the rising-load test, on the other hand, the stress intensity is lower than K_{or} at all times prior to the onset of crack growth. Since the lower values of K correspond to longer incubation times, the effective incubation time of the rising-load test is longer. This relationship is next formulated.

10.5.1 Mathematical Model for Step- or Rising-Load Test

A method of computing K_{or} from the t_i results of single-step tests as well as from K_{Ic} and K_{arr} was suggested in Appendix B of Ref. 1-1. The incubation phase of the step- or rising-load tests was modeled as a succession of load steps (at $K_j = K_1, K_2, K_3$, etc.) of equal spacing (i.e. $\Delta K = K_3-K_2 = K_2-K_1$, etc.) and time duration, Δt. The incubation-time credit for each such step was defined as the ratio of Δt to t_{ij}, the latter being the incubation time of a single-step test performed entirely at the stress intensity K_j. The incubation time of the step- or rising-load test should terminate when the sum of the

successive incubation-time credit terms (or $\Sigma(\Delta t/t_{ij})$) becomes unity. From Equation 10-1, $t_{ij} = t_{io}\,(-\ln \kappa_j)$ and therefore the incubation time of the step-load test should satisfy the condition

$$\Sigma \frac{\Delta t}{t_{ij}} = \Sigma \frac{\Delta t}{t_{io}(-\ln \kappa_j)} = \frac{1}{\dot{\kappa}} \Sigma \frac{\Delta \kappa}{(-\ln \kappa_j)} = 1$$

in which

$$\kappa_j = \frac{K_j - K_{arr}}{K_{Ic} - K_{arr}}, \qquad \Delta\kappa = \frac{\Delta K}{K_{Ic} - K_{arr}};$$

$$\dot{\kappa} = \frac{\dot{K}\, t_{io}}{K_{Ic} - K_{arr}}, \quad \text{and} \quad \dot{K} = \Delta K/\Delta t$$

Adaptation from the step-loading case to that of continuously rising K consists merely of taking the summation to the limit of $\Delta t = 0$ at constant $\dot{K}$:

$$\dot{\kappa} = \Sigma \frac{\Delta \kappa}{(-\ln \kappa_j)} = \int_0^{\kappa_{or}} \frac{d\kappa}{(-\ln \kappa)}$$

in which

$$\kappa_{or} = \frac{K_{or} - K_{arr}}{K_{Ic} - K_{arr}}$$

The integral was evaluated numerically and is tabulated in Table 10-1, which shows the relationship of κ_{or} to $\dot{\kappa}$.

It is implicit in this model that no incubation-time credit is gained from the early part of the rising-load test while K is less than K_{arr}. The duration of this part is $K_{arr}/\dot{K}$ (in a test started at zero load) and is designated "dead" time. The "active" incubation time t_{ia} begins as soon as K reaches K_{arr} and is given by $(K_{or} - K_{arr})/\dot{K}$. Only this active component of the incubation time is derivable from the normalized, reduced stress intensity κ.

The "normalized excess active time", τ_{ea}, listed in Table 10-1 is defined by

$$\tau_{ea} = \frac{t_{ia} - t_i}{t_{io}}$$

in which t_i is the incubation time of a single-step test performed at $K_o = K_{or}$, and t_{ia} is the active component of the incubation time in a rising-load phase terminating at K_{or}. From the definitions of the latter quantities,

$$\tau_{ea} = \frac{K_{or} - K_{arr}}{\dot{K}\, t_{io}} + \ln \kappa_{or} = \frac{\kappa_{or}}{\dot{\kappa}} + \ln \kappa_{or}$$

A plot of $\log \kappa_{or}$ against t_{ia}/t_{io} is linear at values of κ_{or} below about 0.3, the fitted formula being

$$\log \kappa_{or} = 0.31 - 0.42 \frac{t_{ia}}{t_{io}} \qquad (\text{for } t_{ia} \geq 2\, t_{io})$$

An example of the use of these relationships is next presented for a rising-load test at a rate, $\dot{K}$, of 0.10 ksi $in^{1/2}$/h on a material-environment combination with the properties described previously, viz. K_{Ic} = 125 ksi $in^{1/2}$; K_{arr} = 25 ksi $in^{1/2}$; and t_{io}(env) = 250 h. Starting at zero load yields a dead time of 250 h, after which κ is finite. Since $\dot{\kappa}$ = 0.25, the value of κ_{or} obtained from Table 10-1 is 0.40, from which K_{or} = 65 ksi $in^{1/2}$. This rising-load test result is 2.6 times K_{arr}, and therefore it would be a very poor approximation of K_{arr} (or K_{Iscc}).

The normalized excess active time is obtained from Table 10-1 is 0.66. The actual active time is 400 h and the total time prior to crack-growth onset is 650 h.

In the actual course of such a test, K_{arr} remains unknown until it is measured at crack arrest. The analysis of the rising-load phase must therefore await the K_{arr} result. In the present example, at least,

the measured K_{or} is not a suitable approximation of K_{arr} and is instead a measure of the incubation-time constant, $t_{io}(env)$, as next demonstrated.

The dependence of K_{or} on $t_{io}(env)$ may be formulated from the relationships already presented in Table 10-1. For $\kappa_{or} \leq 0.3$, a useful formula is

$$\dot{\kappa} = \frac{\dot{K} t_{io}}{K_{Ic} - K_{arr}} = \frac{0.42\ \kappa_{or}}{0.31 - \log \kappa_{or}} \qquad (\text{for } \kappa \leq 0.3)$$

This relationship indicates the dependence of κ_{or} on both the incubation time constant t_{io} and the imposed loading rate $\dot{K}$. The latter are combined as a simple product in the definition of $\dot{\kappa}$, as shown above. As $\dot{\kappa}$ increases, κ_{or} increases monatonically with it (Table 10-1).

Since κ_{or} represents the (normalized) difference between K_{or} and K_{arr}, this quantity may also be viewed as the error, in effect, of using the rising-load test result, K_{or}, as an approximation of K_{arr}. The dependence of κ_{or} on $\dot{\kappa}$ indicates that as either the loading rate or the incubation-time constant increases, the error represented by κ_{or} also increases.

In the example already considered, K_{Ic} and K_{arr} were 125 and 25 ksi $in^{1/2}$, respectively, and $\dot{K}$ was 0.10 ksi $in^{1/2}/h$. The latter is much lower than the loading-rate range of 5 to 25 ksi $in^{1/2}/h$ used routinely in H_2S rising-load tests. The dependence of K_{or} on t_{io} is illustrated in Table 10-3 for the conditions of the example except that $\dot{K}$ is taken as 10 ksi $in^{1/2}/h$. The error represented by the difference between the listed values of K_{or} and the actual K_{arr} of 25 ksi $in^{1/2}$ is minor at the lowest values of t_{io} but becomes appreciable as t_{io} exceeds about 0.1 hour. This is short relative to the incubation times observed in H_2S testing HY-130 plate and weld-metal specimens, and therefore appreciable differences between K_{or} and K_{arr} must be expected in such specimens.

10.6. Modified Rising-load Test Model.

We now finally return to the modified rising-load test. During the incubation (no-crack-growth) phase, this test is identical to the simple rising-load test in which the stress intensity increases at a constant rate, $\dot{K}$. With the onset of crack growth at K_{or}, the apparatus switches to holding constant displacement. Thus the crack-growth phase is essentially equivalent to that in a bolt-load test, eventually terminating in crack arrest where K_{arr} is measured.

The main advantage of the modified test over the simple rising-load test is in providing K_{arr} as its principal result. Since K_{or} is measured also, an estimate may be made of $t_{io}(env)$.

The main advantage of a rising-load test over an ordinary bolt-load test is in the fact that the specimen is loaded in the test environment rather than in air, with the consequence that the incubation-time constant t_{io} is significantly reduced. The disadvantages include (a) the requirement that relatively sophisticated and costly apparatus be tied up for possibly long times, and (b) reliance for continuous control of displacement on sensitive instruments that may not be as stable in a long-term test as the simple bolt. The test is therefore preferable for use with systems having relatively short values of both t_{io} and t_{go}.

The constant-displacement phase of the test is similar to the simple bolt-load test already considered. In both tests there is a minor increase of v_o, the specimen displacement at the load line, as the crack grows. In the bolt-load case this effect is due to the finite elasticity of the loading bolt, as already discussed.

In the rising-load test the displacement is continuously measured with a clip gauge or LVDT mounted outboard of the load line, as indicated by the sketch in Fig. 5-2. As the crack grows, the output signal from the gauge is held constant by automatic adjustment of the load. A consequence is gradual increase of the displacement at the load line.

Any increase of v_o during crack growth is undesirable because it increases the arrest length of the crack and makes the determination of K_{arr} less exact. Such effects have not been taken into account in development of the present model, in which it is assumed simply that the load-line displacement is constant during crack growth.

The modified rising-load test is thus modeled as a simple rising-load test (at $0 < K < K_{or}$) followed by a constant-displacement test initiated at K_{or}. For the conditions considered previously where K_{or} was 2.6 times K_{arr}, the time for crack-growth onset was 650 h. The additional time for the crack to grow to a length corresponding to a κ' value of 0.03 is 3 t_{go} or 300 h. The total time of 950 h is considerably shorter than that required by alternative methods of estimating K_{arr} in the system considered. To establish K_{arr} as 25 rather than as 28 ksi $in^{1/2}$ requires additional test time. Even so, the modified rising-load test is a relatively efficient way of determining K_{arr} in a single test within a reasonable length of time, and it is therefore considered to be a practical test for this purpose.

10.6.1. Test of Model with EZH-23

The model just described may be used for indicating the time dependence of both the stress intensity and the load during crack growth at constant displacement. The description is exact if the crack growth rate, $\dot{a}$, is proportional to $\sqrt{\kappa}$ as assumed in the original premises. This premise is next critically examined with the aid of the detailed records of the H_2 modified rising-load test of Specimen EZH-23, a description of which was presented in Part 9. A complete record of the load and displacement as a function of time during crack growth was obtained in this one test. The time-base recorder chart speed was 2 in/h, and the load decline appeared to be essentially complete within 30 minutes (= 1 inch on the recorder chart).

The rising-load phase of the test was performed at a $\dot{K}$ value of 2 ksi $in^{1/2}$/h and terminated at a K_{or} value of 71 ksi $in^{1/2}$, at which point the crack-growth phase was signalled by a load drop (at constant clip-gauge displacement) within a 31- minute period from 13.3 to 0.26 kips. The final estimate of K_{arr} was 30 ksi $in^{1/2}$.

The incubation-time constant t_{io} was estimated from the above relationships as 14.5 h. This estimate was based in part on the arbitrary assumption that the fracture toughness, K_{Ic}, of the 10 Ni steel was 130 ksi $in^{1/2}$. This is probably erroneously low, and a more accurate value of K_{Ic} might be 230 ksi $in^{1/2}$. The effect of making such a correction of K_{Ic} (from 130 to 230 ksi $in^{1/2}$) is to change t_{io} from 14.5 to 8.2h.

The recorded load and displacement during only the crack-growth phase of the test are listed in Table 10-2. From the corresponding elastic compliance data, the listed values of the net crack length a_1 were obtained from tabulated elastic compliance data (e.g. Table 5-2), and the accompanying values of K were obtained from appropriate calibration tables (e.g. Table 5-2). The arrest values of a_1 and K thus determined are 1.57" and 25.5 ksi $in^{1/2}$ respectively. The actually measured final crack length was 1.62", however, and the "best estimate" of K_{arr} was 30 ksi $in^{1/2}$. For the present computational purposes only the former, uncorrected figures will be used.

The premise that å is proportional to $\sqrt{K}$ has not been previously tested for conditions approaching crack arrest. Preliminary fitting to the present data yielded the tentative relationship

$$\text{å (in/min)} = 0.02\sqrt{K(\text{ksi } in^{1/2}) - 25.5}$$

Combining this formula with the values of K listed in Table 10-2 yielded the "calculated" values of å listed in the column adjoining the "actual" values of å in Table 10-2. The column headed "error" shows the difference between the calculated and actual values of å for each time interval. The large, positive errors early in the crack growth process can be attributed to nonsteady crack growth, as discussed by Hudak and Wei (10-2).

This phenomenon was specifically omitted from the present treatment in order to simplify the model, and the accompanying "error" does not detract from the validity of the premise that $\dot{a}$ is proportional to $\sqrt{\kappa}$ after the nonsteady crack-growth period has passed.

The errors shown for the conditions approaching crack arrest are probably associated mainly with uncertainties of measurement of the extremely low loads and are not necessarily due to flaws of the model. The much smaller errors in the intermediate crack-length range are due in part to the fact that this was the range empirically fitted. The consistency of the fit over a significant portion of the range seems sufficient, however, to instill confidence in the premise that $\dot{a}$ is proportional to $\sqrt{\kappa}$. The proportionality constant, k, is 0.20"/min if K_{Ic} is taken as 130 or 0.28"/min if K_{Ic} is taken as 230 ksi $in^{1/2}$. The corresponding values of t_{go} are 4 min and 2.8 min respectively.

The crack-growth time to reach a κ value of 0.03 was estimated above as 3 t_{go}, or 12 min for the case where K_{Ic} is 130 ksi $in^{1/2}$. In the present test this time was actually 15 min, the extra 3 min being consumed by the early nonsteady crack growth. The additional time for κ to go from 0.03 to zero was taken as 16 min. Thus the value of t_{arr} at the cutoff κ of .03 was about 4 t_{go}, and that for a κ value of essentially zero was about 8 t_{go}. Since t_{go} was only 4 min, the total time for arrest was not excessive.

10.7. Conclusion

It is considered that the premises and assumptions of the proposed model are sufficiently valid to justify the use of this model in the interpretation of short-time environmental cracking tests, including specifically rising-load tests. The treatment clearly indicates that K_{or}, the stress intensity of crack-growth onset in a step- or rising-load test, is larger than K_{arr} (or K_{Iscc}) by an amount that depends on both the rate of loading in the test and the incubation-time constant, which is itself a function of the material, the environment and the conditions of loading. It is a misleading and potentially dangerous

practice, therefore, to refer to K_{or} as "K_{Iscc}" or even as "apparent K_{Iscc}".

The modified rising-load test procedure described above is suggested as a way of measuring both K_{or} and K_{arr} in a single test. In one case (EZH-23) where complete records of load and displacement in such a test were available, the ratio of K_{or} to K_{arr} was 2.4 and that of t_{io} to t_{go} was 218. Under such conditions the modified rising-load test is an efficient way of evaluating K_{arr} in a relatively short time.

In certain situations the modified rising-load test is impracticable and K_{or} alone must be used as an approximate measure of a material's resistance to cracking in a specified environment. An example drawn from the present work is the H_2S rising-load testing of precracked Charpy specimens, where only K_{or} could be measured. In the case of HY-130 weld D, K_{or} values measured in short-time rising-load tests of precracked Charpy specimens varied from 37 to 51 ksi $in^{1/2}$ (Table 4-1). In the much longer-term load-cell test of the same weld, K_{or} was between 23 and 26 ksi $in^{1/2}$ (Table 5-1). This difference is consistent with the dependence of K_{or} on the loading rate ($\dot{K}$) or test time as derived in the foregoing treatment, and it demonstrates that K_{or} is not a simple property of the material-environment system.

It would be convenient for the present testing purposes if there were a firm relationship between K_{or} and K_{arr}, such that the results of simple rising-load tests of precracked Charpy specimens could be used to estimate the rank order of K_{arr} (or K_{Iscc}) values in screening evaluations. However, the alloy composition effects shown in Figs. 10-1 and 10-2 indicate that such is probably not the case. Both plots show data for failure time (t_f) rather than incubation time (t_i). It now seems reasonable to assume that t_i is some significant fraction of t_f in the constant-load tests depicted in these plots. In Figure 10-1 the respective values of t_{fo} (and probably also t_{io}) vary over a factor of 600 while the respective values of K_{arr}/K_{Ic} were essentially the same in five of the six steels depicted. In Figure 10-2 there is similar agreement of the respective K_{arr} values in spite of the over two-fold difference of the

respective values of t_{fo}. It therefore appears that the incubation-time constant t_{io} is essentially unrelated to K_{arr}. Since K_{or} is a sensitive function of t_{io}, it does not now seem possible to derive significant design-useful information from the results of step- or rising-load tests alone. A major exception to this conclusion is the case where t_{io} is extremely small in comparison with the time of the test, in which event the difference between K_{or} and K_{arr} is also extremely small. Such a condition seems to characterize certain high-strength (>200 ksi) steels tested in H_2S. The steels of primary concern in the present work, however, had yield strengths near 130 ksi. The rising-load and load-cell tests of such steels in H_2S indicated that t_{io} was <u>not</u> extremely short, from which it is concluded that K_{or} may be appreciably larger than K_{arr} in step- and rising-load tests of such steels.

In certain situations such as the present work where only Charpy specimens are available and only K_{or} can be measured as an indication of environmental cracking susceptibility, the limitations of conclusions based on such test results must be kept in mind. It is necessary to realize that K_{or} is not necessarily related in any simple way to K_{arr}, and therefore it cannot be used interchangeably with the latter (or with K_{Iscc}) as a design-useful measure of a material's resistance to environmental cracking. Actually K_{or} depends on both K_{arr} and t_{io} with a contribution also from the imposed loading rate. Usually t_{io} is not a design-useful property because it is an insignificant fraction of the required life of a structure. The present formulations thus indicate the shortcomings of using rising-load test results in design and suggest that data more directly related to K_{arr} are preferable.

11. CONCLUDING DISCUSSION AND SUMMARY

A goal in the design of welded structures is to have the design-controlling properties of all welded-joint elements (i.e. the weld metal and heat-affected zone) match those of the base plate. In HY-130 weldments, for example, the tensile properties of the weld metal approximate those of the base plate to the greatest practicable extent. In structures exposed to degrading environments, however, the design is controlled not by the tensile properties but by the structure's susceptibility to environment-enhanced crack growth. In seawater with applied cathodic polarization, such crack growth is caused primarily by hydrogen introduced from the environment.

The long-term objective of the present program is the development of HY steel weld metals with improved resistance to environmental hydrogen-enhanced subcritical cracking (scc). As an initial step toward satisfying such an objective, the work described in this report had the purpose of qualifying and calibrating two potentially useful laboratory techniques: (a) the preparation of Charpy-size test specimens by induction-levitation melting and chill casting, and (b) the evaluation of the environmental hydrogen cracking susceptibilities of these specimens by the H_2S rising-load method.

The levitation-melted castings were prepared and found to have satisfactory reproducibility of all measured properties, including hardness, tensile and impact properties, and environmental cracking resistance. The latter was gauged by K_{or}, the stress intensity of crack-growth onset in the H_2S rising-load test. The K_{or} data were valid according to a "conservative" interpretation of ASTM E399 (Ref. 1-4).

The values of K_{or} measured on castings made by levitation melting high-purity metal-powder compacts were higher than those of castings made by levitation remelting HY-130 plate, probably because of the latter's

higher impurity content. On this preliminary basis, therefore, the procedure appears to be a potentially useful technique for alloy screening in the development of HY steel weld metals with improved resistance to environmental hydrogen cracking.

The values of K_{or} for the levitation-melted castings (simulated HY-130 weld metals) were lower than those of actual HY-130 weld metals of similar compositions, and both were lower than those of HY-130 plate specimens. The main reason for these differences was microstructural, with K_{or} varying inversely with the grain size. This relationship was confirmed by the repeated finding that H_2S cracking occurred in coarse-grained zones but not in fine-grained zones of HY-130 weld-metal specimens.

A major purpose of the present work was to determine the suitability of the H_2S rising-load test as an accelerated method of comparing various materials' resistances to environmental hydrogen-enhanced scc. The test was based on a suggestion by McIntyre and Priest (1-2) that such a technique can provide measurements of K_{Iscc} in other hydrogenous media. Such an interpretation is suggested in a recent review by Clark and Landes (1-3) that is introduced by the following statements:

"In 1972 McIntyre and Priest reported that the K_{Iscc} values determined for a series of high-strength steels (200 to 400 ksi yield strength) exposed to seawater, hydrogen (H_2) gas, and hydrogen sulfide (H_2S) gas environments were essentially independent of the test environment. In addition, they noted that the corresponding crack-growth rates in the H_2S gas environment were of the order of three to four orders of magnitude faster than that encountered in either seawater or H_2 gas. On the basis of these observations, McIntyre and Priest have proposed that K_{Iscc} testing in H_2S gas can be used as an accelerated test procedure for evaluating a material's stress-corrosion threshold in other hydrogen bearing environments. More specifically, the proposed test procedure involves conventional rising load K_{Ic} fracture-toughness testing in a H_2S environment. The stress-intensity level associated

with the onset of crack growth encountered in such a test is interpreted as the material's K_{Iscc}. Preliminary results involving this accelerated test method show that the time required to determine K_{Iscc} values can be reduced from many hours to a few minutes."

The early-rising-load tests described in these papers were performed in load control (constant $\dot{P}$), which causes self-acceleration of the crack growth. The main result of such a test is K_{or}, which is a function of both $\dot{P}$ and the incubation characteristics of the material-environment combination tested. The suggested equivalence of K_{or} and K_{arr} (or K_{Iscc}) is possible only if the incubation-time constant t_{io} is vanishingly small relative to the time consumed by the test. Although this may have been true of the high-strength steels tested by McIntyre and Priest, it is not generally true of materials with lower yield strengths, as next discussed.

The tests of the precracked Charpy specimens in the present program consisted of H_2S rising-load tests in displacement control (constant $\dot{v}$). Related tests of larger (1T WOL) specimens confirmed that K_{or} is not equivalent to K_{Iscc} (or K_{arr}) in steels of moderate yield strength. Instead, the tests of such steels conducted at ordinary loading rates (values of $\dot{K}$) yielded values of K_{or} that exceed K_{arr} (or K_{Iscc}) by significant amounts (errors) that are themselves sensitive functions of the loading rate ($\dot{K}$). Since K_{or} is thus a function of the test conditions, it is not a simple, single-valued property of the material-environment system suitable for use in design. This conclusion applies also to the results of environmental step-load tests performed at similar average values of $\dot{K}$.

Fortunately, no such ambiguity characterizes K_{arr} (or K_{Iscc}), the threshold stress intensity below which no crack growth will occur at any time. K_{arr} is measurable at crack arrest in a simple constant-displacement test.

In view of the design significance of K_{arr}, a modification of the rising-load test used in both the present work and that for NSRDC (1-1) consisted of switching from the rising-load condition (at constant $\dot{v}$) to the constant-displacement condition (zero $\dot{v}$) at the onset of crack growth. This modified rising-load test allowed the crack to grow to arrest at constant displacement and thereby provided evaluation of both K_{or} and K_{arr} in a single test.

Although the modified rising-load test procedure was applied to specimens of both Charpy and WOL design, usefully measurable crack-arrest values of K_{arr} could not be obtained in the Charpy specimens because of excessive elasticity of the loading system. The resulting, effective spring loading of the Charpy specimen led to an excessive crack length at arrest, and the only measurable test result was K_{or}.

Two 1T WOL specimens of HY-130 Welds D and F, respectively, were tested by the load-cell method, which offered the advantages of both loading in the test environment and continuous load monitoring. Neither specimen yielded a K_{arr} result, however. Weld F experienced arm failure distant from the weld, and Weld D experienced catastrophic crack growth after the stress intensity was increased from 23 to 26 ksi $in^{1/2}$. The latter are bracketing values of K_{or} for a step-loading test of much longer duration (weeks vs hours) than a rising-load test. The significant influence of test time (or $\dot{K}$) on K_{or} is evident from a comparison of this relatively long-term K_{or} result with the K_{or} range of 37 to 52 ksi $in^{1/2}$ measured in rising-load tests of similarly oriented Charpy specimens from the same weld. This confirms that K_{or} depends on the rate or time of testing and is not a simple property of the material-environment combination.

Unlike similar tests of HY-130 plate, the load-cell tests of the ungrooved 1T WOL weld-metal specimens exhibited no evidence of short-length crack arrest associated with crack tunneling. This is additional evidence of the weld metal's lower resistance to environmental hydrogen cracking.

Although the load-cell test method was nominally a constant-displacement technique, its elastic compliance was too large to allow crack arrest at usefully measurable values of the crack length, and therefore K_{arr} could not be determined in such a test. The load-cell method was nevertheless informative in demonstrating both the incubation and tunnel-arrest behavior of the materials tested.

These experiments indicated that limitations of the originally intended laboratory techniques include

a) possibly inadequate simulation of weld-metal microstructure in the levitation-melted castings for the intended alloy screening purposes,

b) possibly inadequate range of measured stress intensity (K_{or}) values in testing future, improved castings by the H_2S rising-load method,

c) inability of the (modified) rising-load test of a Charpy specimen to provide K_{arr} (or K_{Iscc}), and

d) lack of sufficient information on the relationship of the measured K_{or} to the more design-useful K_{arr} (or K_{Iscc}) in either H_2S or the intended actual environment of seawater with applied cathodic polarization.

Because of these limitations, a major effort was made to develop accelerated test methods capable of efficiently measuring K_{arr}. In the simultaneously performed work for NSRDC on HY steel plates, modified rising-load tests and bolt-load tests of 1T WOL specimens provided values of both K_{or} and K_{arr} in both H_2S and H_2. The values of K_{or} were usually about double those of K_{arr} in tests of HY-130 steel specimens consuming several hours or days in H_2S. The fact that K_{arr} is so much smaller than K_{or} is itself a sufficient reason for preferring to measure K_{arr} in small-specimen tests in which the plane-strain validity may be marginal. Accordingly, a major objective of the present work was to determine how K_{arr} might be efficiently measured in screening studies of candidate HY steel weld metals.

Both the present experiments and those for NSRDC suggested improved techniques for determining K_{arr} in minimum test time. Since K_{arr} cannot now be evaluated in Charpy-size specimens of moderate yield strength, the technique development was concentrated on 1T CT and WOL specimens of steels with yield strengths between 80 and 140 ksi. Each specimen is sidegrooved to a depth that will provide a straight crack front at arrest. The slowly rising-load phase of the modified rising-load test is replaced by cyclic loading in the test environment (environmental fatigue) at sufficiently high values of K_{max} to produce rapid crack growth. The cyclic loading is performed in displacement control to allow K_{max} to decrease during the environmental fatigue (pre)cracking. Switching to static loading at the final amplitude (v_{max}) of the fatigue-precracking phase is usually sufficient for the continuation of the environmental crack growth at constant displacement. Suitable control of the displacement leads to eventual crack arrest. This method provides measurement of K_{arr} in minimum time, since the incubation time of the conventional rising-load test is very significantly reduced by the environmental fatigue precracking step.

ACKNOWLEDGEMENTS

The financial support for this work came from the Office of Naval Research Contract N00014-77-C-0372. The ONR administrators are Dr. Philip Clarkin and Dr. Bruce MacDonald, whose continuing interest is appreciated. The work was coordinated closely with a NAVSEA program on "Subcritical Cracking of High Strength Steel Weldments" managed by Dr. H. H. Vanderveldt. Technical coordination was provided by Mr. C. A. Zanis of the David W. Taylor Naval Ship Research and Development Center (DTNSRDC). We wish to thank Mr. Zanis for providing the HY steel weldments tested in this program as well as for his many technical contributions.

Within Westinghouse, Dr. F. C. Hull initiated the preparation and testing of the levitation-melted castings. The levitation melting and hardness readings were performed by William McMunn. The environmental crack-growth testing was performed by L. J. Ceschini, C. M. McGuire, Ronald Smykal, J. R. Malley and G. L. Donahue. Robert Burland assisted with the fractography.

PERMANENT RECORD BOOK ENTRIES

Book Numbers 208076 (all) and
208506, pp. 42-138

REFERENCES

1-1. E. W. Johnson and B. J. Shaw, "Environmental Hydrogen Cracking Susceptibilities of High Strength Steels", Final Report, U.S. Navy Contract N00600-77-C-0991. April 5, 1979.

1-2. P. McIntyre and A. H. Priest, "Accelerated Test Technique for the Determination of K_{Iscc} in Steels", British Steel Corp. Report MG/31/72, 1972.

1-3. W. G. Clark and J. D. Landes "An Evaluation of Rising Load K_{Iscc} Testing" in Stress Corrosion-New Approaches, ASTM STP 610, 1976, pp. 108-127.

1-4. ASTM E399-74, "Standard Method of Test for Plane-Strain Fracture Toughness of Metallic Materials," 1974 Annual Book of ASTM Standards.

1-5. S. R. Novak and S. T. Rolfe, "Modified WOL Specimen for K_{Iscc} Environmental Testing," Journal of Materials, JMLSA, 4 (3), 1969, p. 701.

1-6. B. K. Neale, "The Influence of Crack Shape on Fracture Toughness Testing" International J. of Fracture 12 (3), 1976, p. 499.

1-7. S. R. Novak, "A Fracture Mechanics Analysis of the Kinetics of Stress-Corrosion Crack Growth in a High-Strength 12 Ni- 5 Cr - 3 Mo Maraging Steel", Ph.D. Thesis to University of Pittsburgh, 1977.

2-1. G. Comenetz and J.C.R. Kelly, Jr., "Containment of Hot Matter (Levitation Melting, Cage Melting, and Drip-Pool Melting)," in High Temperature Materials and Technology, Edited by I. E. Campbell and E. M. Sherwood, 1967, The Electrochemical Society, John Wiley and Sons, New York, p. 600.

2-2. J. Heuschkel et al., "Development of a Steel, Weld Metal, and Welding Procedure Capable of Producing 150,000 psi Yield Strength in Heavy Sections," Final Report, U.S. Navy Contract NObs-78823, Dec. 18, 1962.

2-3. ASM Metals Handbook, Vol. 1 of 8th Edition. Table of Rockwell C Hardness Conversions for Steel, p. 1236. ASM, Metals Park, OH, 1973.

3-1. "Rapid Inexpensive Tests for Determining Fracture Toughness" National Materials Advisory Board, National Research Council Publication NMAB-328, National Academy of Sciences, 1976.

4-1. C. A. Zanis, "High Strength Steel Weldment Subcritical Cracking Program", Baseline Study Summary Report, DTNSRDC Annapolis Laboratory, November, 1978.

4-2. T.M.F. Ronald, J. A. Hall and C. M. Pierce, "Usefulness of Precracked Charpy Specimens for Fracture Toughness Screening Tests of Titanium Alloys," Met. Trans 3, 1972,p. 813.

7-1. E. W. Johnson, "Hydrogen Stress Cracking Susceptibilities of High Strength Steels," U.S. Navy Contract N00600-77-C-0991 Second Quarterly Report, March 30, 1978.

7-2. T. K. Hellen and S. J. Protheroe, Computer Aided Design, 6 (1), 1974, p. 15.

8-1. B. J. Shaw and E. W. Johnson, "The Role of the Fatigue Precrack as a Component of the Incubation Time in Hydrogen Embrittlement of HY-180 Steel", draft of scientific paper to be submitted in 1979 for journal publication.

8-2. A. S. Tetelman and A. J. McEvily, Jr. Fracture of Structural Materials p.308 (1967), Wiley and Sons, New York.

10-1. R. P. Wei, S. R. Novak and D. P. Williams, "Some Important Considerations in the Development of Stress Corrosion Cracking Test Methods," Materials Research and Standards, 12 (9), 1972, p. 25 (ASTM).

10-2. S. J. Hudak, Jr., and R. P. Wei, "Consideration of Nonsteady State Crack Growth in Materials Evaluation and Design", Paper for Proceedings of the 5th International Conference on Structural Mechanics in Reactor Technology, Berlin, August, 1979.

10-3. W. D. Benjamin and E. A. Steigerwald, "Environmentally Induced Delayed Failures in Martensitic High-Strength Steels," Tech. Rep. AFML-TR-68-80 Wright-Patterson Air Force Base, OH (1968). Same data also replotted in Met. Trans. 2, 1971, p. 606.

10-4 A. A. Sheinker, "Effect of Rare Earth Additions on Stress Corrosion Cracking of 4340 Steel," Technical Report ER-7814-3 to Office of Naval Research for Contract N00014-74-C-0365, Jan. 1978.

Table 2-1. Correlation of Yield and Ultimate Strengths with Rockwell C Hardness of Wrought HY Steels and Comparison with Data in ASM Metals Handbook (Ref. 2-3).

R_c	0.2%-Offset YS (ksi)	Ref. 2-2 UTS (ksi)	Ref. 2-3 UTS (ksi)
20	100	112	110
21	102	114	113
22	105	117	115
23	107	119	118
24	110	121	121
25	112	123	124
26	115	126	127
27	118	129	131
28	121	131	134
29	123	134	138
30	126	137	142
31	130	140	146
32	133	144	150
33	136	147	154
34	139	151	159
35	143	154	163
36	147	158	168
37	151	163	172
38	155	168	176
39	160	173	181
40	165	179	186
41	169	186	191
42	174	193	196
43	179	201	201
44	184	212	206
45	188	224	212
46	193	232	219
47	198	239	225
48	203	244	232
49	207		239
50	212		245

TABLE 2-2 Nominal Compositions and Mechanical Properties of HY-130/150 Levitation-Melted Castings.

No.	Reference	Nominal Composition, wt %										Impact ft-lbs	Hardness R_C	Approximate UTS(ksi)
		C	Mn	Si	Ni	Cr	Mo	V	W	Cu	Ce+La			
0-1	VM514	0.07	1.36	0.02	2.52	0.90	1.33	0.62				90	34.2	152
0-2	VM517	0.10	0.66	0.01	2.52	1.08	2.49	0.34				75	36.7	161
0-3	VM526	0.11	0.95	0.036	3.28	0.65	1.18	0.88				90	36.7	161
0-4	VM529	0.07	1.56	0.007	3.32	0.45	2.67	0.11				34	34.1	151
0-5	Casting X1	0.10	0.25	--	4.75	1.0	0.6	--	1		0.05	34	37.0	163
0-6	Casting X2	0.10	0.25	--	4.75	0.8	0.6	0.1	0.5	0.3	0.05	60	38.1	168
0-7	McKay SMA	0.10	0.9	0.3	3.4	0.45	0.75					90	35.2	155
0-8	Airco	0.10	1.8	0.3	2.2	1.0	0.6					24	36.9	163
0-9	Linde	0.10	1.6	0.35	2.6	0.75	0.9					23	39.6	176

Table 2-3. Average Rockwell C Hardness of Levitation-Melted Castings Derived by Remelting HY-130 Steel Plate

Series L			Series R		
Specimen ID	Average R_C	SD*	Specimen ID	Average R_C	SD*
L-2	35.3	1.2	R-1	36.5	2.5
L-3	35.7	2.3	R-2	34.8	1.7
L-4	33.4	1.1	R-3	34.9	2.0
L-5	36.8	0.9	R-4	35.6	1.9
overall Avg.	35.3	1.4	R-5	35.4	1.8
			R-6	36.7	0.9
			R-7	36.3	0.9
			R-8	34.9	0.5
			R-9	36.4	1.3
			R-10	35.3	1.0
			overall Avg.	35.7	0.7

*SD = Standard Deviation. The SD listed next to the overall average R_C hardness was calculated from the individual-specimen average R_C hardness values alone.

Table 2-4. Average Rockwell C Hardness of Levitation Melted Castings of Series A

Single-melted Castings Tested in As-cast Condition

Specimen ID	Average R_C	SD*
A-11	35.3	1.0
A-12	34.8	1.3
A-13	34.7	0.8
A-15	35.1	1.2
A-16	35.2	1.2
A-17	33.7	1.0
A-20	33.3	1.3
overall Avg.	34.6	0.8

Single-melted Castings Tested After Machining to Charpy Bars

Specimen ID	Average R_C	SD*
A-4	30.6	1.0
A-6	32.7	1.0
A-3	35.5	0.9
A-2	33.8	0.8
overall Avg.	33.	2.

Double-melted Castings Tested in As-cast Condition

Specimen ID	Average R_C	SD*
A-21R	35.8	0.7
A-23R	35.7	0.7
A-25R	34.0	2.1
A-27R	37.9	0.9
A-29R	37.6	1.2
overall Avg.	36.2	1.6

*SD = Standard Deviation. The SD listed next to the overall average R_C hardness was calculated from the individual-specimen average R_C hardness values alone.

Table 2-3. Average Rockwell C Hardness of Levitation-Melted Castings Derived by Remelting HY-130 Steel Plate

Series L			Series R		
Specimen ID	Average R_c	SD*	Specimen ID	Average R_c	SD*
L-2	35.3	1.2	R-1	36.5	2.5
L-3	35.7	2.3	R-2	34.8	1.7
L-4	33.4	1.1	R-3	34.9	2.0
L-5	36.8	0.9	R-4	35.6	1.9
overall Avg.	35.3	1.4	R-5	35.4	1.8
			R-6	36.7	0.9
			R-7	36.3	0.9
			R-8	34.9	0.5
			R-9	36.4	1.3
			R-10	35.3	1.0
			overall Avg.	35.7	0.7

*SD = Standard Deviation. The SD listed next to the overall average R_c hardness was calculated from the individual-specimen average R_c hardness values alone.

Table 2-5

Results of Mechanical Tests of Charpy-size Castings of Series A

Specimen ID	0.2% Offset YS (ksi)	UTS (ksi)	El. (%)	R.A. (%)
A-1	122	156	15	58
A-5	111	156	16	65
A-13	117	167	15	54
A-16	113	163	14	54
A-20	113	151	14	58
A-23R	120	163	15	55
Avg.	116.0	159.3	14.8	57.3
Std. Dev.	4.4	6.0	0.8	4.2

Specimen ID	CVN Impact ft-lbs	Lateral Expansion (in)
A-2	63	.038
A-3	48	.028
A-15	60	.036
A-21R	69	.040
Avg.	60	.036
Std. Dev.	9	.005

Table 2-6. Chemical Compositions of HY-130 Steel Plates Remelted by Levitation to Make Castings of Series L, R and P.

HY-130 Plate ID = Casting Series =	D, F Base Metal L, R	FKS P
% C	0.11	0.11
Mn	0.85	0.76
P	0.005	0.005
S	0.006	0.004
Si	0.24	0.31
Ni	4.91	5.00
Cr	0.54	0.42
Mo	0.52	0.53
V	0.09	0.043
Cu		0.022
Ti		0.008
Al		0.021
N		0.011
As		0.004
Sb		0.001
Sn		0.006
Co		0.002
O		0.0032

Table 3-1. Precracked Charpy Specimen Elastic Compliance and K Calibration Data: P in kips, v in mils, K in ksi $in.^{1/2}$

	For v measured at specimen				For $v_m = 1.95P$	
					Effective	
a_1(in.)	a/W	v/P	K/P	K/v	v_t/P	K/v_t
0.01	0.228	1.83	20.7	11.3	3.78	5.5
0.02	0.254	1.94	22.1	11.4	3.89	5.7
0.03	0.279	2.06	23.6	11.5	4.01	5.9
0.04	0.305	2.20	25.2	11.5	4.15	6.1
0.05	0.330	2.36	26.9	11.4	4.31	6.2
0.06	0.355	2.54	28.8	11.3	4.49	6.4
0.07	0.381	2.74	30.8	11.2	4.69	6.6
0.08	0.406	2.98	33.0	11.1	4.93	6.7
0.09	0.431	3.26	35.4	10.9	5.21	6.8
0.10	0.457	3.59	38.1	10.6	5.54	6.9
0.11	0.482	3.96	41.2	10.4	5.91	7.0
0.12	0.508	4.41	44.6	10.1	6.36	7.0
0.13	0.533	4.94	48.6	9.8	6.89	7.1
0.14	0.558	5.56	53.1	9.6	7.51	7.1
0.15	0.584	6.31	58.2	9.2	8.26	7.0
0.16	0.609	7.21	67.2	9.3	9.16	7.3
0.17	0.635	8.30	74.3	9.0	10.25	7.2
0.18	0.660	9.65	82.8	8.6	11.60	7.1
0.19	0.685	11.34	93.0	8.2	13.29	7.0

Table 3-2. Conditions and Results of H_2S Rising-Load Tests of Precracked Charpy Castings

Specimen ID	Net Precrack Length(in)	$\dot{K}$ (ksi$\sqrt{in}$/h)	K_{or} ksi$\sqrt{in}$
A-4	0.043	15	21
A-6	.029	15	33
A-11	.069	5	28
A-17	.062	5	24
A-25R	.059	5	34
Series A Avg.			28.0
SD			5.6
P-C	.040	14	18
R-3	.057	5	21
R-6	.034(?)	14	16
Series P/R Avg.			18.3
SD			2.5

Table 4-1. Conditions and Results of H_2S Crack-Growth Tests Of Precracked Charpy Specimens of HY-130 Weld D.

First Phase - Vertical Notch

Specimen	Net Precrack Length(in)	$\dot{K}$ (ksi$\sqrt{in}$/h)	K_{or} (ksi$\sqrt{in}$)
D1-3	.064	18	>50
D1-2	.064	13	37
D1-1	.115		52

Second Phase - Horizontal Notch

D2-2	.062	5	18
D2-1	.010	5	70

Table 5-1. Weld Specimens D-5 and F-5 Load Cell Tests-Daily Readings of Load (kips) and K (ksi $in^{1/2}$)

Weld Specimen ID		D-5		F-5	
		Load	K	Load	K
#Days of Step 1:	0	5.64	23	5.51	23
	1	5.23	23	5.40	23
	2	5.26	23	5.36	23
	3	--		--	
	4	--		--	
	5	--		--	
	6	5.19	23	5.32	23
	7	5.18	23	5.30	23
	8	5.20	23	5.31	23
	9	5.18	23	5.30	23
	10	--		--	
	11	--		--	
	12	--		--	
	13	5.14	23	5.19	23
#Days of Step 2:	0	6.40	26	6.40	26
	1	0.07	--	1.05	--
	1	0	0	0	0

Table 5-2. 1T WOL Specimen Calibration and Effects of Added Loading-System Elastic Compliance (C_s) and Piston Load (P_p)

	Standard Calibration			K/v_{eff} (ksi$\sqrt{in}$/mil) for C_s, P_p combinations								P/v_{eff} (kips/mil)		
C_s (mils/kip)=				0	0.085	1.0		2.0		3.0		0	1.0	
P_p (lbs)=				0	0	0	47	0	47	0	47	0	0	47
a_1 (in)	a/W	K/P ($in^{-3/2}$)	v_o/P (C_e) (mils/kip)	K/v_o (ksi$\sqrt{in}$/mil)										
0	0.301	4.11	.592	6.94	6.07	2.58	2.60	1.59	1.61	1.14	1.16	1.689	.628	.633
0.1	.340	4.48	.717	6.24	5.59	2.61	2.63	1.65	1.67	1.21	1.23	1.395	.582	.587
0.2	.379	4.87	.864	5.64	5.13	2.61	2.63	1.70	1.72	1.26	1.28	1.157	.536	.540
0.3	.418	5.31	1.036	5.12	4.74	2.61	2.64	1.75	1.78	1.32	1.35	0.965	.491	.497
0.4	.458	5.81	1.242	4.68	4.38	2.59	2.62	1.79	1.82	1.37	1.40	.805	.446	.451
0.5	.497	6.41	1.489	4.30	4.07	2.58	2.61	1.84	1.87	1.43	1.46	.672	.402	.407
0.6	.536	7.15	1.794	3.99	3.81	2.56	2.60	1.88	1.92	1.49	1.53	.557	.358	.364
0.7	.575	8.09	2.177	3.72	3.58	2.55	2.59	1.94	1.98	1.56	1.60	.459	.315	.320
0.8	.615	9.30	2.677	3.47	3.37	2.53	2.58	1.99	2.04	1.64	1.69	.374	.272	.277
0.9	.654	10.91	3.354	3.25	3.17	2.51	2.56	2.04	2.09	1.72	1.77	.298	.230	.235
1.0	.693	13.12	4.31	3.04	2.98	2.47	2.53	2.08	2.14	1.79	1.85	.232	.188	.193
1.1	.732	16.24	5.75	2.82	2.78	2.41	2.49	2.10	2.18	1.86	1.94	.174	.148	.153
1.2	.771	20.85	8.04	2.59	2.56	2.31	2.41	2.08	2.18	1.89	1.99	.1244	.1106	.1156
1.3	.811	28.07	12.02	2.34	2.32	2.16	2.30	2.00	2.14	1.87	2.01	.0832	.0768	.0819
1.4	.850	40.43	19.72	2.05	2.04	1.95	2.15	1.86	2.06	1.78	1.98	.0507	.0483	.0532
1.5	.889	64.8	37.5	1.73	1.72	1.68	2.00	1.64	1.96	1.60	1.92	.0267	.0260	.0309
1.6	.928	126.6	93.8	1.35	1.35	1.34	1.96	1.32	1.94	1.31	1.93	.0107	.0105	.0155
1.65	.948	206	182	1.13	1.13	1.13	2.14	1.12	2.13	1.11	2.12	.0055	.0055	.0104
1.70	.967	420	480	0.88	0.88	0.87	2.93	0.87	2.93	0.87	2.93	.0021	.0021	.0070
1.75	.987	1685	3130	0.54	0.54	0.54	8.80	0.54	8.80	0.54	8.80	.0003	.0003	.0052
1.783	1.000			0	0	0	∞	0	∞	0	∞	0	0	0

Table 5-3. EZH-2 Load-cell Test in H_2S: Daily Reading of Load (kips)

Step No.		1	2	3	4	5	6
K(ksi$\sqrt{in}$)		14.9	16.6	19.0	21.3		
Nom. P(kips)		2.5	2.8	3.2	3.6	3.0	3.6
Day of Step:	0	2.52	2.80	3.20	3.60	3.00	3.60
	1	2.52	2.80	3.20	3.60	2.91	1.02
	2	2.52	2.80	--	3.59	2.76	
	3	--	2.76	--	--	--	
	4	2.52	2.80	3.20	--	--	
	5	2.52	--	3.20	3.60	--	
	6	2.52	2.80	3.20	3.58	2.72	
	7	2.52	2.80		3.58	2.65	
	8	2.52	2.80		2.82	2.64	
	9	2.52	--		2.72	2.61	
	10	2.52	2.76		2.72	--	
	11		--		--	--	
	12		--		2.72	--	
	13		2.76		2.60	2.64	
	14		2.76		2.52		
	15		2.76		2.52		
	16		2.76		2.52		
	17				2.48		
	18				--		
	19				2.52		
Comment		Precrack a_{ledge} = 0.30"			Crack grew 0.12" at surface		

Table 5-4. FKZ-S1 Load-cell and Bolt-load Test in H_2S: Daily Readings of Load (kips)

		Load-cell Test Steps				Bolt-Load Steps		
Step No.		1	2	3	4	5	6	7
K(ksi$\sqrt{in}$)		27	30	35	39	44		
Nom. P(kips)		5.0	5.6	6.4	7.2	8.2	10.0	11.0
Day of Step:	0	5.00	5.60	6.40	7.23	8.24	10.00	11.0
	1	4.97	5.60	6.40	7.19	--	--	--
	2	4.97	5.60	--	7.19	8.24	--	--
	3	--	5.54	--	--	7.84	--	0.32
	4	4.97	5.60	6.40	--	7.64	--	
	5	4.97	--	6.40	6.94	7.60	--	
	6	4.87	5.57	6.40	7.00	6.89	--	
	7	4.87	5.57		7.02	6.89		
	8	4.97	5.57		7.18	--	--	
	9	4.97	--		7.10	6.89	--	
	10	4.97	5.51				--	
	11		--				--	
	12		--				--	
	13		5.51				9.90	
	14		5.51					
	15		5.51					
	16		5.51					
Comments						Minor tunnel growth		Major crack growth

TABLE 10-1 Incubation-Time Relationships in Rising-Load Tests: Relationships of $\dot{\kappa}$, κ_{or}, and Normalized Excess Active Time Over That of Single-Step Tests.

$\dot{\kappa}$	κ_{or}	$(t_{ia} - t_i)/t_{io}$
0.0001	0.00075	0.89
0.0002	0.00148	0.88
0.0003	0.00210	0.88
0.0007	0.0044	0.87
0.0013	0.0075	0.86
0.0024	0.0125	0.83
0.0036	0.0175	0.82
0.0049	0.0225	0.80
0.0062	0.0275	0.80
0.0077	0.0325	0.80
0.0091	0.0375	0.80
0.010	0.040	0.80
0.020	0.069	0.80
0.030	0.095	0.79
0.040	0.117	0.78
0.050	0.137	0.77
0.060	0.157	0.76
0.070	0.175	0.76
0.080	0.192	0.75
0.100	0.225	0.73
0.120	0.252	0.72
0.150	0.290	0.71
0.20	0.348	0.68
0.25	0.396	0.66
0.30	0.439	0.64
0.40	0.515	0.62
0.50	0.575	0.59
0.60	0.626	0.57
0.70	0.670	0.55
0.80	0.708	0.54
1.00	0.770	0.51
1.25	0.825	0.47
1.50	0.867	0.44
1.75	0.900	0.41

Table 10-2. Record of crack growth in modified H_2 rising-load test of 10 Ni Specimen EZH-23.

time (min)	P (kips)	$v_{0.65}$ (mils/kip)	a_1 (in)	K (ksi$\sqrt{in}$)	calc'd å (in/min)	actual å (in/min)	error
0	13.28	22.0	0.32	71.3	0.14		
0.5					.13	0.02	0.11
1	12.78	22.0	0.34	70.0	.13		
2.5					.13	.07	.06
4	9.08	22.1	0.55	61.7	.12		
5.5					.11	.12	-.01
7	4.68	22.2	0.91	51.5	.10		
8.5					.09	.09	.00
10	2.18	22.2	1.19	44.4	.09		
11.5					.07	.08	-.01
13	0.78	22.2	1.42	34.6	.06		
14					.05	.05	.00
15	0.38	22.2	1.52	28.4	.034		
18.5					.026	.006	.020
22	0.28	22.2	1.56	26.2	.017		
26.5					.008	.001	.007
31	0.26	22.2	1.57	25.5	.000		

Table 10-3 Dependence of K_{or} on t_{io}

(at $\dot{K}$ = 10 ksi$\sqrt{in}$/h,
K_{arr} = 25 ksi$\sqrt{in}$
K_{Ic} = 125 ksi$\sqrt{in}$)

t_{io} (hours)	K_{or} (ksi$\sqrt{in}$)
0.0010	25.1
.0025	25.2
.010	25.6
.025	26.3
.10	29.0
.25	33.0
1.0	47.5
2.5	65.
10.	102.
25.	121.
100.	125.

412C889

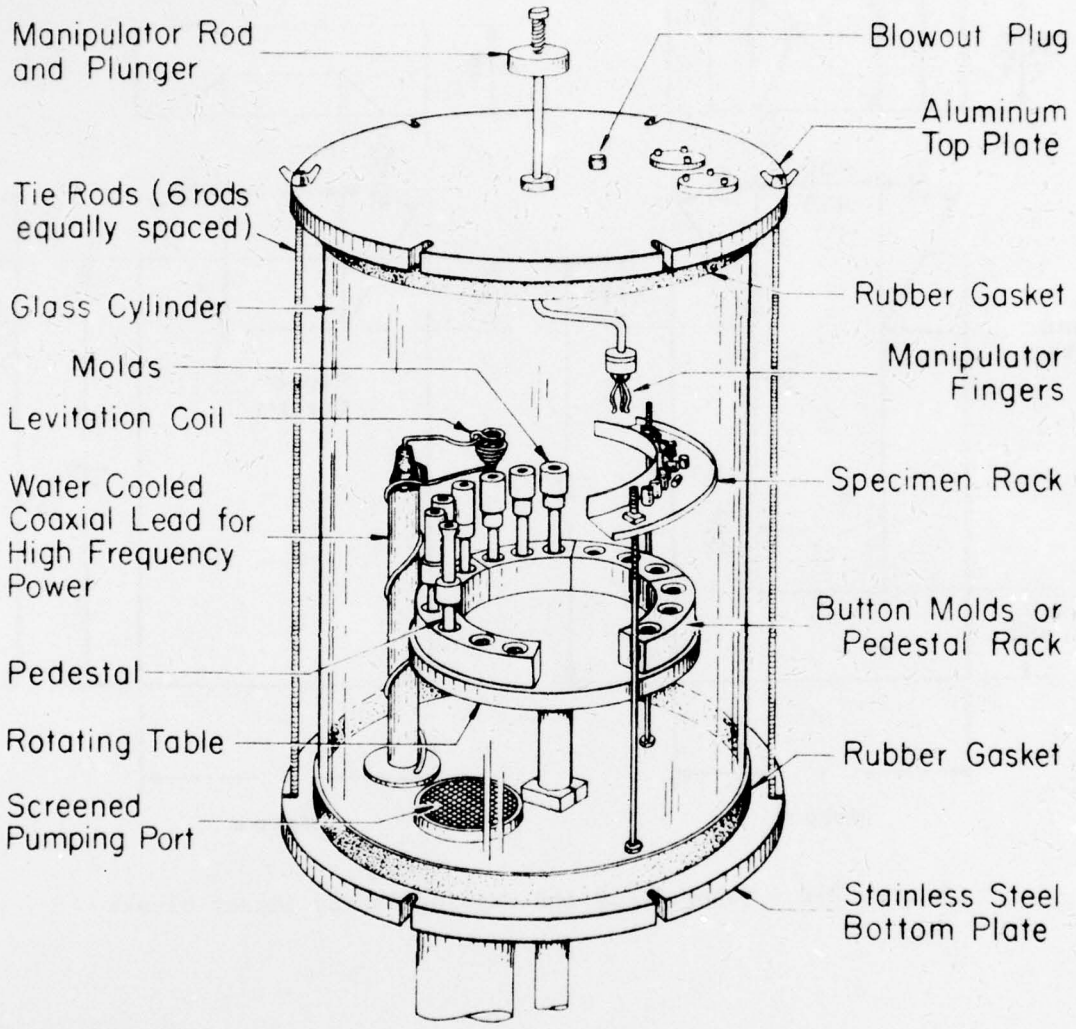

Figure 2-1 - Levitation melting furnace. Melting atmosphere is high-purity inert gas.

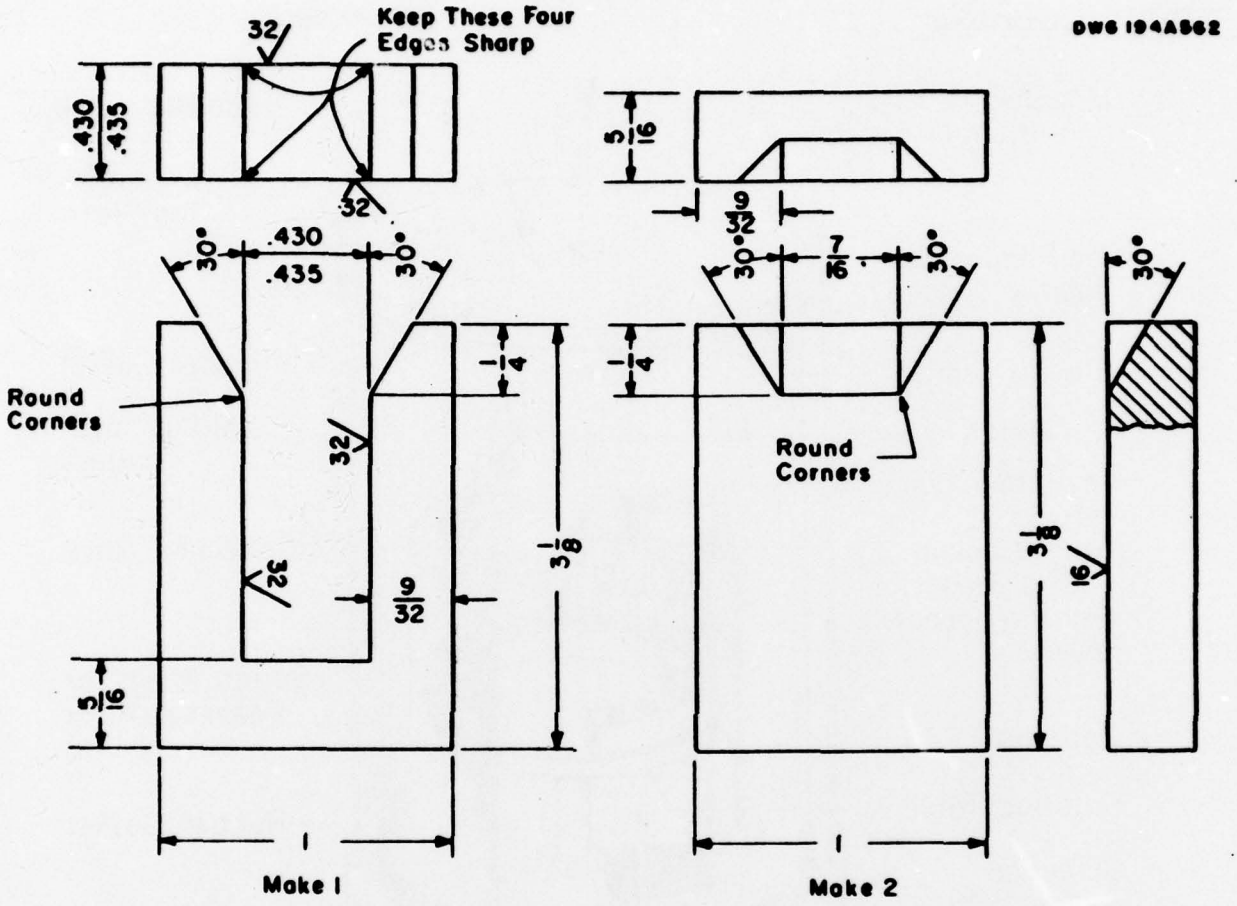

Figure 2-2 - Copper mold for casting Charpy impact blanks

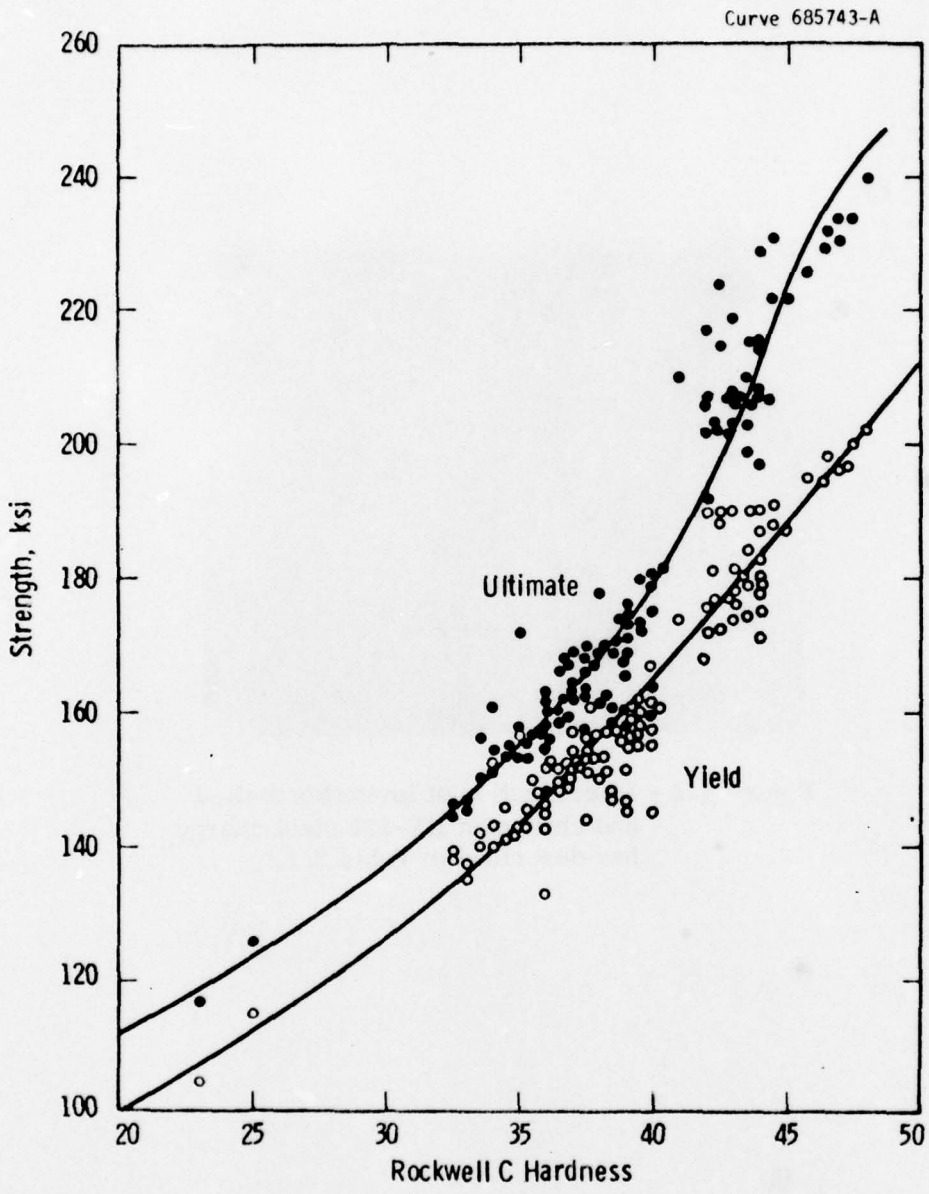

Figure 2-3- Correlation of Rockwell C hardness with yield and ultimate tensile strengths of wrought HY type steels.

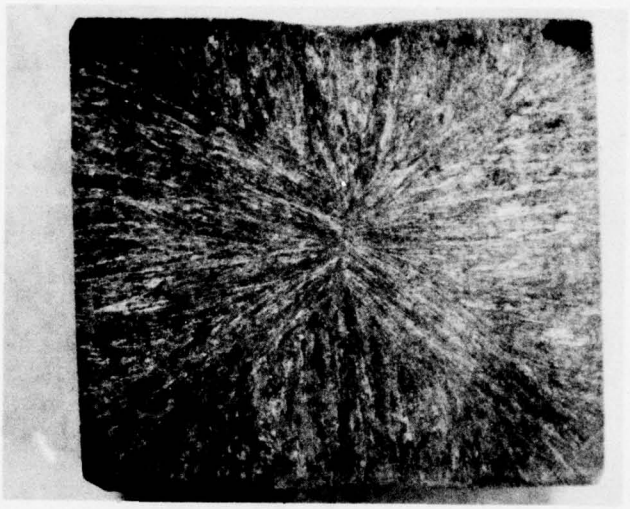

Figure 2-4 - Macrosection of levitation melted and chill-cast HY-150 steel charpy bar described in Table 3.1.

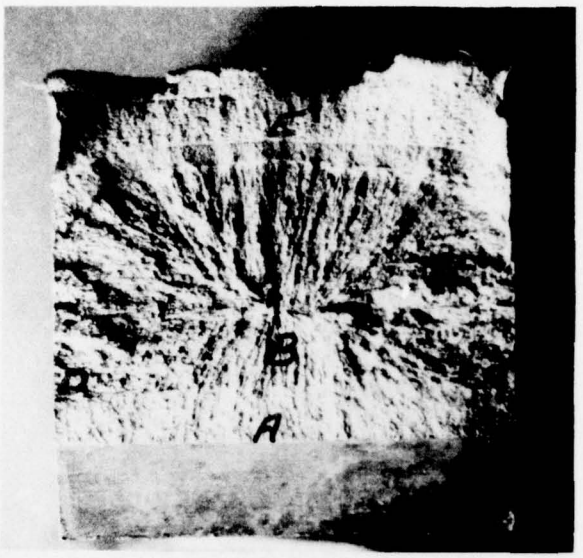

x 6.5

Fig. 3-1 Optical macrograph of the fracture surface of Specimen A-4. Position A indicates the pre-fatigue zone, B the center of the hydrogen embrittled fracture surface and E the ductile fracture surface produced by overloading in air. A scanning electron microscope view of the brittle zone B is shown in Fig. 3-9

x 5

Fig. 3-2 Optical macrograph of fracture surface of Specimen A-11

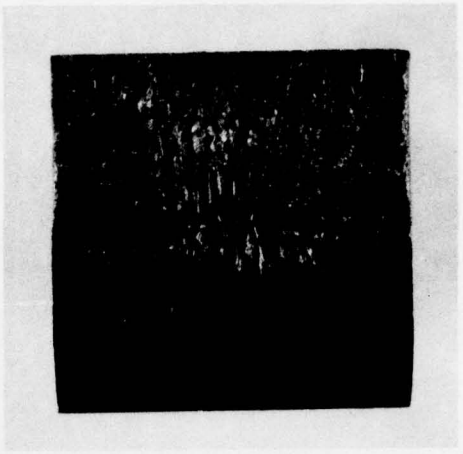

x 5

Fig. 3-3 Optical macrograph of fracture surface of Specimen A-17

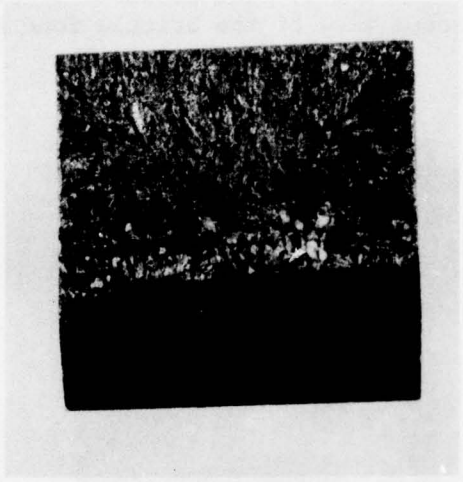

x 5

Fig. 3-4 Optical macrograph of fracture surface of Specimen A-25R

x 10

Fig. 3-5 Optical macrograph of fracture surface of Specimen P-C. A scanning electron microscope view of the intergranular fracture surface is shown in Fig. 3-8.

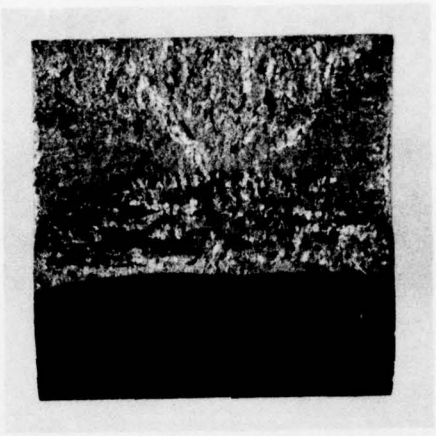

x 5

Fig. 3-6. Optical macrograph of fracture surface of Specimen R-3

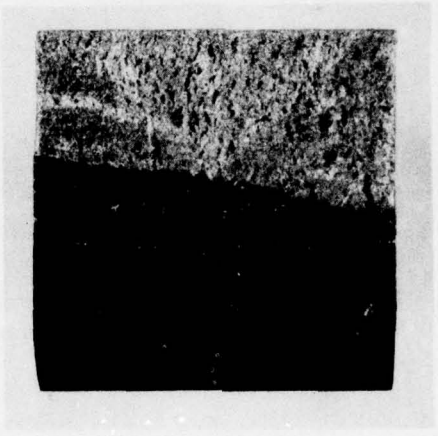

x 5

Fig. 3-7 Optical macrograph of fracture surface of Specimen R-6

Angle of view 36°

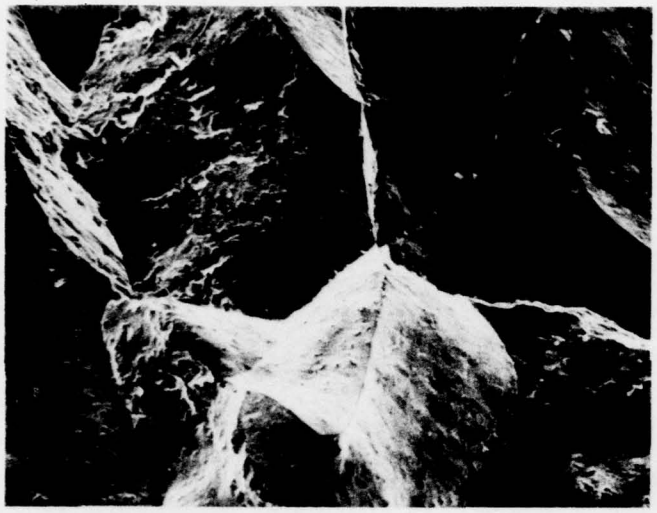

44°

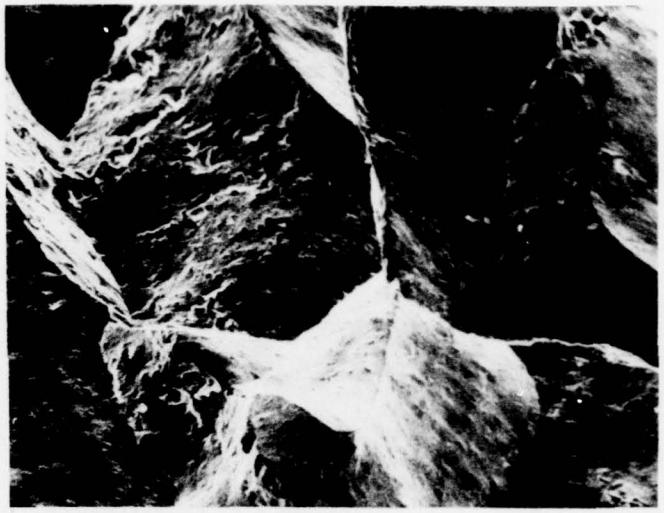

x 500

Fig. 3-8. Scanning electron microscope stereo views of the fracture surface of the center of Specimen P-C showing 100% intergranular fracture produced in the H_2S environment. See. Fig. 3-5.

RM-81213

Angle of view 37° 45°

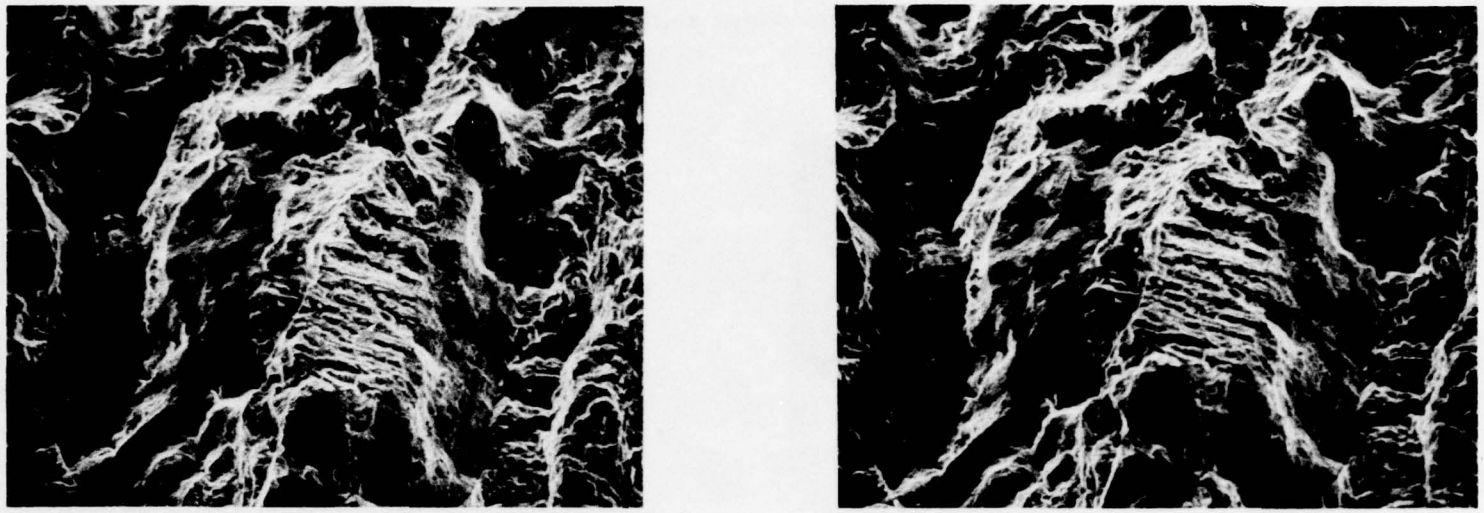

x 500

Fig. 3-9. Scanning electron microscope stereo views of the fracture surface of Specimen A-4. This H_2S-environment fracture surface is a mixture of cleavage and intergranular fracture and was taken from position B in Fig. 3-1.

Figure 4-1 - Macroetched full-thickness (1.5") section through Weld D, showing size of weld bead.

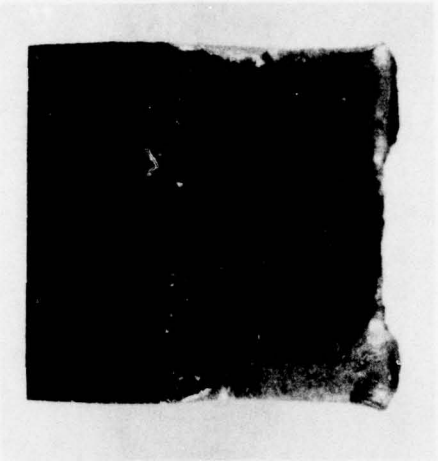

Figure 4-2 - Charpy specimen D1-2 fracture surface, showing serrated H_2S crack front

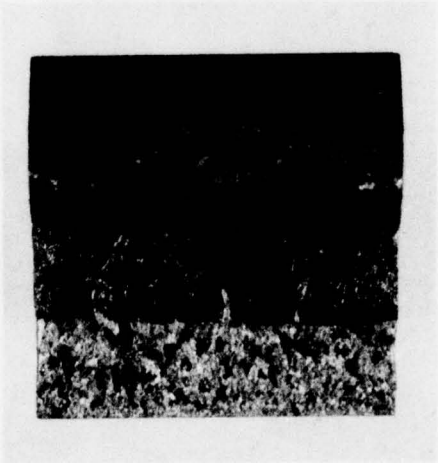

Figure 4-3 - Charpy specimen D2-2 fracture surface

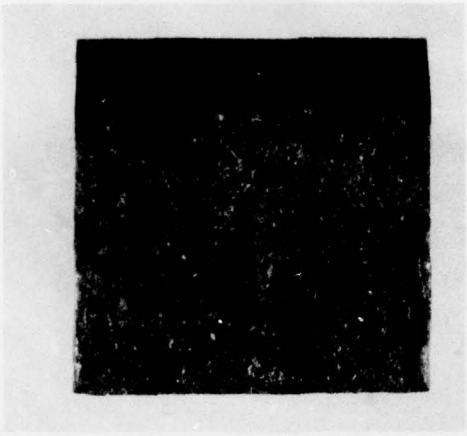

Figure 4-4 - HY-130 weld-metal Charpy specimen D2-1 fracture surface

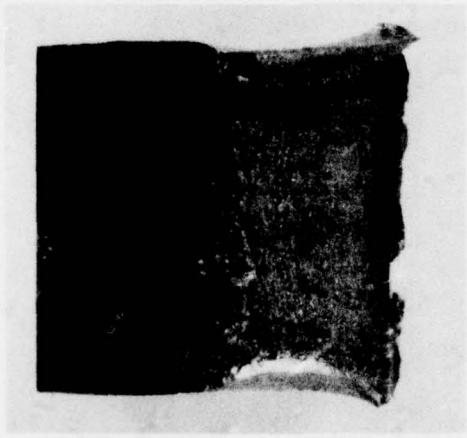

Figure 4-5 - HY-130 Weld-metal Charpy specimen F1-2 fracture surface

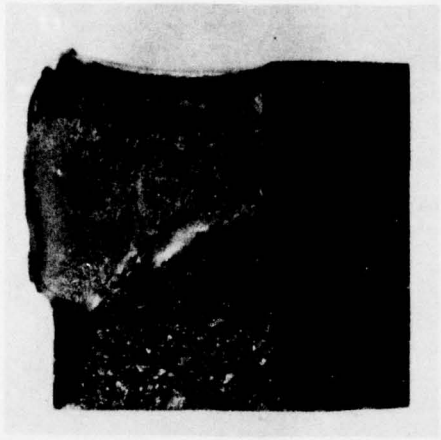

Figure 4-6 - HY-130 weld metal Charpy specimen F1-3 fracture showing arc-shaped H_2S crack front in only lower (coarse-grained) half of specimen

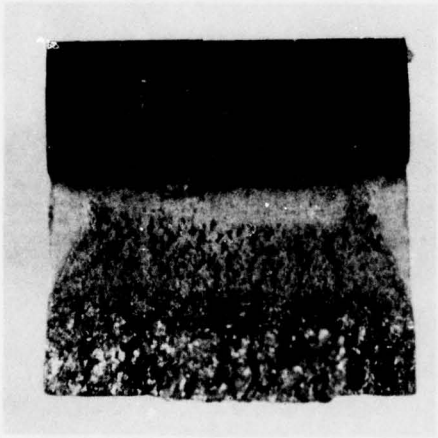

Figure 4-7 - HY-130 weld metal Charpy specimen F2-3 fracture

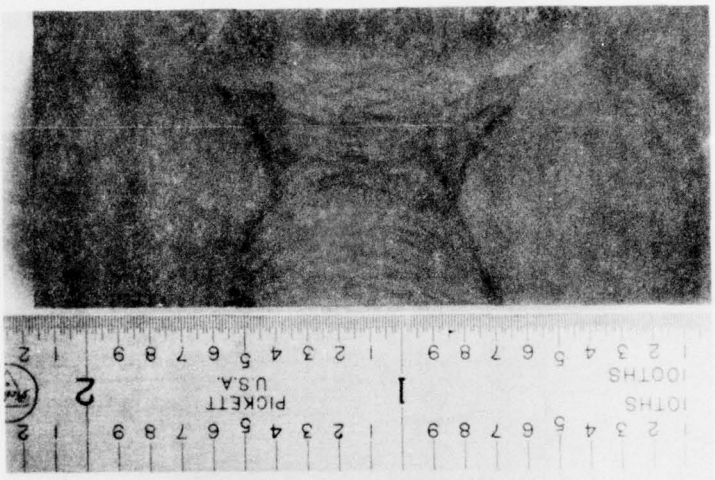

Figure 4-8 - Macroetched section of upper 2/3 of Weld Q, showing coarse-grained final surface passes

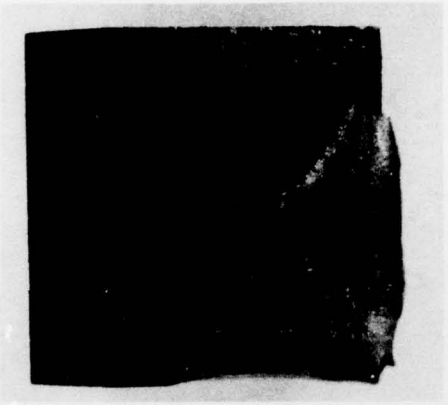

Figure 4-9 - Weld-metal Charpy specimen QS1-1 fracture, showing diagonal H_2S crack front

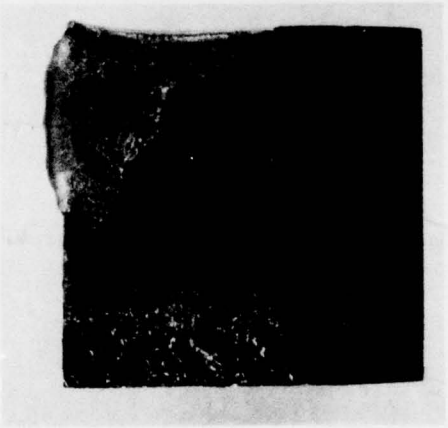

Figure 4-10 - Weld-metal Charpy specimen QS1-3, showing diagonal H_2S crack front

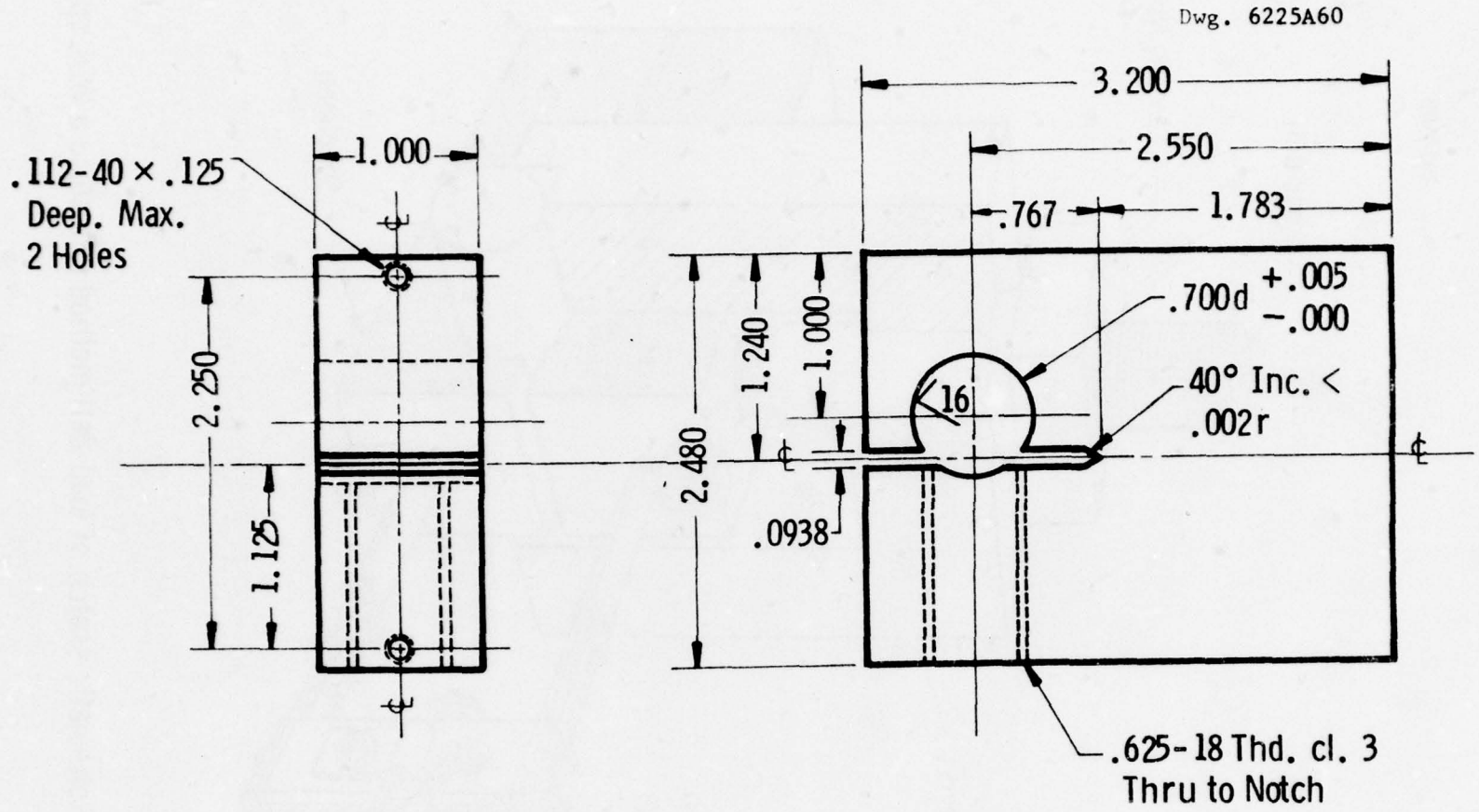

Fig. 5-1 — 1T WOL specimen modified for bolt loading

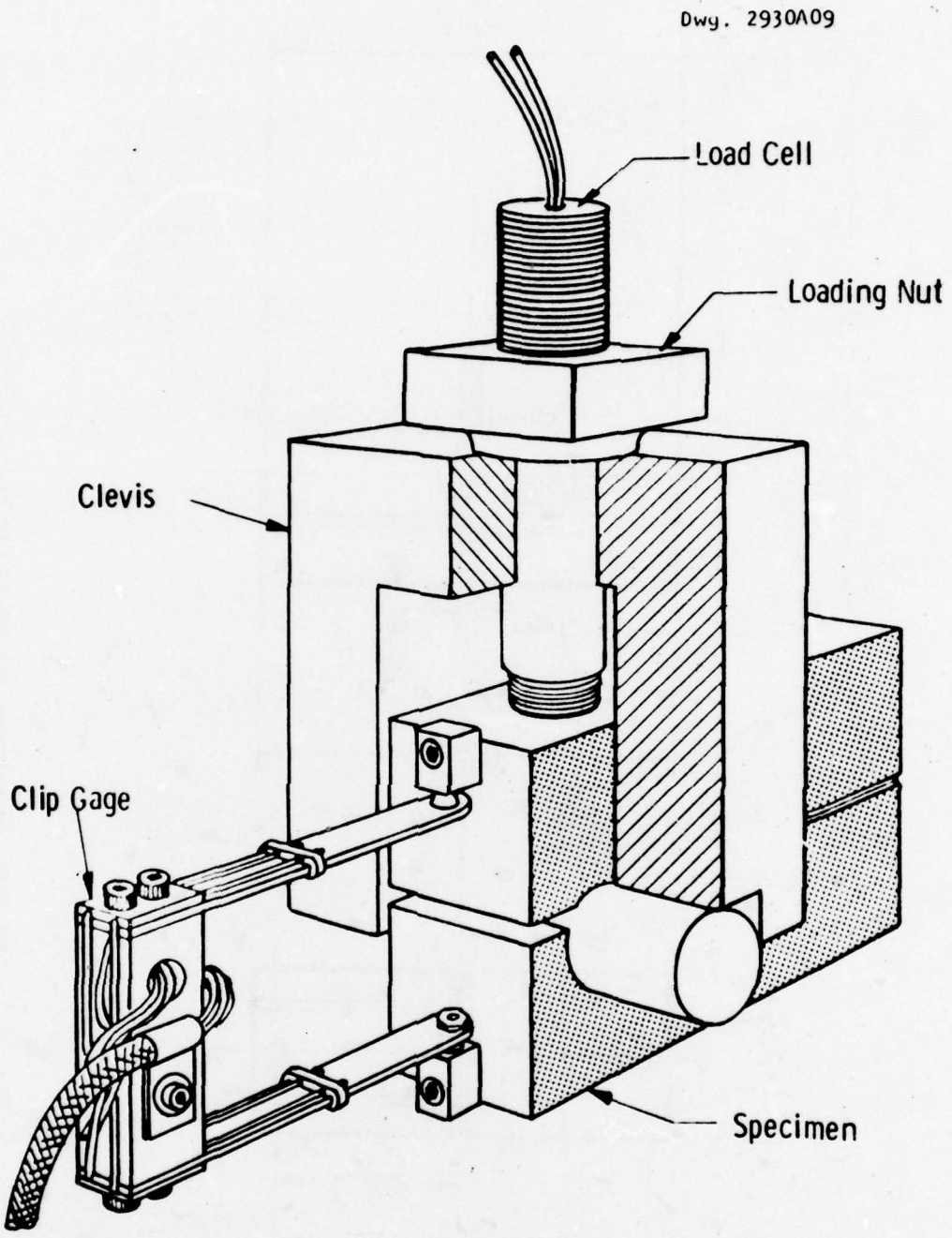

Fig. 5-2 — Schematic sketch of load-cell method of testing a WOL specimen

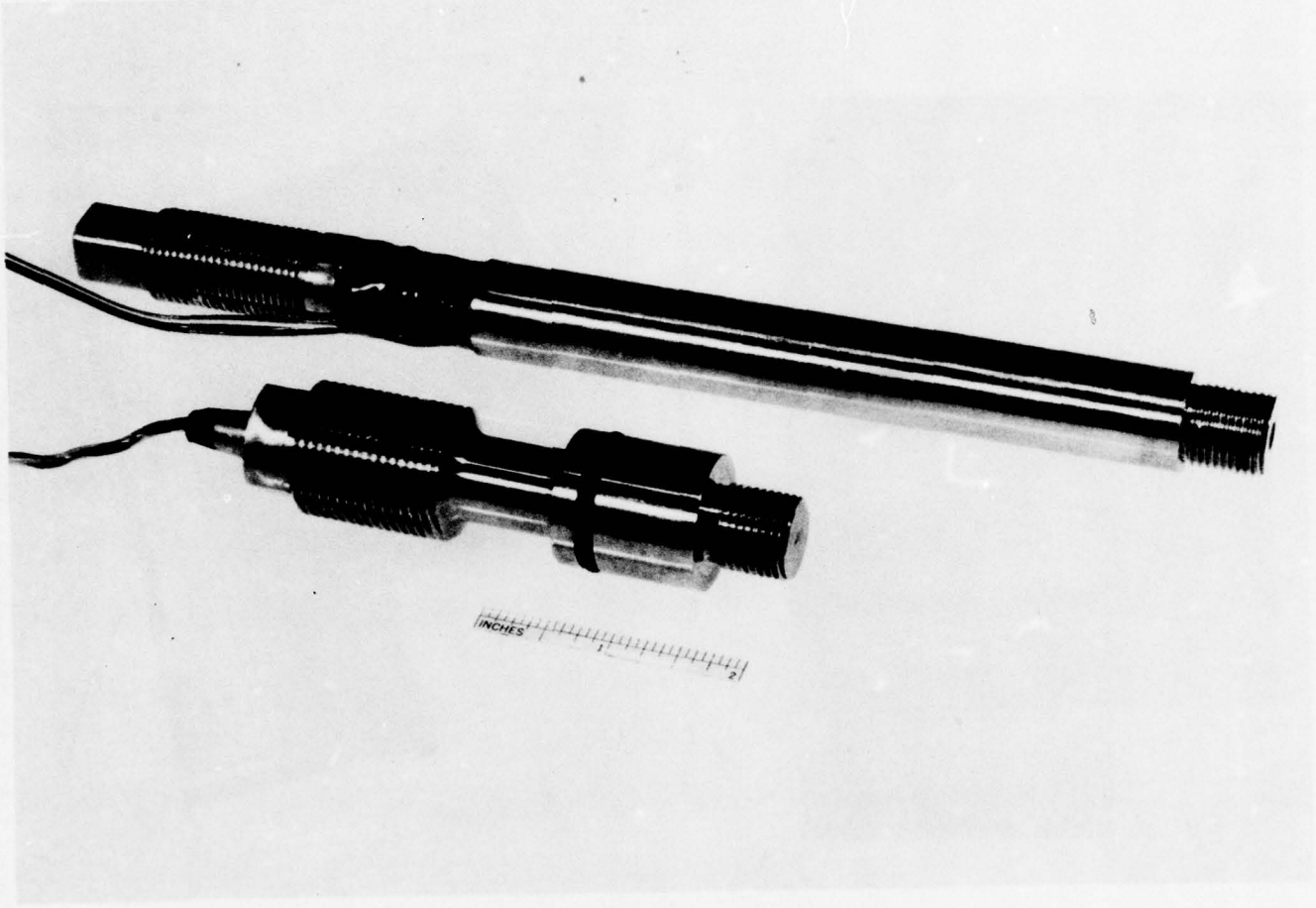

Fig. 5-3 – Photograph of two designs of load-cell device. (O-ring of lower device serves as pressure seal in gaseous environment testing)

RM-72482

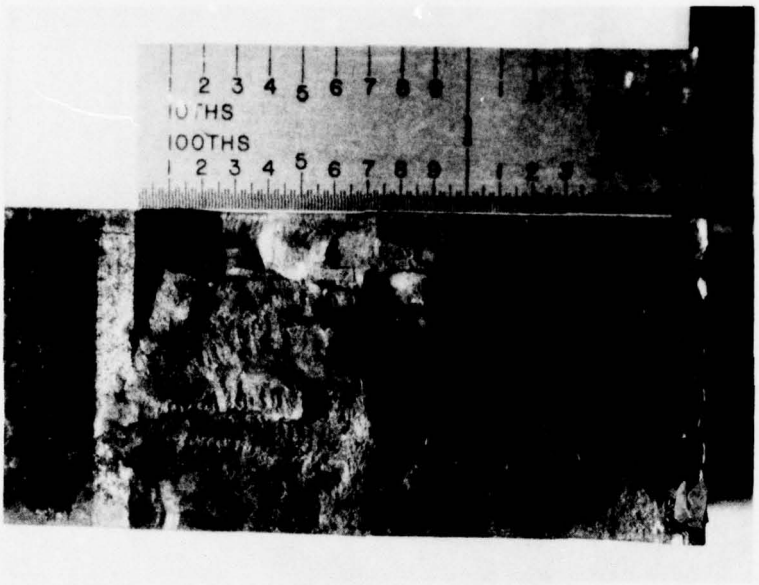

Figure 5-4 - HY-130 weld specimen D-5 fracture

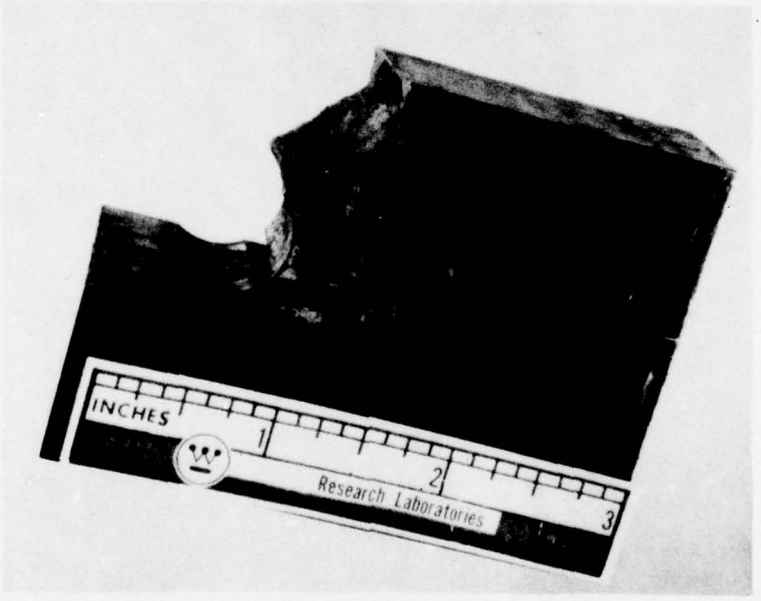

Figure 5-5 - 1T WOL weld specimen F-5 fracture (through arm) in H_2S load-cell test

Dwg. 7701A54

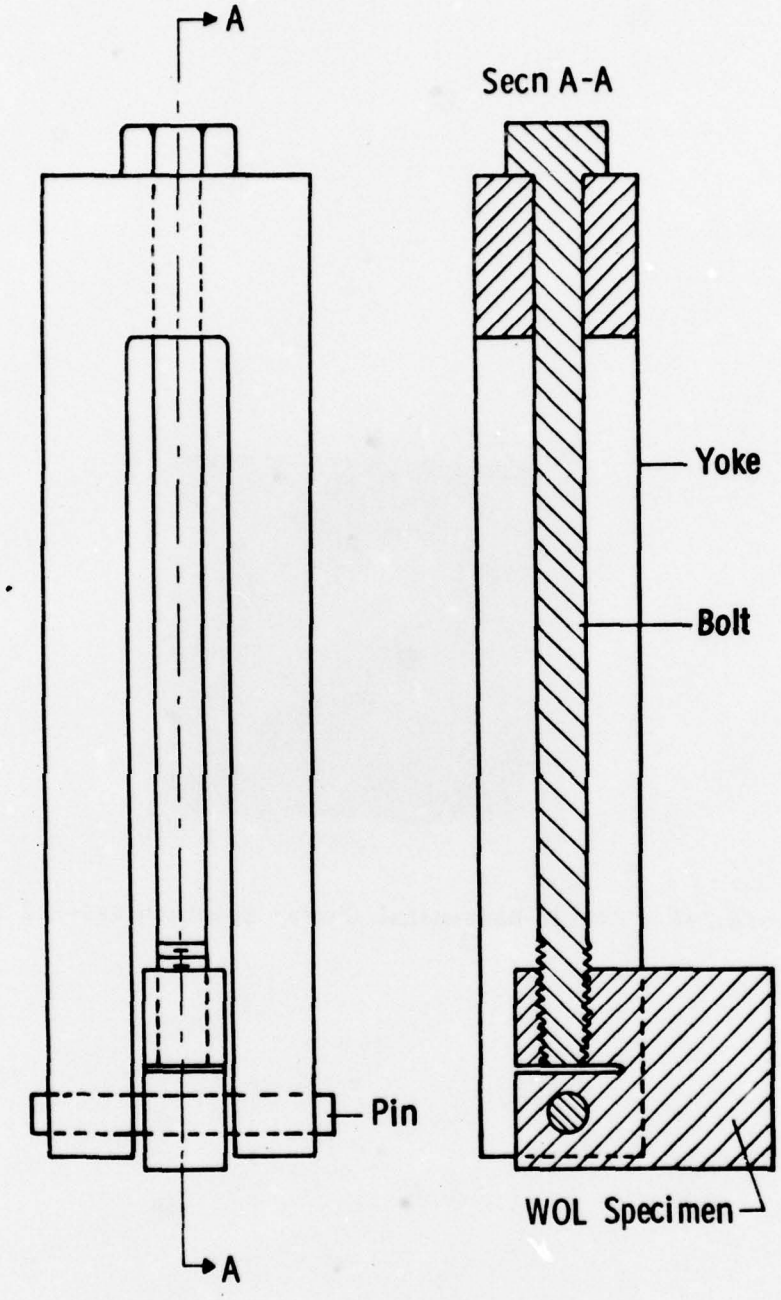

Fig. 5-6 — Spring-loaded specimen model. The "yoke" and "pin" are assumed to be fully rigid while the "bolt" and "specimen" are elastic.

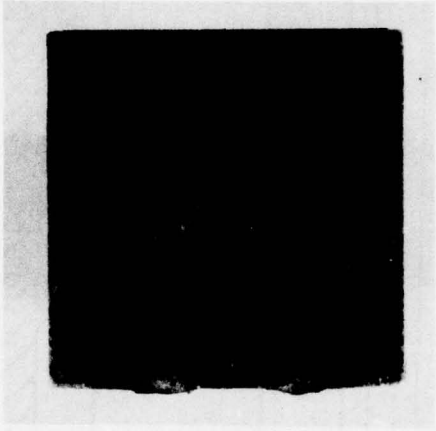

Figure 7-1 - HY-130 base-metal Charpy specimen FKS-R22 fracture

ERH-6

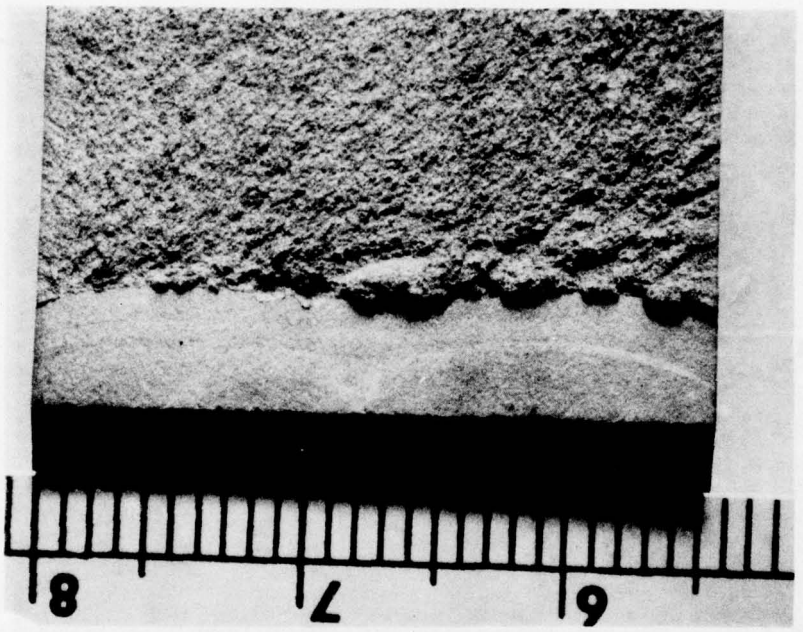

Scale in Centimeters

Fig. 8-1. An overview of the fracture surface found or sample ERH-6 (9Ni 4Co HY-180) which was tested in hydrogen gas at 190 psia. Note the irregular appearance of the fatigue crack front.

X 20

Fig. 8-2. A low magnification SEM view of the tip of the fatigue crack. The overhanging lips conceal parts of the fatigue crack.

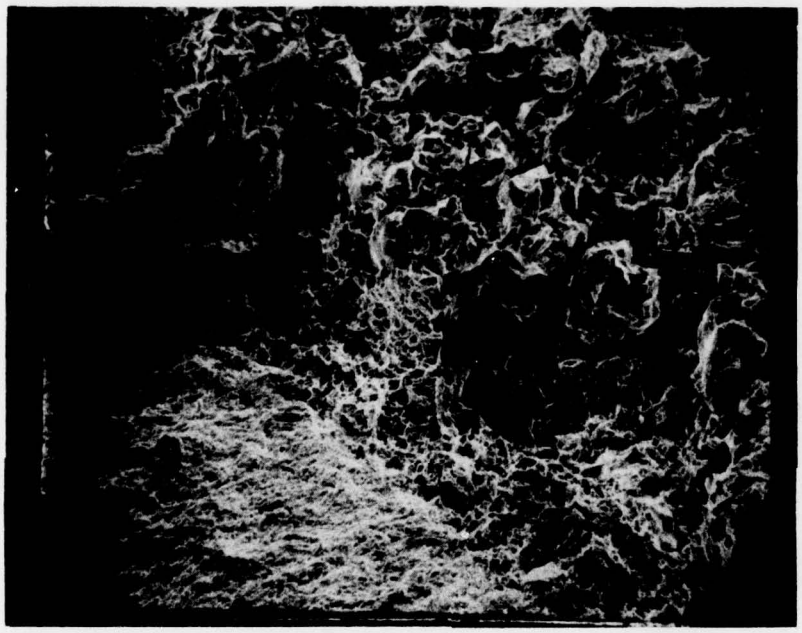

X 200

Fig. 8-3. An enlarged view of the center of Fig. 8-2 showing a ribbon of dimpled rupture between the fatigue crack tip (LHS) and the intergranular fracture (RHS).

X 180

Fig. 8-4. A view of an overhanging lip showing a "featureless zone" between the fatigue crack on the left and the intergranular fracture on the right.

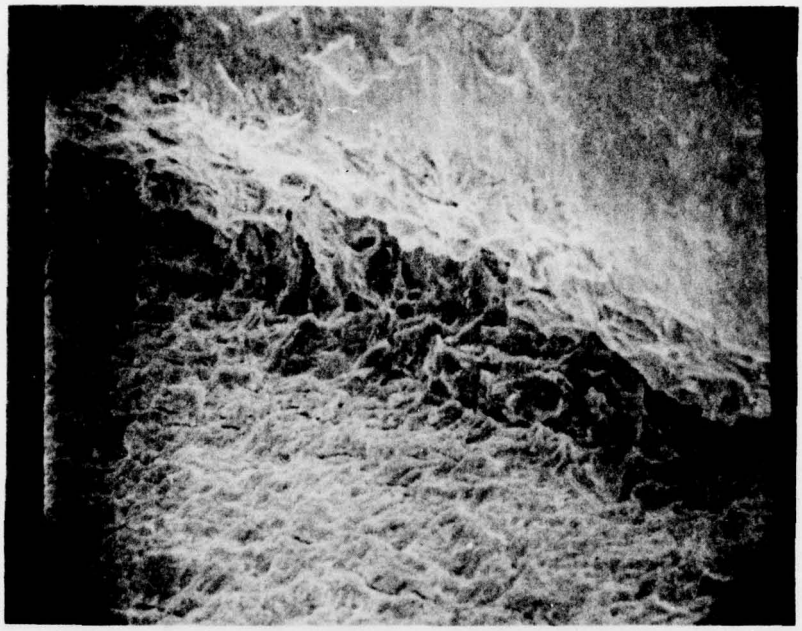

X 900

Fig. 8-5 The sample was tilted to give a clear view of the fatigue crack tip under the lip shown in Fig. 8-4. Note the relative absence of dimpled rupture compared with the fatigue crack tip shown in Figure 8-3.

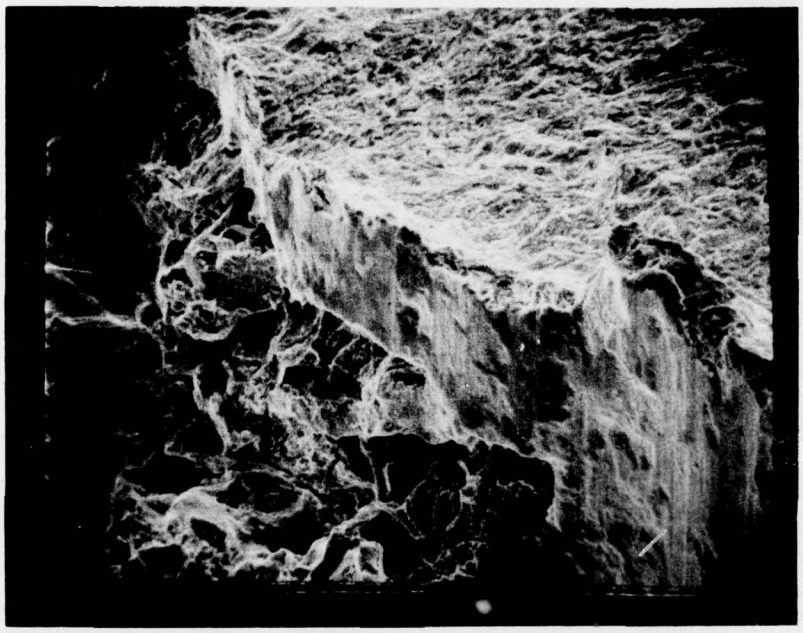

X 500

Fig. 8-6. A view of the fracture surface taken in the 7.1 cm position in Fig. 8-1. The sample was rotated so that the picture is taken from a point facing the fatigue crack on the right. The featureless zone has scrape marks generated in the final shear failure. The intergranular fracture on the left extends under the fatigue crack plane.

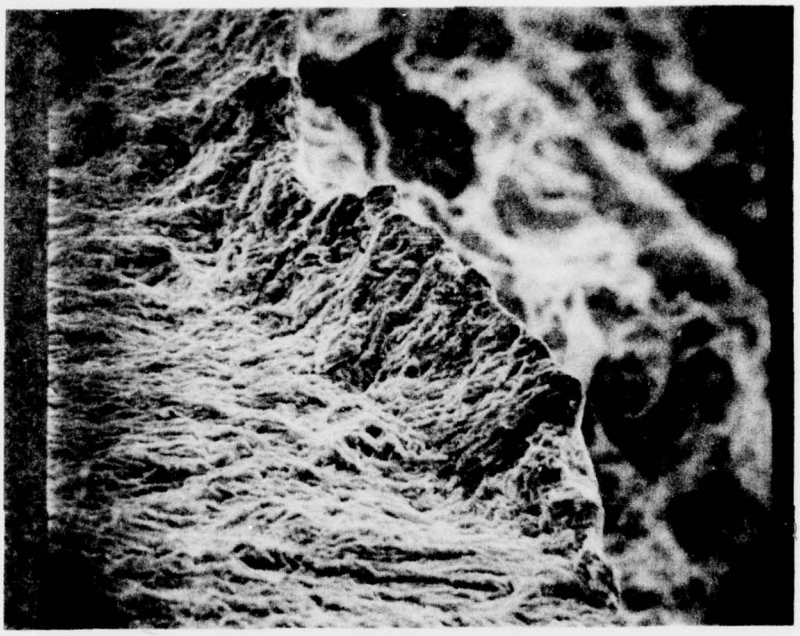

X 800

Fig. 8-7. A view of the fracture surface shown in Fig. 8-6 taken from a point above the fatigue crack on the left. The final shear separation of the cracks has resulted in a severe deformation of the (normally flat) fatigue crack plane.

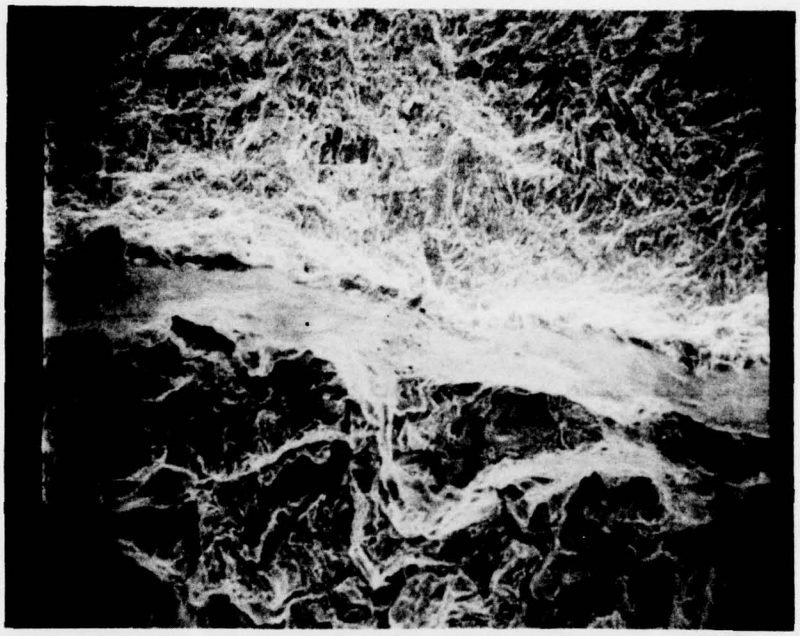

X 500

Fig. 8-8. A view of the fracture surface from a point above the hydrogen induced fracture at the bottom, facing the fatigue crack at the top. Note the evidence of smeared dimples in the "featureless zone" seperating the two fracture surfaces.

Dwg. 7685A50

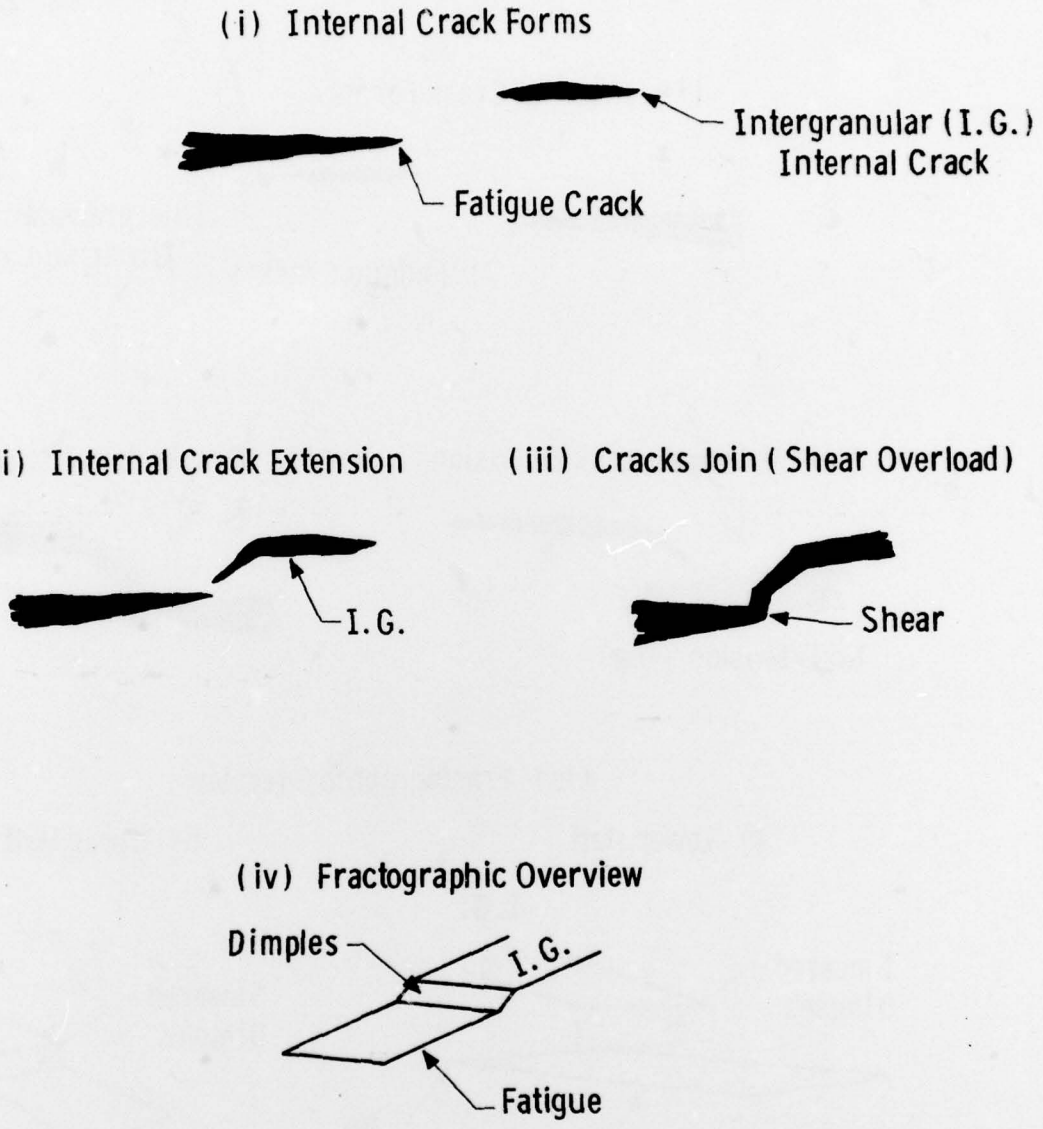

Fig.8-9—Cracking sequence in H_2 test giving dimpled rupture between the tip of the fatigue crack and the main hydrogen embrittled crack (Fig.8-3)

Dwg. 7685A52

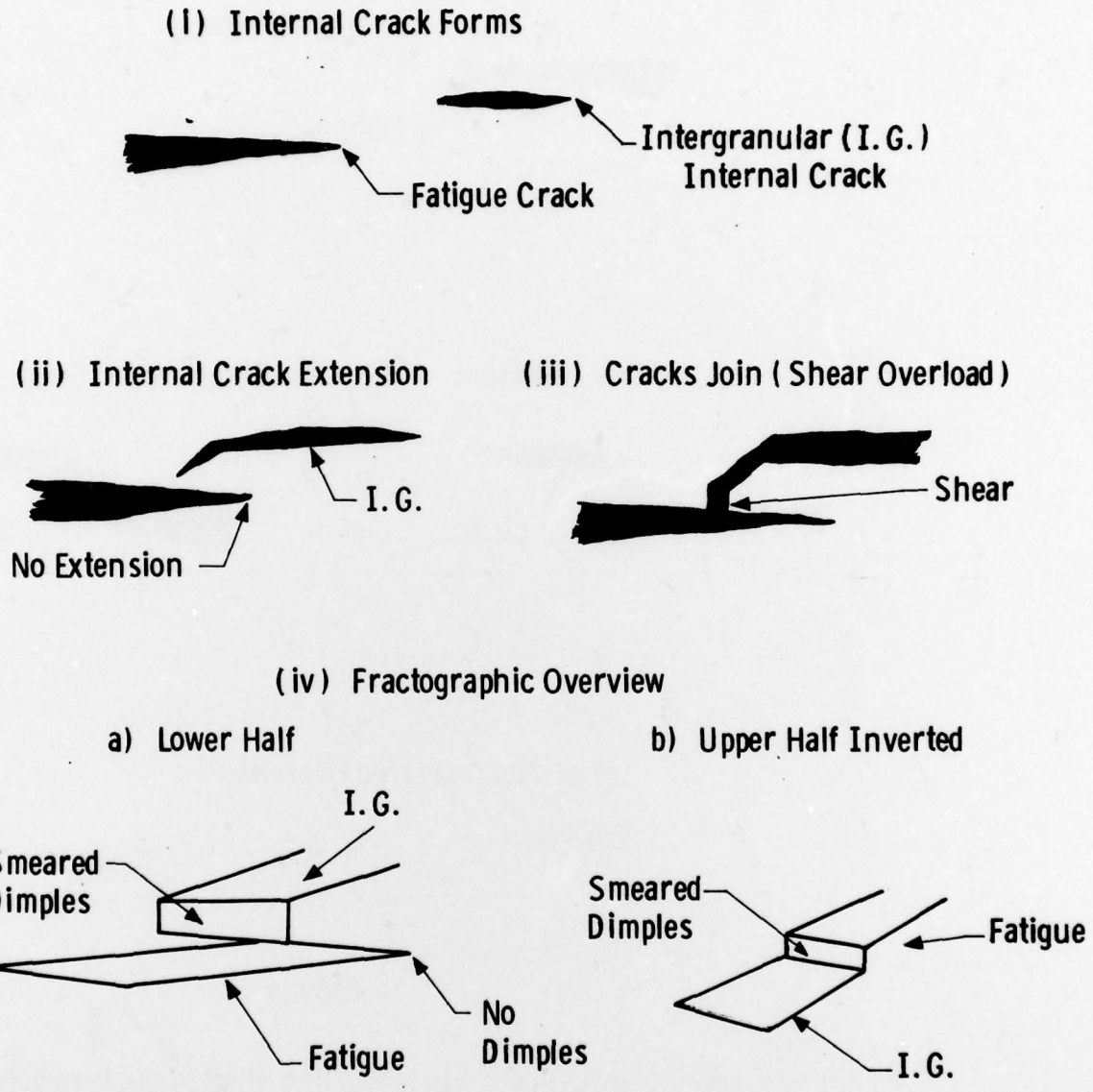

Fig. 8.10 - Cracking sequence in H_2 test leading to a) a featureless zone of smeared dimples and a ligament overhanging the main fatigue crack (Fig. 8.4) The absence of dimples is shown in Fig. 8.5 b) A featureless zone separating the fatigue crack and the intergranular crack (right hand part of Fig. 8.6)

Dwg. 7685A51

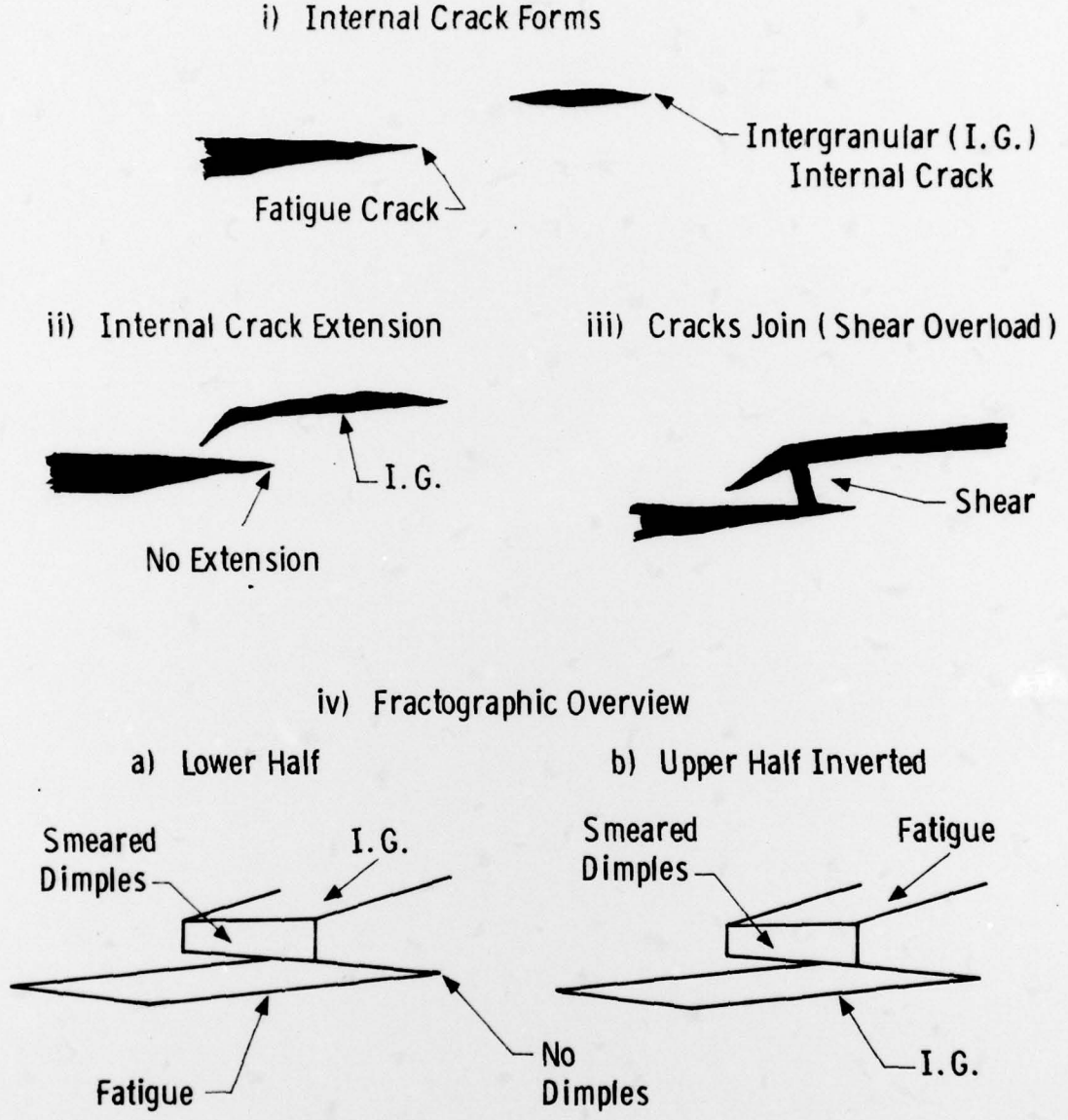

Fig. 8.11 -Cracking sequence in H_2 test leading to a fracture appearance a) similar to that of Fig. 8.10 (iv) and b) a featureless zone overhanging an intergranular fracture as found in Fig. 8.6

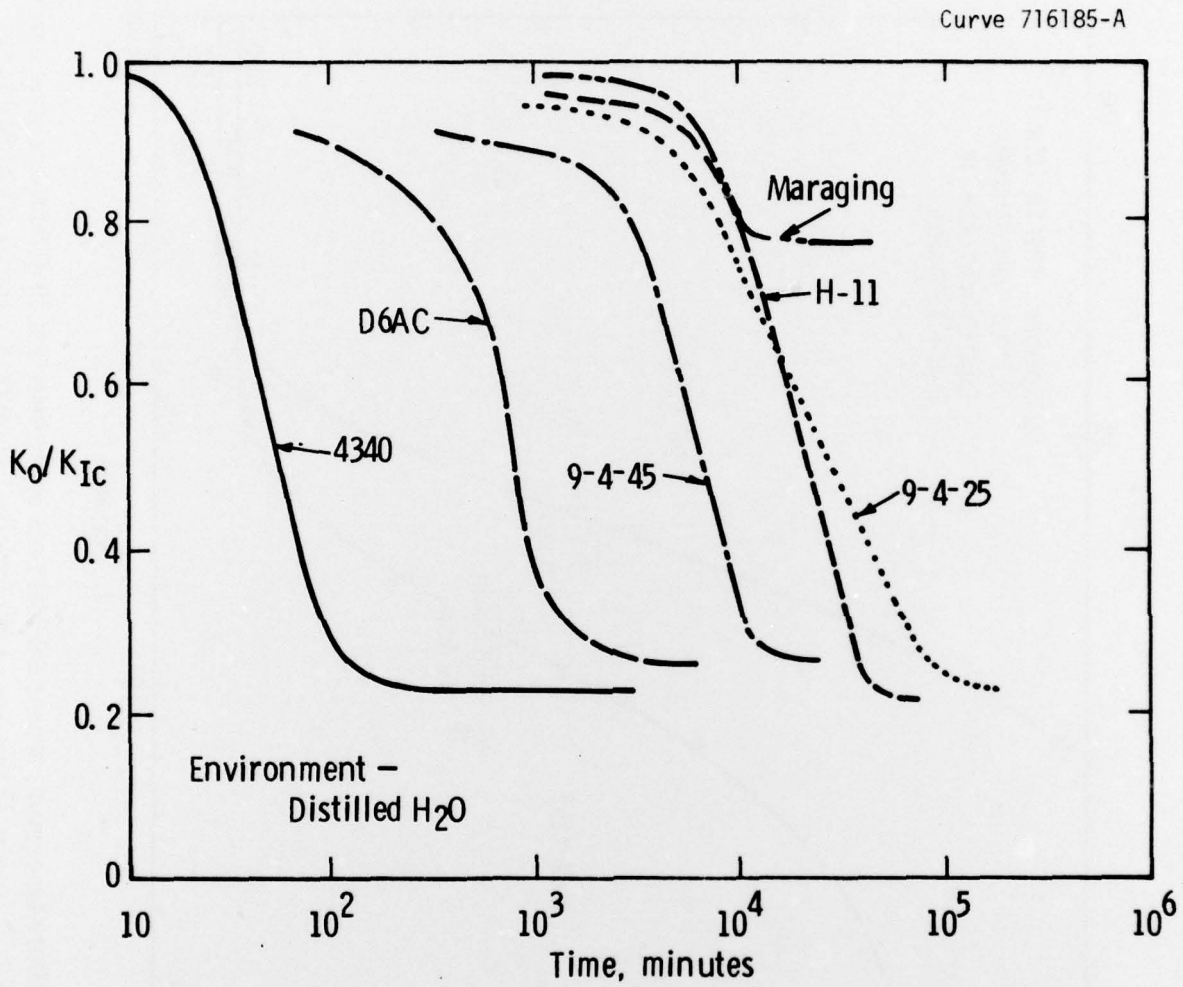

Fig. 10-1– Summary plot of normalized stress intensity against failure time (log scale) for six high-strength (σ_y = 200 ksi) steels, demonstrating 600-fold range of failure-time constant t_{fo} with steel type (reproduced from data of Benjamin and Steigerwald, Ref. 10-3).

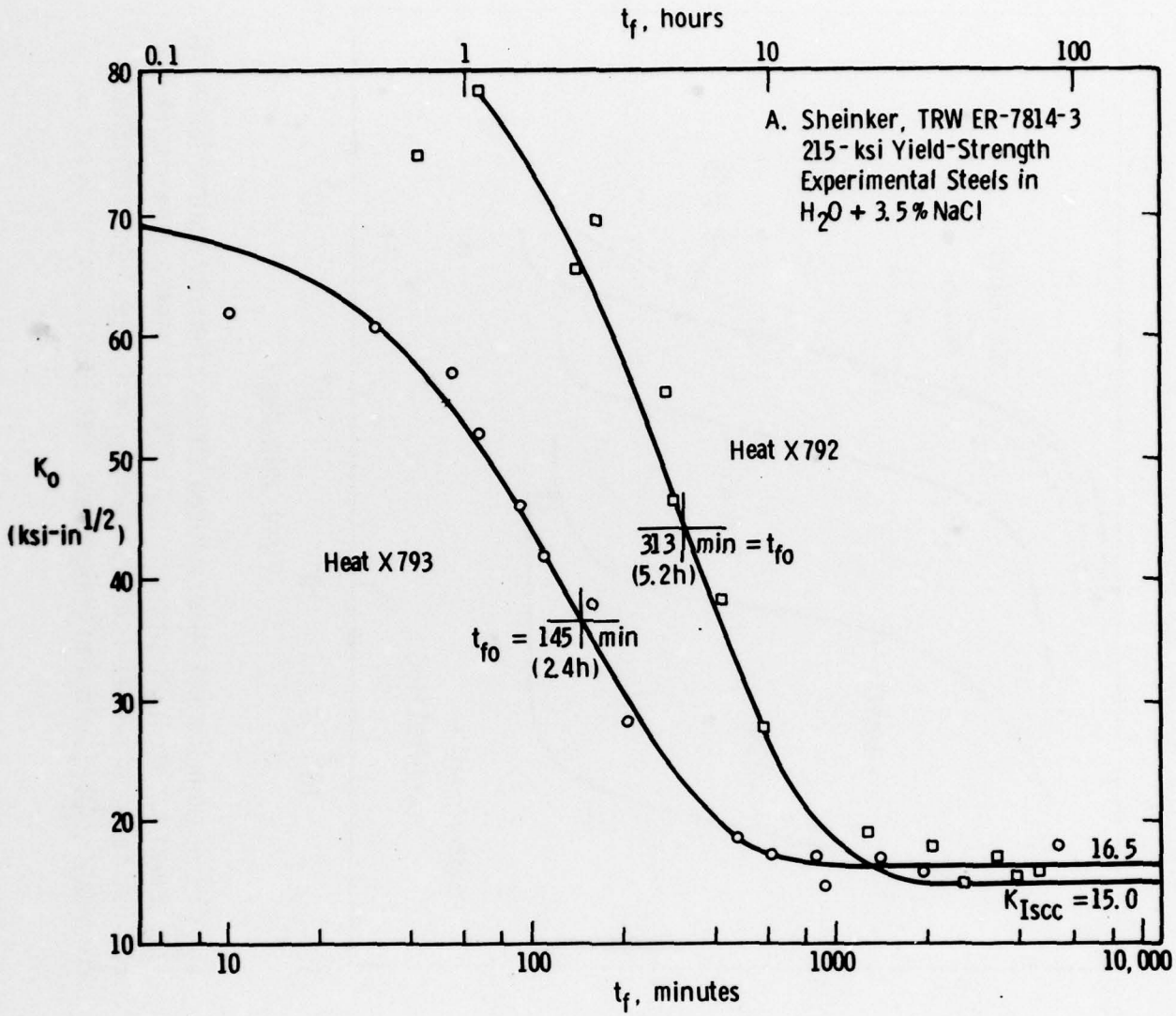

Fig. 10-2— Failure-time results of constant-load tests by Sheinker (Ref. 10-4) fitted by curves having the formula $K_o = K_{Iscc} + (K_{Ic} - K_{Iscc}) \exp(-t_f/t_{fo})$ in which K_{Ic} and t_{fo} are constants for each material

BASIC DISTRIBUTION LIST

Technical and Summary Reports April 1978

Organization	Copies
Defense Documentation Center Cameron Station Alexandria, VA 22314	12
Office of Naval Research Department of the Navy 800 N. Quincy Street Arlington, VA 22217	
ATTN: Code 471	1
Code 102	1
Code 470	1
Commanding Officer Office of Naval Research Branch Office Building 114, Section D 666 Summer Street Boston, MA 02210	1
Commanding Officer Office of Naval Research Branch Office 536 South Clark Street Chicago, IL 60605	1
Office of Naval Research San Francisco Area Office 760 Market Street, Room 447 San Francisco, CA 94102	1
Naval Research Laboratory Washington, DC 20375	
ATTN: Codes 6000	1
6100	1
6300	1
6400	1
2627	1
Naval Air Development Center Code 302 Warminster, PA 18964 ATTN: Mr. F. S. Williams	1
Naval Air Propulsion Test Center Trenton, NJ 08628 ATTN: Library	1
Naval Construction Batallion Civil Engineering Laboratory Port Hueneme, CA 93043 ATTN: Materials Division	1
Naval Electronics Laboratory San Diego, CA 92152 ATTN: Electron Materials Sciences Division	1
Naval Missile Center Materials Consultant Code 3312-1 Point Mugu, CA 92041	1
Commanding Officer Naval Surface Weapons Center White Oak Laboratory Silver Spring, MD 20910 ATTN: Library	1
David W. Taylor Naval Ship Research and Development Center Materials Department Annapolis, MD 21402	1
Naval Undersea Center San Diego, CA 92132 ATTN: Library	1
Naval Underwater System Center Newport, RI 02840 ATTN: Library	1
Naval Weapons Center China Lake, CA 93555 ATTN: Library	1
Naval Postgraduate School Monterey, CA 93940 ATTN: Mechanical Engineering Department	1

BASIC DISTRIBUTION LIST (cont'd)

Organization	Copies
Naval Air Systems Command Washington, DC 20360 ATTN: Codes 52031 52032	1
Naval Sea System Command Washington, DC 20362 ATTN: Code 035	1
Naval Facilities Engineering Command Alexandria, VA 22331 ATTN: Code 03	1
Scientific Advisor Commandant of the Marine Corps Washington, DC 20380 ATTN: Code AX	1
Naval Ship Engineering Center Department of the Navy Washington, DC 20360 ATTN: Code 6101	1
Army Research Office P.O. Box 12211 Triangle Park, NC 27709 ATTN: Metallurgy & Ceramics Program	1
Army Materials and Mechanics Research Center Watertown, MA 02172 ATTN: Research Programs Office	1
Air Force Office of Scientific Research Bldg. 410 Bolling Air Force Base Washington, DC 20332 ATTN: Chemical Science Directorate Electronics & Solid State Sciences Directorate	1 1
Air Force Materials Laboratory Wright-Patterson AFB Dayton, OH 45433	1
Library Building 50, Rm 134 Lawrence Radiation Laboratory Berkeley, CA	1
NASA Headquarters Washington, DC 20546 ATTN: Code RRM	1
NASA Lewis Research Center 21000 Brookpark Road Cleveland, OH 44135 ATTN: Library	1
National Bureau of Standards Washington, DC 20234 ATTN: Metallurgy Division Inorganic Materials Div.	1 1
Director Applied Physics Laboratory University of Washington 1013 Northeast Forthieth Street Seattle, WA 98105	1
Defense Metals and Ceramics Information Center Battelle Memorial Institute 505 King Avenue Columbus, OH 43201	1
Metals and Ceramics Division Oak Ridge National Laboratory P.O. Box X Oak Ridge, TN 37380	1
Los Alamos Scientific Laboratory P.O. Box 1663 Los Alamos, NM 87544 ATTN: Report Librarian	1
Argonne National Laboratory Metallurgy Division P.O. Box 229 Lemont, IL 60439	1
Brookhaven National Laboratory Technical Information Division Upton, Long Island New York 11973 ATTN: Research Library	1
Office of Naval Research Branch Office 1030 East Green Street Pasadena, CA 91106	1

C
April 1978

SUPPLEMENTARY DISTRIBUTION LIST

Technical and Summary Reports

Dr. T. R. Beck
Electrochemical Technology Corporation
10035 31st Avenue, NE
Seattle, Washington 98125

Professor I. M. Bernstein
Carnegie-Mellon University
Schenley Park
Pittsburgh, Pennsylvania 15213

Professor H. K. Birnbaum
University of Illinois
Department of Metallurgy
Urbana, Illinois 61801

Dr. Otto Buck
Rockwell International
1049 Camino Dos Rios
P.O. Box 1085
Thousand Oaks, California 91360

Dr. David L. Davidson
Southwest Research Institute
8500 Culebra Road
P.O. Drawer 28510
San Antonio, Texas 78284

Dr. D. J. Duquette
Department of Metallurgical Engineering
Rensselaer Polytechnic Institute
Troy, New York 12181

Professor R. T. Foley
The American University
Department of Chemistry
Washington, D.C. 20016

Dr. G. A. Gehring
Ocean City Research Corporation
Tennessee Avenue & Beach Thorofare
Ocean City, New Jersey 08226

Dr. D. A. S. Green
Martin Marietta Corporation
1450 South Rolling Road
Baltimore, Maryland 21227

Professor R. H. Heidersbach
University of Rhode Island
Department of Ocean Engineering
Kingston, Rhode Island 02881

Professor H. Herman
State University of New York
Material Sciences Division
Stony Brook, New York 11794

Professor J. P. Hirth
Ohio State University
Metallurgical Engineering
Columbus, Ohio 43210

Dr. D. W. Hoeppner
University of Missouri
College of Engineering
Columbia, Missouri 65201

Dr. E. W. Johnson
Westinghouse Electric Corporation
Research and Development Center
1310 Beulah Road
Pittsburgh, Pennsylvania 15235

Professor R. M. Latanision
Massachusetts Institute of Technology
77 Massachusetts Avenue
Room E19-702
Cambridge, Massachusetts 02139

Dr. F. Mansfeld
Rockwell International Science Center
1049 Camino Dos Rios
P.O. Box 1085
Thousand Oaks, California 91360

Professor A. E. Miller
University of Notre Dame
College of Engineering
Notre Dame, Indiana 46556

Dr. Jeff Perkins
Naval Postgraduate School
Monterey, California 93940

C
April 1978

SUPPLEMENTARY DISTRIBUTION LIST
(Continued)

Professor H. W. Pickering
Pennsylvania State University
Department of Material Sciences
University Park, Pennsylvania 16802

Professor R. W. Staehle
Ohio State University
Department of Metallurgical Engineering
Columbus, Ohio 43210

Dr. E. A. Starke, Jr.
Georgia Institute of Technology
School of Chemical Engineering
Atlanta, Georgia 30332

Dr. Barry C. Syrett
Stanford Research Institute
333 Ravenswood Avenue
Menlo Park, California 94025

Dr. R. P. Wei
Lehigh University
Institute for Fracture and
Solid Mechanics
Bethlehem, Pennsylvania 18015

Professor H. G. F. Wilsdorf
University of Virginia
Department of Materials Science
Charlottesville, Virginia 22903